

Final Report

**Marine Species Density
Models for the Arctic
Environmental Impact
Statement (EIS) Study Area**

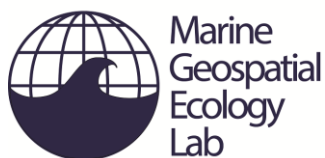
Submitted to:

Naval Facilities Engineering Command Atlantic
for Fleet Forces Command under
Contract No. N62470-15-D-8006 (T011)
issued to HDR, Inc.



Prepared by

Rob S. Schick, Jason J Roberts, and Pat N. Halpin



Marine Geospatial Ecology Lab
Duke University

Submitted by:



San Diego, CA

November 2017

Suggested Citation:

Schick, R.S., J.J. Roberts, and P.N. Halpin. 2017. *Marine Species Density Models for the Arctic Environmental Impact Statement (EIS) Study Area. Final Report*. Prepared for U.S. Fleet Forces Command. Submitted to Naval Facilities Engineering Command Atlantic, Norfolk, Virginia, under Contract No. N62470-15-D-8006, Task Order TO11, issued to HDR, San Diego, California. November 2017.

Table of Contents

List of Tables.....	6
List of Figures.....	7
Acronyms and Abbreviations.....	12
Introduction.....	13
Report Structure	14
Background	15
Bowhead whales	16
Beluga whales.....	16
Walrus	17
Gray whales.....	17
Seals.....	17
Objective.....	18
Methods.....	18
Data Summary.....	19
Bowhead Whales.....	24
Beluga Whales.....	25
Gray Whales	26
Walrus	27
Bearded Seals	28
Small Pinnipeds	29
Unidentified Pinnipeds.....	30
Baleen Whales.....	31
Data Cleaning.....	32
Data Modeling -- Detection Functions	32
Sighting Hierarchies by Platform.....	34
Multiple Covariate Distance Sampling.....	35
Availability Bias— $g(0)$	35
Data Modeling -- Processing and Preparation of Environmental Covariates.....	36
Data Modeling -- Generalized Additive Models	38
Data Modeling -- Density Prediction	39
Temporal Dimensions	39
Spatial Dimensions.....	39
Results.....	40

Detection Functions.....	40
Generalized Additive Model.....	40
Predicted Density—Surfaces & Total Abundance	41
Bowhead Whales.....	42
Beluga Whales.....	49
Gray Whales	53
Walrus	59
Bearded Seals	66
Small Pinnipeds	68
Unidentified Pinnipeds.....	74
Baleen Whales.....	81
Discussion.....	83
Species-level Predictions.....	83
Bowhead Whales.....	83
Beluga Whales.....	83
Gray Whales	84
Walrus	85
Bearded Seals	85
Small Pinnipeds & Unidentified Pinnipeds.....	86
Baleen Whales.....	86
Modeling and Analytical Caveats.....	86
Future Work.....	88
Covariates	88
Additional Data Sources.....	89
Modeling Species Jointly.....	90
Summary	90
Literature Cited	91
Appendix A - Detection Functions.....	97
Sightings Hierarchies	97
Fitted Detection Functions	99
Bowhead Whales.....	99
Beluga Whales.....	101
Gray Whales	103
Walrus	104

Bearded Seals	106
Small Pinnipeds	107
Unidentified Pinnipeds.....	109
Baleen Whales.....	110
Appendix B - Generalized Additive Models.....	113
Detailed Summaries of the GAM Models for Each Species	113
Bowhead Whales.....	113
Beluga Whales.....	114
Gray Whales	115
Walrus	116
Bearded Seals	117
Small Pinnipeds	119
Unidentified Pinnipeds.....	120
Baleen Whales.....	121

List of Tables

Table 1. Summary of survey effort, by year, in the ASAMM database from 2000-2016. The Length column represents the cumulative on-effort tracklines covered in 1,000s of kilometers.....	20
Table 2. Summary of survey effort during 2000-2016 split out over each of the four main survey months. Values are in 1,000s of km, and represent the cumulative on-effort distance covered on the trackline.....	21
Table 3. Summary of sightings during 2000-2016. Sightings represent the cumulative number of individuals sighted while on-effort.....	21
Table 4. Summary of sightings by species (whales) and year during 2000-2016. Sightings represent the cumulative number of individuals sighted while on-effort for a given year..	22
Table 5. Summary of sightings by species (pinnipeds) and year during 2000-2016. Sightings represent the cumulative number of individuals sighted while on-effort for a given year.....	23
Table 6. Summary of sightings during 2000-2016 by species/guild and month. Sightings represent the cumulative number of individuals sighted while on-effort.	23
Table 7. Summary table highlighting the final model for the detection function we chose for each species.*	33
Table 8. Species-specific availability bias values used to correct the observed group size estimates into final abundance values used in modeling. If no correction was available, we used a $g(0)$ estimate of 1	36
Table 9. Summary of the static covariates used in the density surface prediction.*	37
Table 10. Summary of the dynamic environmental predictors used in the GAM analysis....	37
Table 11. Summary table highlighting the final covariates included in each species or guild-specific GAM. Further details given in each summary section.	41
Table 12. Predicted abundances and CV, overall and by month. Two groups only contain the total abundance (bearded seals, and baleen whales).....	42

List of Figures

Figure 1. Study area of the ASAMM project with individual survey transect lines depicted in light gray. Some survey blocks (e.g., 8, 9, and 10) are less well surveyed.....	19
Figure 2. All on-transect sightings of bowhead whales (<i>Balaena mysticetus</i>) in the ASAMM study area. Bowheads were primarily seen nearshore in the Alaskan Beaufort Sea. Note the high number of sightings of bowheads east of Point Barrow.	24
Figure 3. All on-transect sightings of beluga whales (<i>Delphinapterus leucas</i>) in the ASAMM study area. In contrast to bowheads, belugas were seen farther offshore in the Alaskan Beaufort Sea. Note the especially high number of sightings northeast of Point Barrow. Large groups were also seen quite near the shore in the Chukchi Sea between Cape Lisburne and Wainwright.	25
Figure 4. All on-transect sightings of gray whales (<i>Eschrichtius robustus</i>) in the ASAMM study area. Very few gray whales were seen east of Point Barrow in the Alaskan Beaufort Sea. Most whales were seen west of Point Hope, and in the so-called “gray whale garden” north and east of Wainwright, Alaska.	26
Figure 5. All on-transect sightings of walrus (<i>Odobenus rosmarus</i>) in the ASAMM study area. Very few walrus were seen east of Point Barrow in the Alaskan Beaufort Sea. Most walrus sightings were either coastal, or located in Hannah Shoal in the Northeast Chukchi Sea (Block 14).	27
Figure 6. All on-transect sightings of bearded seals (<i>Erignathus barbatus</i>) in the ASAMM study area. While they were seen throughout the study area, bearded seals seemed biased toward shallower waters, especially in the Alaskan Beaufort Sea.	28
Figure 7. All on-transect sightings of small pinnipeds in the ASAMM study area. As with bearded seals, locations of small pinnipeds were biased toward shallower waters, especially in the Alaskan Beaufort Sea, where relatively few were seen deeper than the shelf-break.....	29
Figure 8. All on-transect sightings of unidentified pinnipeds in the ASAMM study area. The sighting patterns were very similar to that of small unidentified pinnipeds.....	30
Figure 9. All on-transect sightings of the three species that comprise the baleen whale guild--fin whales (<i>Balaenoptera physalus</i>), humpback whales (<i>Megaptera novaeangliae</i>), and minke whales (<i>Balaenoptera acutorostrata</i>). There were no sightings of these sub-Arctic migrants in the Alaskan Beaufort Sea; most whales were seen in the southern Chukchi Sea near Point Hope.	31
Figure 10. Hierarchical structure of the number of bowhead whale sightings by year and by platform. Sightings colored in red are below the 60 sighting group threshold suggested in Buckland et al. (2001) as the threshold needed to fit a detection function.....	34

Figure 11. (A) Predicted densitology for bowhead whales (2000-2016). Bowheads observed on-transect are shown with orange dots. (B) Predicted CV surface.....	43
Figure 12. (A) Predicted density for bowhead whales in July (2000-2016). Bowheads observed on-transect are shown with orange dots. (B) Predicted CV surface.....	45
Figure 13. (A) Predicted density for bowhead whales in August (2000-2016). Bowheads observed on-transect are shown with orange dots. (B) Predicted CV surface.....	46
Figure 14. (A) Predicted density for bowhead whales in September (2000-2016). Bowheads observed on-transect are shown with orange dots. (B) Predicted CV surface.....	47
Figure 15. (A) Predicted density for bowhead whales in October (2000-2016). Bowheads observed on-transect are shown with orange dots. (B) Predicted CV surface.....	48
Figure 16. (A) Predicted densitology for beluga whales (2000-2016). Belugas observed on-transect are shown with orange dots. (B) Predicted CV surface.	49
Figure 17. (A) Predicted density for beluga whales in July (2000-2016). Belugas observed on-transect are shown with orange dots. (B) Predicted CV surface.	50
Figure 18. (A) Predicted density for beluga whales in August (2000-2016). Belugas observed on-transect are shown with orange dots. (B) Predicted CV surface.....	51
Figure 19. (A) Predicted density for beluga whales in September (2000-2016). Belugas observed on-transect are shown with orange dots. (B) Predicted CV surface.....	52
Figure 20. (A) Predicted density for beluga whales in October (2000-2016). Belugas observed on-transect are shown with orange dots. (B) Predicted CV surface.....	53
Figure 21. (A) Predicted densitology for gray whales (2000-2016). Gray whales observed on-transect are shown with orange dots. (B) Predicted CV surface.	54
Figure 22. (A) Predicted density for gray whales in July (2000-2016). Gray whales observed on-transect are shown with orange dots. (B) Predicted CV surface.	55
Figure 23. (A) Predicted density for gray whales in August (2000-2016). Gray whales observed on-transect are shown with orange dots. (B) Predicted CV surface.....	56
Figure 24. (A) Predicted density for gray whales in September (2000-2016). Gray whales observed on-transect are shown with orange dots. (B) Predicted CV surface.....	57
Figure 25. (A) Predicted density for gray whales in October (2000-2016). Gray whales observed on-transect are shown with orange dots. (B) Predicted CV surface.....	58
Figure 26. (A) Predicted densitology for walrus (2000-2016). Walrus observed on-transect are shown with orange dots. (B) Predicted CV surface.	60

Figure 27. (A) Predicted density for walrus in July (2000-2016). Walrus observed on-transect are shown with orange dots. (B) Predicted CV surface.	62
Figure 28. (A) Predicted density for walrus in August (2000-2016). Walrus observed on-transect are shown with orange dots. (B) Predicted CV surface.	63
Figure 29. (A) Predicted density for walrus in September (2000-2016). Walrus observed on-transect are shown with orange dots. (B) Predicted CV surface.	64
Figure 30. (A) Predicted density for walrus in October (2000-2016). Walrus observed on-transect are shown with orange dots. (B) Predicted CV surface.	65
Figure 31. (A) Predicted densitology for bearded seals (2000-2016). Bearded seals observed on-transect are shown with orange dots. (B) Predicted CV surface.	67
Figure 32. (A) Predicted densitology for small pinnipeds (2000-2016). Small pinnipeds observed on-transect are shown with orange dots. (B) Predicted CV surface.	69
Figure 33. (A) Predicted densitology for small pinnipeds in July (2000-2016). Small pinnipeds observed on-transect are shown with orange dots. (B) Predicted CV surface.	70
Figure 34. (A) Predicted densitology for small pinnipeds in August (2000-2016). Small pinnipeds observed on-transect are shown with orange dots. (B) Predicted CV surface.	71
Figure 35. (A) Predicted densitology for small pinnipeds in September (2000-2016). Small pinnipeds observed on-transect are shown with orange dots. (B) Predicted CV surface.	72
Figure 36. (A) Predicted densitology for small pinnipeds in October (2000-2016). Small pinnipeds observed on-transect are shown with orange dots. (B) Predicted CV surface.	73
Figure 37. (A) Predicted densitology for unidentified pinnipeds (2000-2016). Unidentified pinnipeds observed on-transect are shown with orange dots. (B) Predicted CV surface.	75
Figure 38. (A) Predicted densitology for unidentified pinnipeds in July (2000-2016). Unidentified pinnipeds observed on-transect are shown with orange dots. (B) Predicted CV surface.	77
Figure 39. (A) Predicted densitology for unidentified pinnipeds in August (2000-2016). Unidentified pinnipeds observed on-transect are shown with orange dots. (B) Predicted CV surface.	78
Figure 40. (A) Predicted densitology for unidentified pinnipeds in September (2000-2016). Unidentified pinnipeds observed on-transect are shown with orange dots. (B) Predicted CV surface.	79
Figure 41. (A) Predicted densitology for unidentified pinnipeds in October (2000-2016). Unidentified pinnipeds observed on-transect are shown with orange dots. (B) Predicted CV surface.	80

Figure 42. (A) Predicted densitology for baleen whales (2000-2016). Baleen whales observed on-transect are shown with orange dots. (B) Predicted CV surface.....	82
Figure 43. Plot of the Distance to 200-m Isobath covariate. Note how far areas in block 23 are from the 200-m isobath covariate (i.e., they have high distance values).....	85
Figure 44. Initial predicted density for bowhead whales in the ASAMM study area prior to inclusion of the soap smoother.	88
Figure 45. Beluga whale sightings/platform hierarchy.....	97
Figure 46. Gray whale sightings/platform hierarchy.	97
Figure 47. Walrus sightings/platform hierarchy.....	98
Figure 48. Bearded seal sightings/platform hierarchy.....	98
Figure 49. Small pinnipeds sightings/platform hierarchy.	98
Figure 50. Small pinnipeds sightings/platform hierarchy.....	98
Figure 51. Baleen whale sightings/platform hierarchy.....	99
Figure 52. Final detection function chosen for the MMS Otter platform for bowhead whales shows a decent fit with three covariates included in the detection function model: 1) Maximum Visibility, 2) Depth Observed, and 3) Observer.....	99
Figure 53. Final detection function chosen for the MML Otter platform for bowhead whales. The single covariate included indicates that as bowhead group size increases, so does detection probability.	100
Figure 54. Final detection function chosen for the MML Commander platform for bowhead whales includes covariates for both glare (VisImp) and log group size. As with the MML Otter, as group size increases, so does detectability.....	100
Figure 55. Final detection function chosen for the MMS Otter platform for beluga whales. Some heaping may be evident, but we kept the distance bins as depicted. Left truncation distance was higher than in the MML Otter.....	101
Figure 56. Final detection function chosen for the MML Otter platform for beluga whales. A single covariate—maximum visibility—was included. The detection function indicates somewhat paradoxically that as the visibility improves, detection decreases. It is possible that with a broader search field, observers are scanning over a larger area and thus missing some sightings.	102
Figure 57. Final detection function chosen for the MML Commander platform for beluga whales. As with bowhead whales, the Commander is the platform with the most sightings and the best fit. Five covariates were included in the best model for detection.	102

Figure 58. Final detection function chosen for the combined Otter platforms for gray whales. Intuitively, as visibility increases, so does detection.	103
Figure 59. Final detection function chosen for the MML Commander platform for gray whales. While the detection function is more complicated than with the Otters, the fit is excellent.....	104
Figure 60. Final detection function chosen for the MML Otter platform for walrus. There were relatively few walrus seen from this platform, and the sightings rate decays very quickly with distance from the trackline.	105
Figure 61. Final detection function chosen for the MML Commander platform for walrus. The detection function decays quickly for this platform as well, though not as quickly as for the Otter.....	105
Figure 62. Final detection function chosen for the MML Otter platform for bearded seals.	106
Figure 63. Final detection function chosen for the MML Commander platform for bearded seals. With approximately double the number of observations, the fit is improved; however the ESHW for both platforms is still quite short.....	107
Figure 64. Final detection function chosen for the MML Otter platform for small pinnipeds. Though there are relatively few sightings—especially as compared to the Commander—the fit is still quite good.	108
Figure 65. Final detection function chosen for the MML Commander platform for small pinnipeds.	108
Figure 66. Final detection function chosen for the MML Otter platform for unidentified pinnipeds. Though the ESHW is higher than the Commander, the fit is generally poor.	109
Figure 67. Final detection function chosen for the MML Commander platform for unidentified pinnipeds.....	110
Figure 68. Final detection function chosen for baleen whale (fin, humpback, and minke whale). There is a large ESHW, though this appears driven by humpbacks which are seen at farther distances from the trackline. Minke whales have the lowest detection rate of the three baleen whale species.	111

Acronyms and Abbreviations

°	Degree(s)
AIC	Akaike Information Criterion
AMM	Arctic marine mammal
ASAMM	Aerial Survey of Arctic Marine Mammals
BOEM	Bureau of Ocean Energy Management
CV	Coefficient of Variation
DFO	Canadian Department of Fisheries and Oceans
ESHW	Effective strip half-width
ESRI	Environmental Systems Research Institute
GAM	Generalized Additive Model
km	Kilometer(s)
m	Meter(s)
MCDS	Multiple Covariate Distance Sampling
MMS	Minerals Management Service
MML	Marine Mammal Laboratory
NOAA	National Oceanic and Atmospheric Administration
NSIDC	National Snow and Ice Data Center
REML	Restricted Maximum Likelihood
ROMS	Regional Ocean Modeling System
SRTM	Shuttle Radar Topography Mission
U.S.	United States

Introduction

The Arctic is a dynamic and rapidly changing ecosystem; it is dynamic in the sense that the pattern of annual ice melt and ice freeze up drives a large part of the ecological structure and function of the system; and changing in the sense that as global temperatures increase, these increases are being felt most acutely in the Arctic (Tynan and DeMaster 1997, Moore and Huntington (2008), Kovacs et al. (2011), Screen and Williamson (2017)). The Arctic is also an area that is used extensively by humans and by many marine mammals (Laidre et al. 2015). Because the ecological structure of the system is so heavily ice-dominated, the distribution of Arctic marine mammals (hereafter AMMs) is driven by the interaction between their own biological needs and the availability of suitable habitat. In the case of AMMs, this typically includes some open (ice-free) water. Despite decades of research into AMMs (Moore and Huntington 2008, Laidre et al. (2015)), few synoptic descriptions of density exist for AMMs. This gap is critical in the face of a changing climate. In order for humans to use the Arctic in sustainable ways, we must first understand how our use may impact individual animals of different species. One of the ways we can do that is by understanding the distribution and abundance over space and through time. In this report, we take a first step towards such a synopsis by describing and quantifying the distribution of AMMs in two seas adjacent to Alaska - the Chukchi Sea and the Alaskan Beaufort Sea. To do this, we use the decades-long Aerial Survey of Arctic Marine Mammals (ASAMM) project—conducted by the National Oceanic and Atmospheric Administration's (NOAA's) Marine Mammal Laboratory (MML). While other datasets exist on the distribution and abundance of marine mammals, ASAMM is the longest running, and covers the broadest spatial extent. Therefore, we focus our initial modeling efforts using this rich dataset.

Report Structure

This is the final report for the Arctic Density Modeling project completed for the United States (U.S.) Navy (Contract #N62470-15-D-8006). This report down is structured as follows:

1. **Introduction** to the system and the problem we are addressing
2. Review and summary of the **Materials & Methods** we employ throughout the project
3. **Results** from the detection function fitting stage/process
4. **Results** from the spatial models, i.e. the generalized additive model (gam) fits to the observed data
5. **Results** from predicting density using the gam and detection function output
6. **Discussion** of the current results, and issues to be addressed in the future
7. **Literature Cited**

Background

Many species of marine mammals occupy Arctic and sub-Arctic waters. Core Arctic species and sub-Arctic species exist, with the key distinction being whether the species depends on the Arctic ecosystem for all life history aspects or not (Laidre et al. 2008). In the western Arctic, the core Arctic marine mammals include: bowhead whale (*Balaena mysticetus*), beluga whale (*Delphinapterus leucas*), walrus (*Odobenus rosmarus*), bearded seal (*Erignathus barbatus*), and ringed seal (*Pusa hispida*). (Note that polar bears (*Ursus arctos*) are also considered a core Arctic marine mammal (Laidre et al. 2008), although we do not address them here. This is for two related reasons: 1) the ASAMM concentrated on the at-sea distribution of AMMs; and 2) many sightings of polar bears were on land. This violates some of the assumptions of distance sampling. Though this can be addressed, it requires special treatment of the issue including needing ancillary movement data for the on-land portion (Marques et al. 2013). These core AMM species are categorized as follows: 1) ice-obligate, 2) ice-associated, and 3) sub-arctic species that seasonally migrate into Arctic waters (Moore and Huntington 2008). The sub-Arctic species include gray whale (*Eschrichtius robustus*), humpback whale (*Megaptera novaeangliae*), minke whale (*Balaenoptera acutorostrata*), fin whale (*Balaenoptera physalus*), harbor porpoise (*Phocoena phocoena*), spotted seal (*Phoca largha*), ribbon seal (*Histiophoca fasciata*), harp seal (*Pagophilus groenlandicus*), and hooded seal (*Cystophora cristata*). For the sub-Arctic baleen whales, there is an important distinction; gray whales are thought to be seasonally *resident* in Arctic waters, while humpback, minke and fin whales are thought to be seasonally *migrant* (Moore 2016). Here we concentrate on five species (four core Arctic, and one sub-Arctic), as well as three guilds. The five species are: bowhead whale, beluga whale, gray whale, walrus, and bearded seal; the three guilds are small unidentified pinnipeds, unidentified pinnipeds, and sub-Arctic baleen whales—a guild comprised of minke whale, humpback whale, and fin whale.

Because the Arctic is dominated by sea ice, use of the Arctic habitat by marine mammals is dynamic through space and time, with, for example, species entering waters north of the Bering Strait as winter ice begins to recede and open water expands. Because there is a great degree of interannual variability in ice cover, and because ice cover is changing rapidly (Walsh 2008, Jeffries, Overland, and Perovich 2013), the timing of the distribution and abundance of each species varies a great deal. Depending on whether the species is a core Arctic species (e.g., bowhead whale), or a sub-Arctic migrant (e.g., gray whale), the northern and eastern extents of their distributions can significantly differ between years. Even within the core Arctic species, northern extents of habitat range can differ dramatically, e.g., the northernmost extent of beluga whales is approximately 81 °N (Suydam, Lowry, and Frost 2005, Suydam et al. 2001), whereas for bowhead whales it is approximately 73 °N (Citta et al. 2015). Because of this shifting habitat within a changing climate, understanding synoptic densities of AMMs remains a challenge. In an effort to account for these dynamic habitats, we include two different time-specific predictor covariates - Distance to Ice Edge, and Ice Concentration (details on each are provided in the **Methods** section).

Research into the ecology of AMMs has been taking place since at least the 1970s (Burns, Montague, and Cowles 1993). Much of this research has focused on bowhead whales, because of the joint pressures of managing subsistence harvests for native peoples, and exploration for offshore oil and natural gas resources. The ASAMM project is a major on-going research project that was started by Minerals Management Service (MMS) in 1979 (Moore and Reeves 1993, Clarke, Kennedy, and Ferguson 2016). Currently run by NOAA's MML, this project conducts annual summertime (July—October) aerial surveys in the Chukchi and Alaskan Beaufort seas. In addition to this large-scale survey, there have been many studies of AMMs, including aerial surveys in the Canadian Beaufort Sea (Harwood et al. 2009); satellite tracking studies of bowheads (Citta et al. 2015); belugas (Suydam, Lowry, and Frost 2005, Suydam et al. 2001); walrus (Jay, Fischbach, and Kochnev 2012, Jay et al. 2017); and several ice-associated seal species (Harwood et al. 2015), point-based counts (George et al. 2004), and acoustic detections (Moore et al. 2006). Besides these dedicated marine mammal studies, there have been large scale oceanographic studies of the region, e.g., (Grebmeier et al. 2006). This research is critical to our understanding of the environmental covariates that drive individual species distributions (e.g., Ashjian et al. (2010)).

What have we learned from this work, and what gaps still exist in our knowledge? First, the broad-scale habitat-use patterns for bowhead whales have been ascertained, at least for the present-day climate. The combination of aerial- and vessel-based surveys, acoustic detection, land-based visual detections, traditional knowledge from subsistence hunters, and satellite telemetry have produced a plethora of data, and reasonably fine-scale understanding of habitat use.

Bowhead whales

The current understanding of the distribution of bowhead whales posits that as the winter ice recedes, bowheads in the Bering-Chukchi-Beaufort stock make their way into the Arctic, passing closely by Point Barrow on their way to summer feeding grounds in the Canadian Beaufort Sea. As the summer progresses into fall, bowheads begin a westward migration and feed in nearshore waters of the Canadian and Alaskan Beaufort seas east of Point Barrow. As the fall progresses, whales migrate west past Point Barrow fanning out into the Chukchi Sea before ultimately making their way down into the northern Bering Sea as the ice closes in (Moore and Reeves 1993).

Beluga whales

Belugas are a core, ice-associated, Arctic species (Moore and Huntington 2008). In the ASAMM study area, two distinct stocks are present: the eastern Chukchi Sea, and the eastern Beaufort Sea populations (Hauser et al. 2017). Previous tagging work (Suydam et al. 2005, Suydam et al. 2001) has documented broad scale use of the area, while more recent work has shown that the distribution and habitat features that predict habitat use differ both by stock, and within-stock, by sex (Hauser et al. 2017). For example, Chukchi belugas respond strongly to the Barrow Canyon feature, while Beaufort belugas responded more to Distance to Coast Line and Distance to Ice-Edge covariates. Unfortunately, neither the

gender, nor the stock, can be determined from aerial surveys. Thus, stock-specific response to habitat covariates may be harder to ascertain.

Walrus

Walrus are benthic foragers often seen in great numbers in the Arctic (Fay 1982). They are a core ice-associated species, and are often seen hauled on landfast ice, or pack ice (Jay, Fischbach, and Kochnev 2012, Jay et al. 2017, Moore and Huntington 2008). These aggregations can number in the tens of thousands (Janet Clarke, Leidos Corporation, *pers. comm.*). Their approximate annual cycle is to overwinter in the Bering Sea (Fay 1982), and as ice leads develop, they migrate northward into the northern Chukchi Sea (Jay et al. 2012); recent radio-tagging evidence suggests that, as new ice minimums occur, walrus go farther north (Jay, Fischbach, and Kochnev 2012, Jay et al. 2017). Peak abundance in the northeastern Chukchi Sea is in July and August, which is an area of high benthic productivity (Dunton et al. 2005). As the summer progresses into fall (e.g. September), walrus shift their distribution to the south, although still coastally biased (Jay, Fischbach, and Kochnev 2012). Jay, Fischbach, and Kochnev (2012) have found that walrus are now seen in more open-water habitat with lower ice concentration values than they were during the 1980s.

Gray whales

Gray whales are typically considered to be a sub-Arctic species that use Arctic habitats as ice recedes. They are benthic feeders that migrate into the Chukchi Sea as summer progresses, and tend to use several known hotspots, including the gray whale garden, Hanna shoal, and areas off Point Lay (Clarke, Kennedy, and Ferguson 2016). Gray whales are rarely seen east of Point Barrow.

Seals

There are few synoptic descriptors of the distribution and abundance of pinnipeds other than walrus throughout the Arctic. While the ASAMM survey extends back several decades, from the start it has focused on large whales. Therefore the intensity of collection and identification of seal sightings has varied over the duration of the survey. In addition, most Arctic seals are small and the ASAMM planes fly at high altitudes (Ferguson and Clarke 2013), making identification of these sightings difficult, more so as weather and sighting conditions degrade. Thus, when seals are seen during ASAMM, they tend to be lumped into one of two sighting categories, stratified by size: 1) small unidentified pinnipeds; and 2) unidentified pinnipeds. The species that comprise these two groups include: walrus, bearded seal, ringed seal, and spotted seal. Some span both categories (e.g. a juvenile walrus could be in the small category, while an adult could be in the unidentified category). Bearded seals, because of their unique morphology (big body, small head) tend to be easier to identify to species than other Arctic ice-seal species. There have been aerial surveys for ringed and bearded seals in the Alaskan Beaufort Sea (Burns and Harbo 1972, Burns, Shapiro, and Fay 1981); however, most of the spatial modeling done for these species occurred in the Bering Sea (Bengtson et al. 2005, Conn et al. 2013, Conn et al. 2014, Ver Hoef et al. 2014). And while these surveys have been conducted, they are typically

conducted during the winter-ice period, as opposed to the summertime open-water period. Consequently there have been few attempts to quantify the distribution and abundance of Arctic ice-seals during the ice-free period over broad scale areas. (See Aerts et al. (2013) for an example of a fine-scale analysis of selected ice-seal species.)

Objective

The objectives of this work include: modeling the distribution and abundance of different species/guilds of AMMs, and determining if distribution and abundance can be explained by a complex interaction between what we observe (where the species are, what they are doing, how likely we are to see them, how many individuals there are, and what habitats they are associated with), the quantitative links between the observations and the habitat, and how certain we are of where favorable habitat exists for these different species. All of this is complicated by the fact that a) the timing of yearly patterns of ice distribution dictates what habitat is available, and b) the yearly patterns of ice distribution are changing.

Methods

Here we outline both the species-observation data as well as the analytical techniques and workflow that we have embraced in this project. We begin with a description of the primary dataset available in the region, the 37-year time series of the distribution and abundance of AMMs collected as part of the ASAMM project. This project has been funded over its lifetime by the U.S. Navy, the MMS (now Bureau of Ocean Energy Management [BOEM]), and MML. Though the primary focus of ASAMM has always been bowhead whales, over the decades the ASAMM team has collected data on all AMMs seen in the Chukchi and Alaskan Beaufort seas (**Figure 1**). We refer the reader to the primary and gray literature for details on the survey itself (Moore and Reeves 1993, Clarke, Kennedy, and Ferguson 2016, Ferguson and Clarke 2013). As mentioned in the introduction, there are several other datasets in the area. These include two years of strip-transect aerial surveys for beluga whales and bowhead whales; these surveys were conducted in the Canadian Beaufort Sea by the Canadian Department of Fisheries and Oceans (DFO). In 2013, DFO flew a series of line-transect surveys in the eastern High-Arctic, e.g. off Greenland and Baffin Island. Neither of these two datasets was available to us, and hence were not included here. In addition, there were plane- and vessel-based surveys conducted in the Chukchi Sea; these were part of the oil and natural gas exploration efforts conducted by Shell Oil Company. These are now available on-line through the Alaska Ocean Observing System; however we did not include them during this first phase for two reasons: 1) the spatial and temporal extent of the surveys lies entirely within the ASAMM study area; and 2) the experience and training of the observers varied substantially, which suggested some of the data were of uneven quality (Janet Clarke, Leidos Corporation, *pers. comm.*).

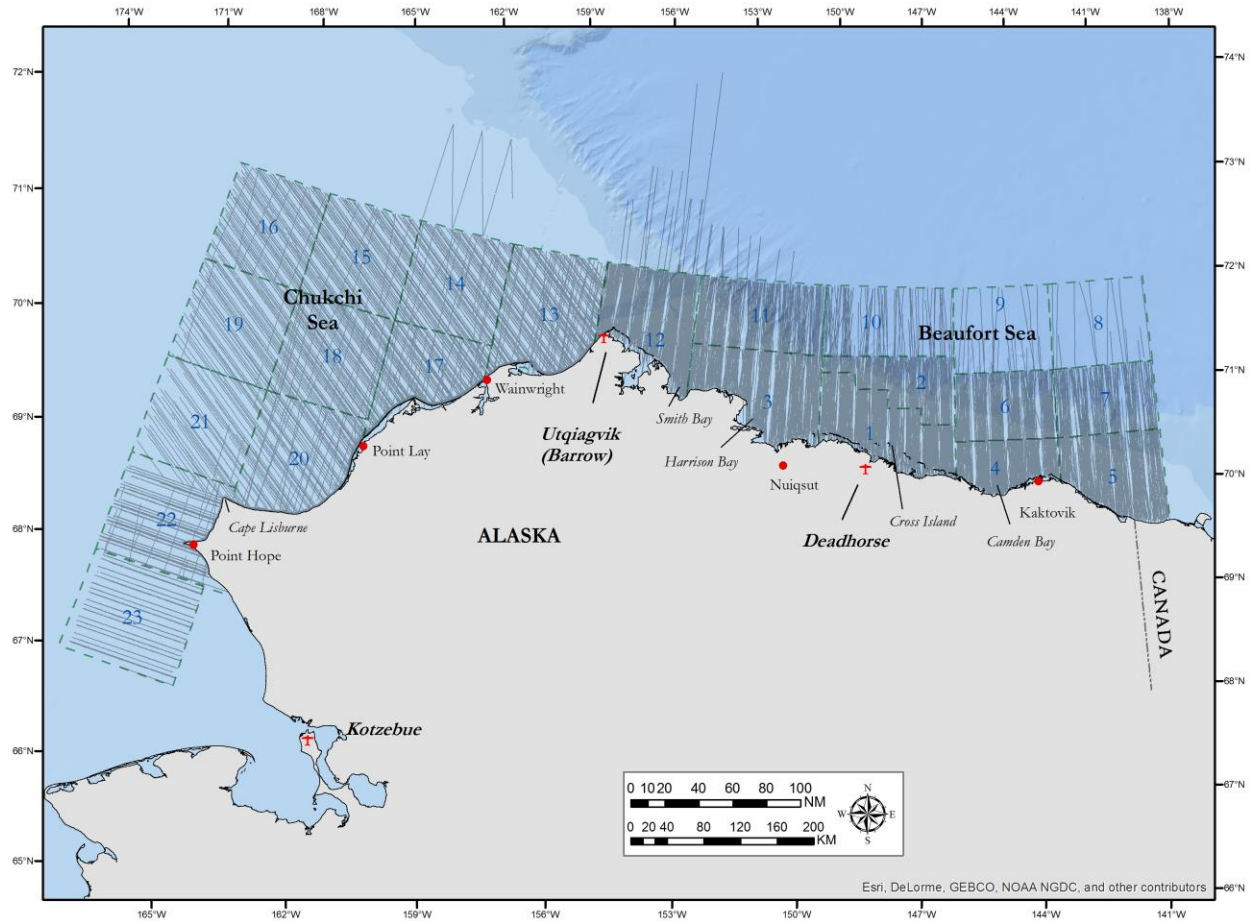


Figure 1. Study area of the ASAMM project with individual survey transect lines depicted in light gray. Some survey blocks (e.g., 8, 9, and 10) are less well surveyed.

The four steps of our analytical process are:

1. Review and clean the aerial survey data.
2. Fit species-specific detection functions to the observed data.
3. Fit Generalized Additive Models (GAMs) to explain the relationship between species abundance and environmentally relevant predictor variables.
4. Use these fitted relationships to predict the species-specific density of animals across space.

Data Summary

ASAMM has been active since 1979; we are using a more recent subset of these data as part of this analysis--including 2000 through 2016. The reason for this is three-fold. First, the U.S. Navy wishes to predict density close to “modern-day,” under the assumption that patterns may have changed significantly over the past 30+ years. Second, 2000 is seen as the approximate start of the “new-normal” environmental conditions in the Arctic (Jeffries, Overland, and Perovich 2013). Third, the Arctic is changing rapidly (Moore and Huntington

2008); given that change it makes sense to model species-environment relationships under existing conditions. Though these conditions are likely to change in the future, by modeling with data observed more recently, we hope to capture extant relationships.

In broad terms, the aerial surveys are flown in the summer and early fall, from July through October. The protocol follows standard line-transect methodology, and covers a consistent set of survey blocks in the Chukchi and Beaufort seas (**Figure 1**).

Here we briefly summarize the data collected as part of the ASAMM project. We first enumerate the survey effort by year, and then provide five tabular summaries of the on-effort observation data (**Tables 1-6**). Following the tabular summaries, we show the spatial extent of species-specific sightings (**Figures 2-9**).

Table 1. Summary of survey effort, by year, in the ASAMM database from 2000-2016. The Length column represents the cumulative on-effort tracklines covered in 1,000s of kilometers.

Year	Length (1,000 km)
2000	31.43
2001	25.93
2002	41.44
2003	26.81
2004	41.85
2005	26.51
2006	36.31
2007	25.91
2008	138.15
2009	211.60
2010	190.74
2011	318.40
2012	446.16
2013	318.96
2014	360.80
2015	405.49
2016	473.21
Total	3,119.70

Table 2. Summary of survey effort during 2000-2016 split out over each of the four main survey months. Values are in 1,000s of km, and represent the cumulative on-effort distance covered on the trackline.

Year	July	August	September	October	Total
2000	NA	NA	19.66	11.77	31.43
2001	NA	NA	17.42	8.50	25.92
2002	NA	24.28	14.84	2.31	41.43
2003	NA	NA	19.65	7.15	26.80
2004	NA	NA	32.89	8.96	41.85
2005	NA	NA	14.82	11.69	26.51
2006	NA	NA	24.55	11.77	36.32
2007	NA	NA	17.67	8.23	25.90
2008	4.73	32.77	41.30	40.86	119.66
2009	36.01	26.19	85.88	55.12	203.20
2010	51.77	28.68	65.97	44.33	190.75
2011	40.23	68.12	140.43	36.50	285.28
2012	109.20	122.46	114.26	96.96	442.88
2013	72.03	114.39	108.63	23.91	318.96
2014	81.27	103.05	97.21	79.27	360.80
2015	64.97	100.49	149.70	90.33	405.49
2016	110.56	129.49	146.64	86.52	473.21
Total	570.77	749.92	1,111.52	624.18	3,056.39

Table 3. Summary of sightings during 2000-2016. Sightings represent the cumulative number of individuals sighted while on-effort.

Species or Guild	Sightings
Baleen Whales	66
Bearded Seals	171
Beluga Whales	2,431
Bowhead Whales	1,637
Gray Whales	775
Small Pinnipeds	4,436
Unidentified Pinnipeds	520
Walrus	2,128
Total	12,164

Table 4. Summary of sightings by species (whales) and year during 2000-2016. Sightings represent the cumulative number of individuals sighted while on-effort for a given year.

Year	Bowhead Whales	Beluga Whales	Gray Whales	Baleen Whales	Total
2000	30	13	1	NA	44
2001	12	22	2	NA	36
2002	29	82	0	NA	111
2003	39	62	0	NA	101
2004	88	60	0	NA	148
2005	33	38	0	NA	71
2006	58	33	4	NA	95
2007	48	5	1	NA	54
2008	55	8	19	NA	82
2009	62	44	90	NA	196
2010	78	15	40	NA	133
2011	41	170	99	2	312
2012	156	355	97	15	623
2013	141	288	56	6	491
2014	200	590	133	9	932
2015	185	395	76	20	676
2016	382	251	157	14	804
Total	1,637	2,431	775	66	4,909

Table 5. Summary of sightings by species (pinnipeds) and year during 2000-2016. Sightings represent the cumulative number of individuals sighted while on-effort for a given year.

Year	Walrus	Bearded Seal	Small Pinniped	Unidentified Pinniped	Total
2000	NA	NA	NA	NA	0
2001	NA	NA	NA	NA	0
2002	NA	NA	NA	NA	0
2003	NA	NA	NA	NA	0
2004	NA	NA	NA	NA	0
2005	NA	NA	NA	NA	0
2006	NA	NA	NA	NA	0
2007	4	NA	NA	NA	4
2008	21	24	NA	2	47
2009	89	32	179	13	313
2010	162	2	230	59	453
2011	459	44	638	43	1,184
2012	288	6	688	99	1,081
2013	240	42	542	63	887
2014	141	4	618	65	828
2015	269	7	712	106	1,094
2016	455	10	829	70	1,364
Total	2128	171	4,436	520	7,255

Table 6. Summary of sightings during 2000-2016 by species/guild and month. Sightings represent the cumulative number of individuals sighted while on-effort.

Species or Guild	July	August	September	October	Total
Baleen Whales	9	30	23	4	66
Bearded Seals	42	35	57	22	156
Beluga Whales	677	762	636	337	2,412
Bowhead Whales	75	342	874	342	1,633
Gray Whales	278	261	151	63	753
Small Pinnipeds	919	1,403	1,179	858	4,359
Unidentified Pinnipeds	124	128	166	83	501
Walrus	528	644	691	148	2,011
Total	2,652	3,605	3,777	1,857	11,891

Bowhead Whales

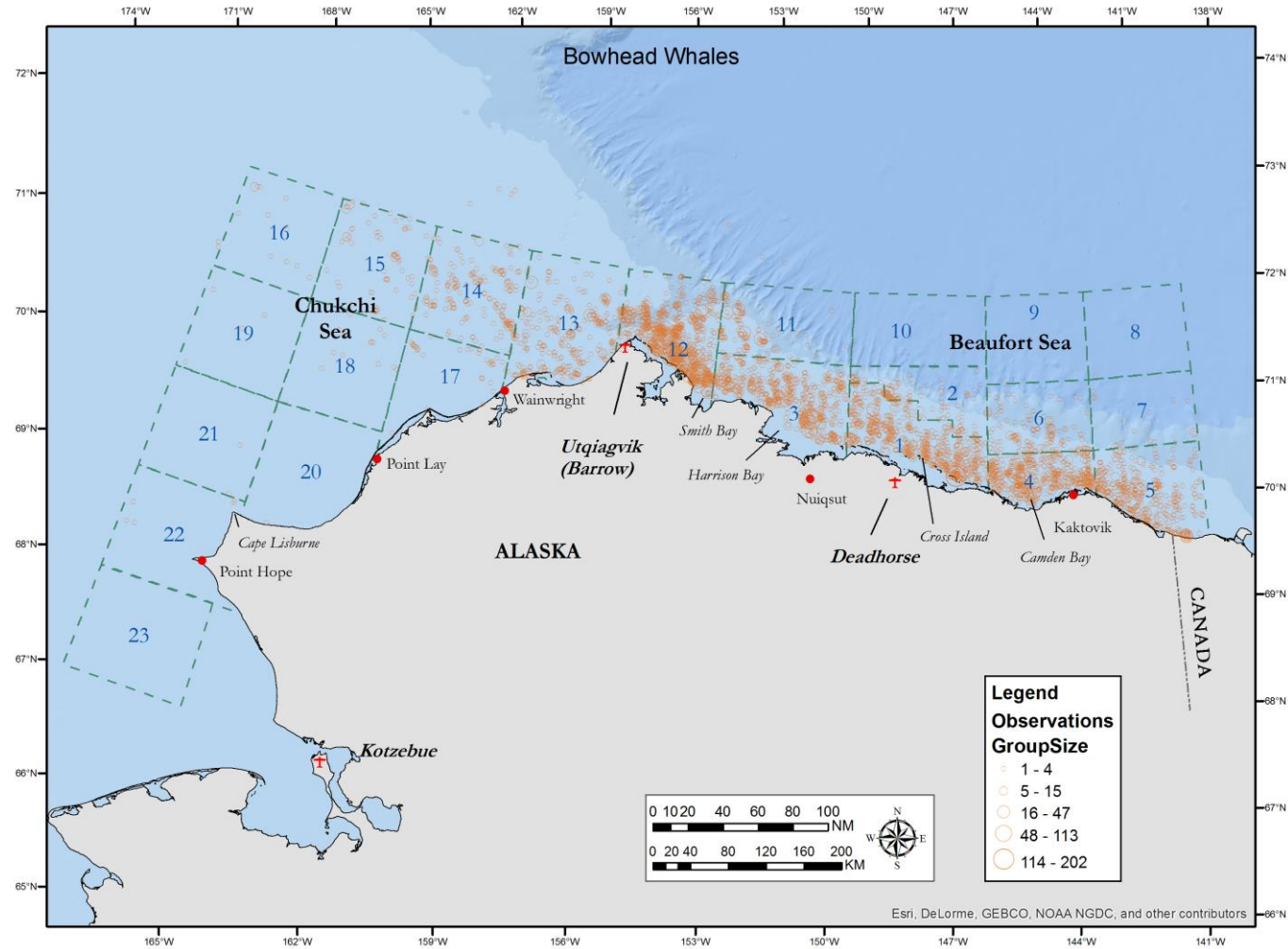


Figure 2. All on-transect sightings of bowhead whales (*Balaena mysticetus*) in the ASAMM study area. Bowheads were primarily seen nearshore in the Alaskan Beaufort Sea. Note the high number of sightings of bowheads east of Point Barrow.

Beluga Whales

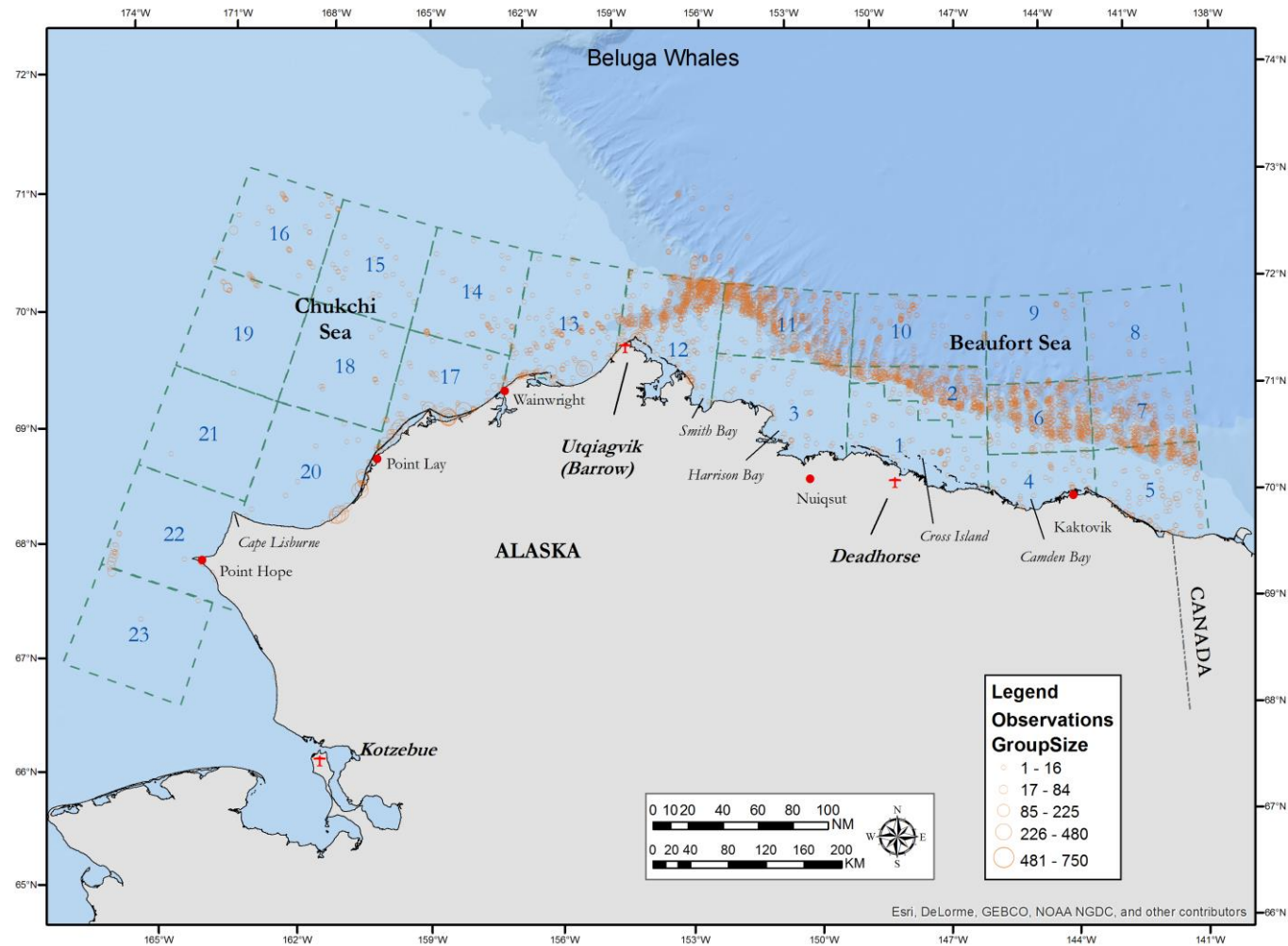


Figure 3. All on-transect sightings of beluga whales (*Delphinapterus leucas*) in the ASAMM study area. In contrast to bowheads, belugas were seen farther offshore in the Alaskan Beaufort Sea. Note the especially high number of sightings northeast of Point Barrow. Large groups were also seen quite near the shore in the Chukchi Sea between Cape Lisburne and Wainwright.

Gray Whales

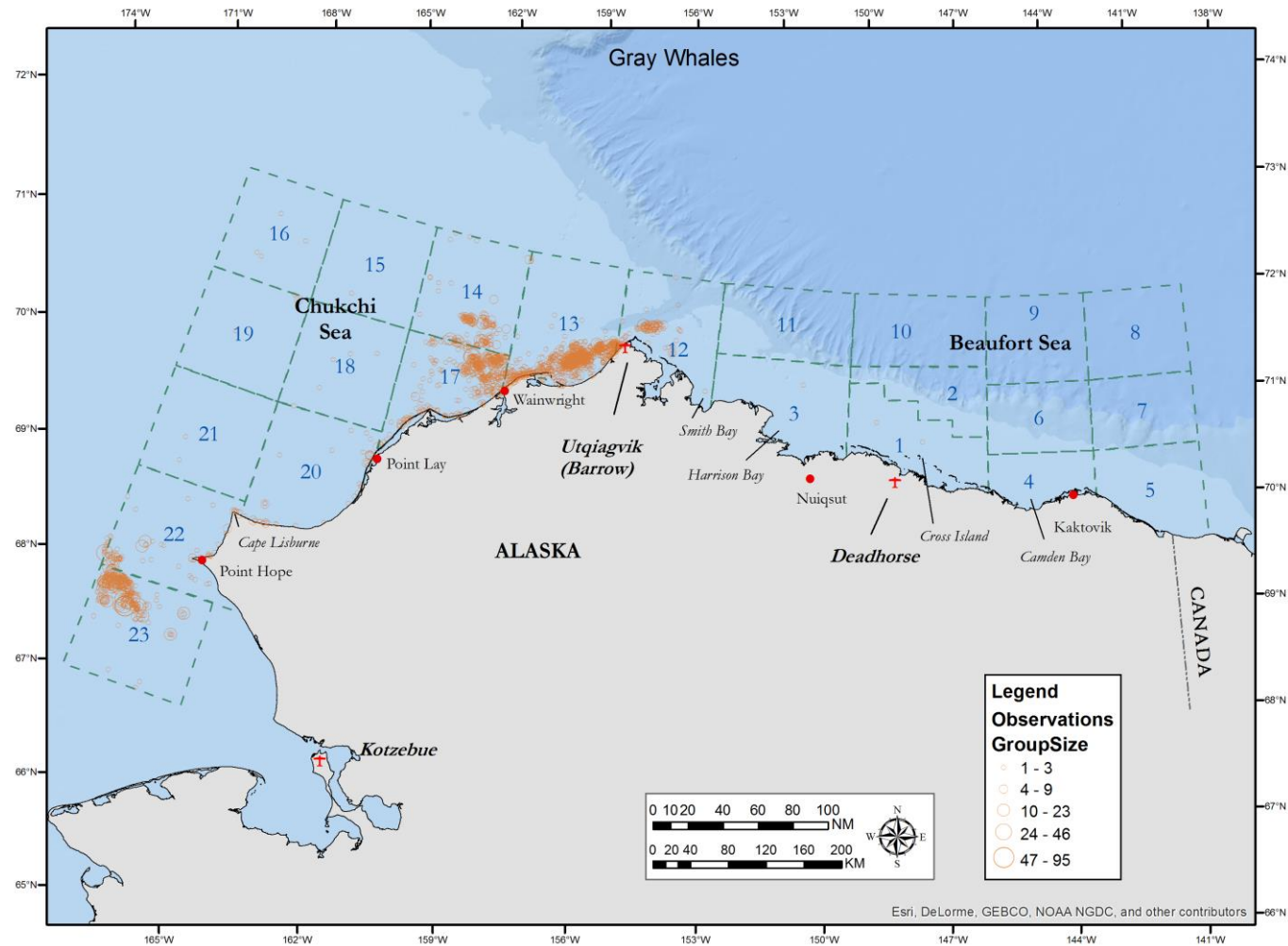


Figure 4. All on-transect sightings of gray whales (*Eschrichtius robustus*) in the ASAMM study area. Very few gray whales were seen east of Point Barrow in the Alaskan Beaufort Sea. Most whales were seen west of Point Hope, and in the so-called “gray whale garden” north and east of Wainwright, Alaska.

Walrus

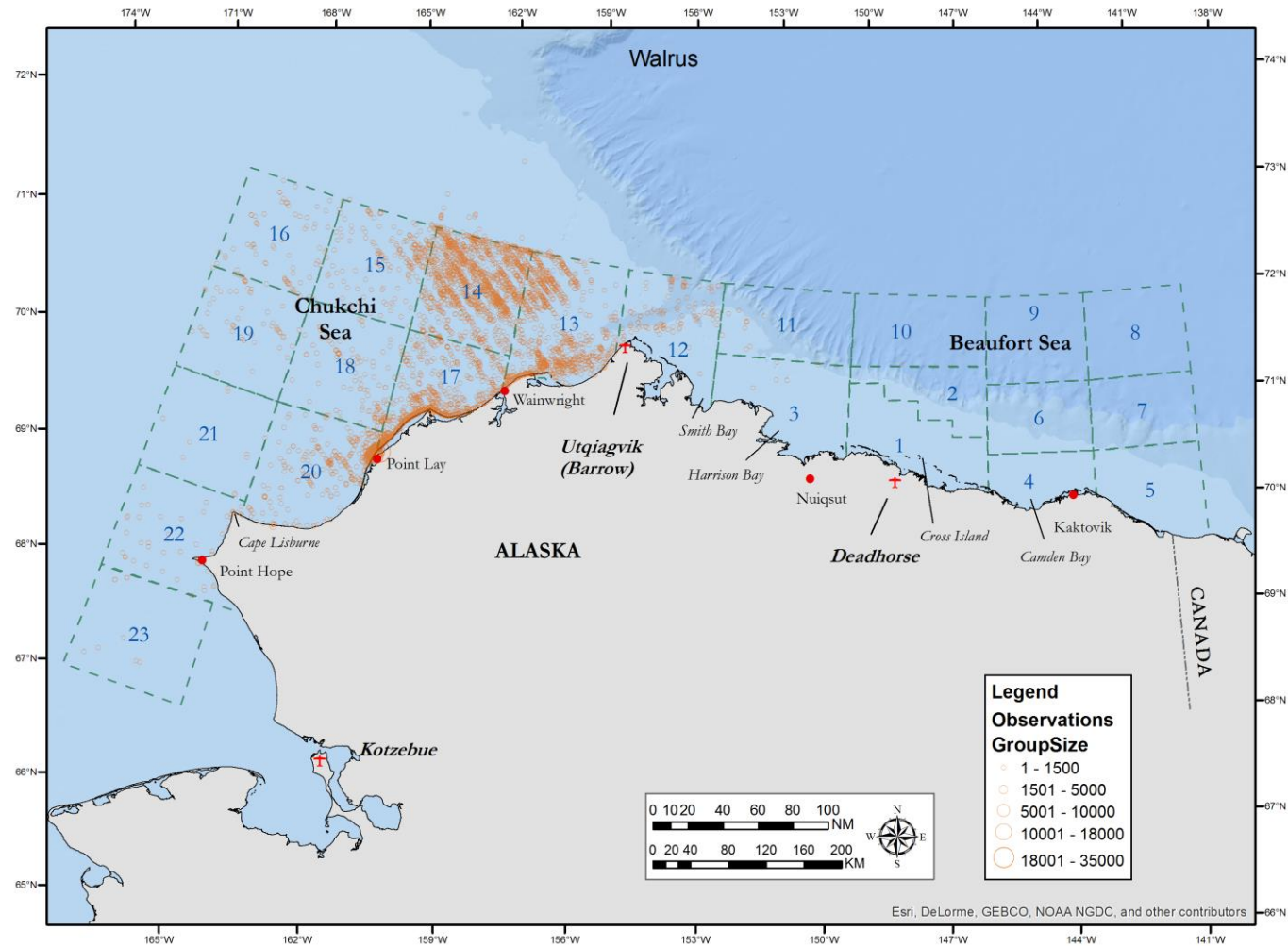


Figure 5. All on-transect sightings of walrus (*Odobenus rosmarus*) in the ASAMM study area. Very few walrus were seen east of Point Barrow in the Alaskan Beaufort Sea. Most walrus sightings were either coastal, or located in Hannah Shoal in the Northeast Chukchi Sea (Block 14).

Bearded Seals

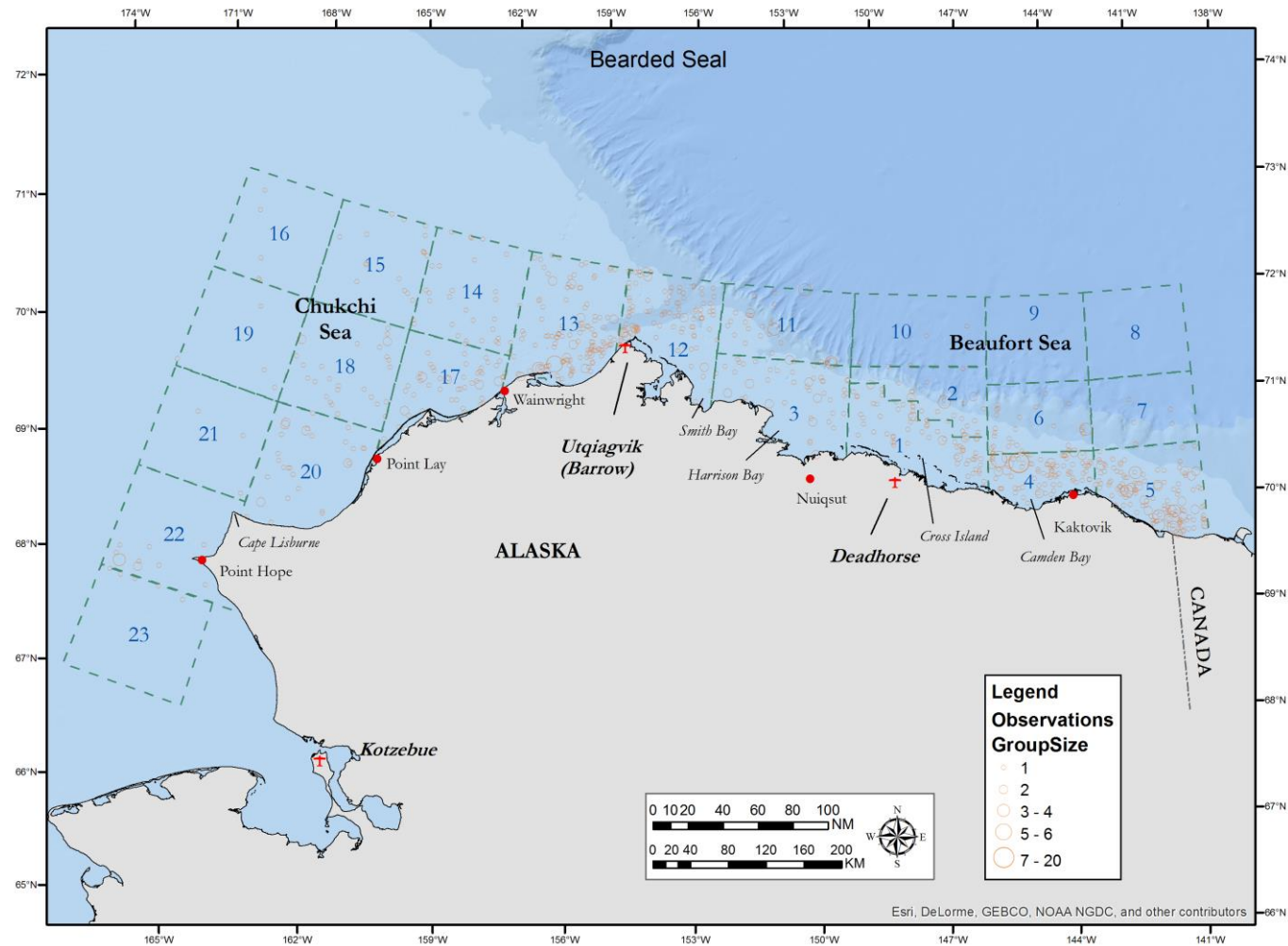


Figure 6. All on-transect sightings of bearded seals (*Erignathus barbatus*) in the ASAMM study area. While they were seen throughout the study area, bearded seals seemed biased toward shallower waters, especially in the Alaskan Beaufort Sea.

Small Pinnipeds

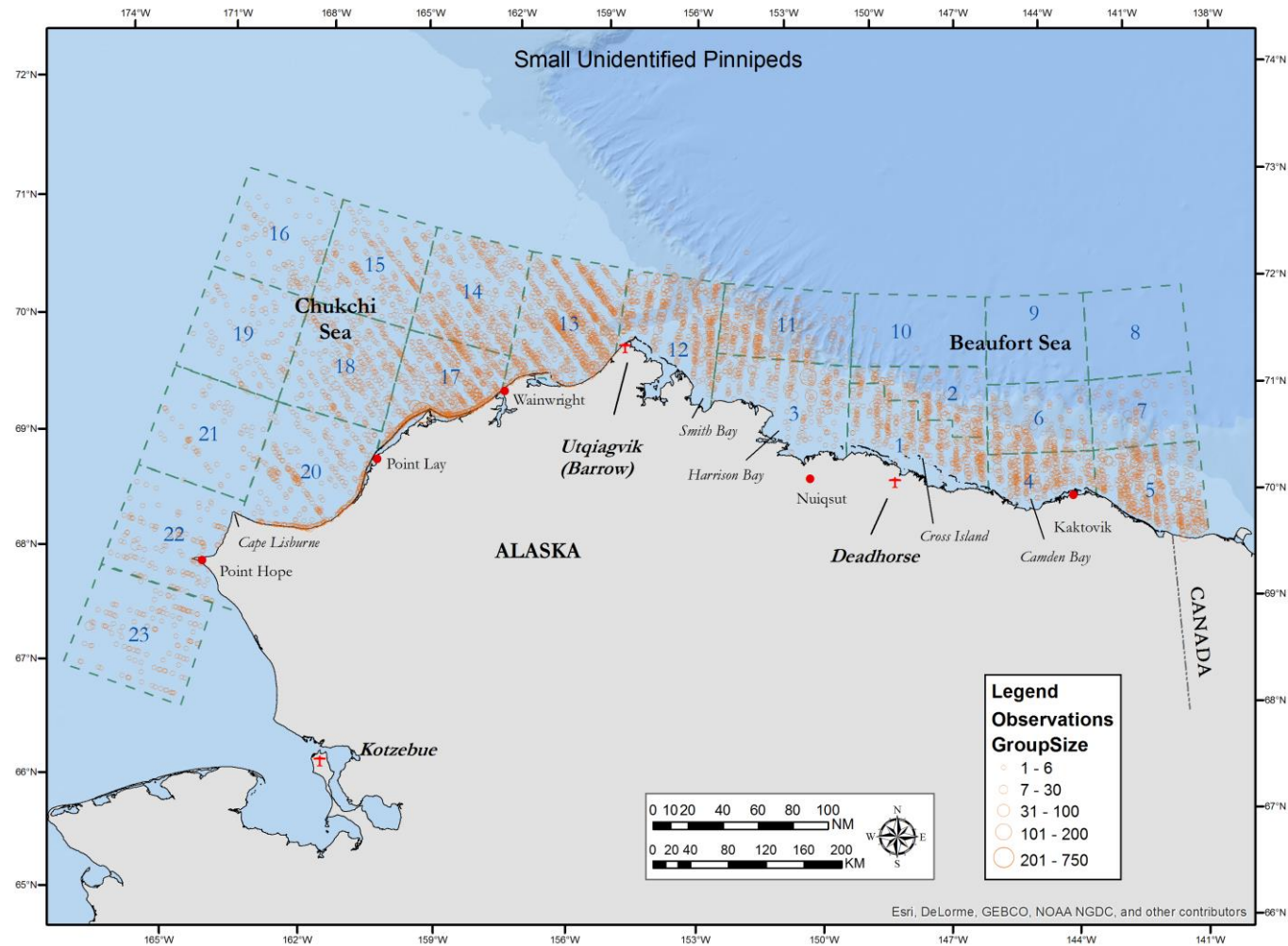


Figure 7. All on-transect sightings of small pinnipeds in the ASAMM study area. As with bearded seals, locations of small pinnipeds were biased toward shallower waters, especially in the Alaskan Beaufort Sea, where relatively few were seen deeper than the shelf-break.

Unidentified Pinnipeds

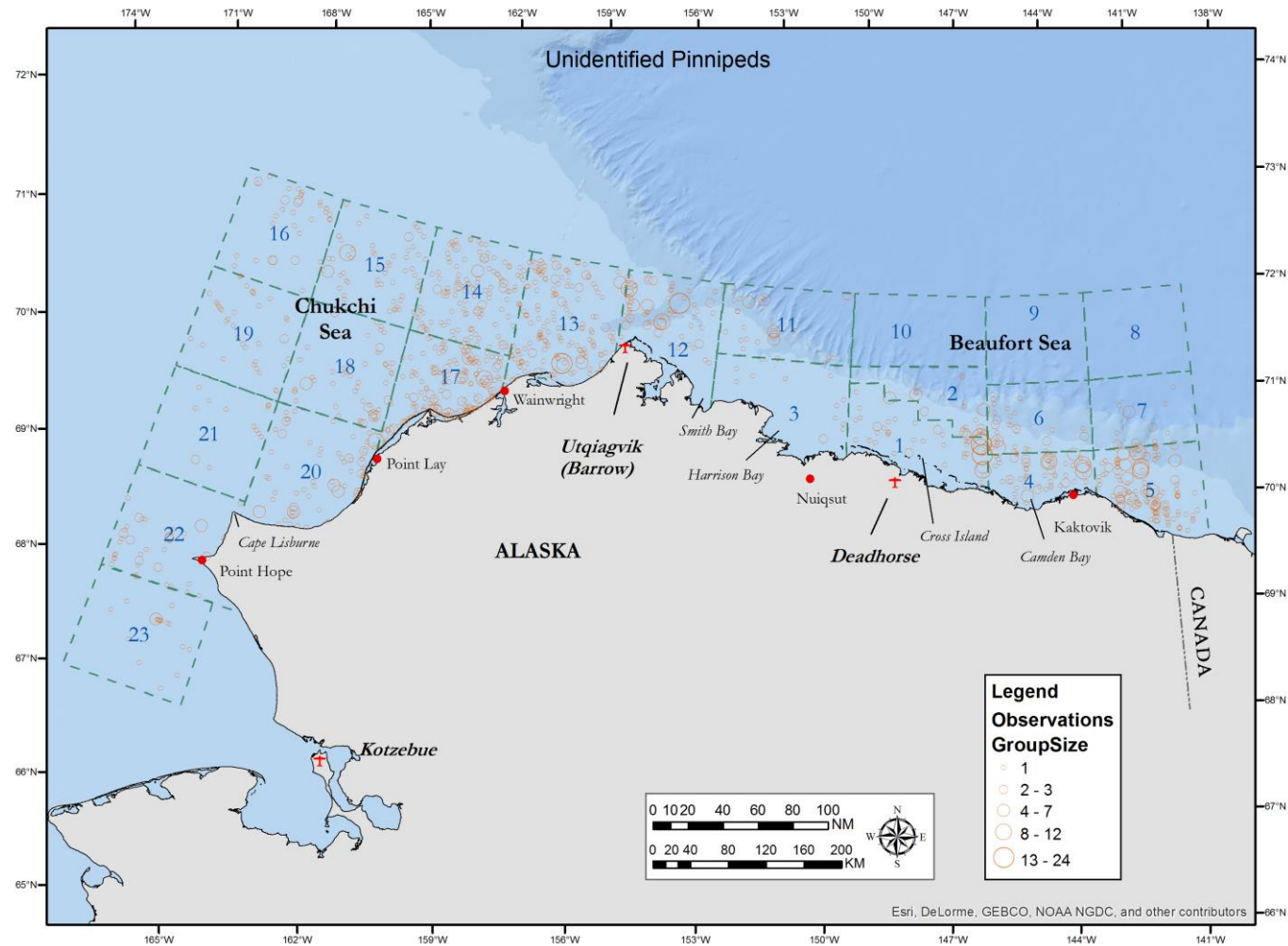


Figure 8. All on-transect sightings of unidentified pinnipeds in the ASAMM study area. The sighting patterns were very similar to that of small unidentified pinnipeds.

Baleen Whales

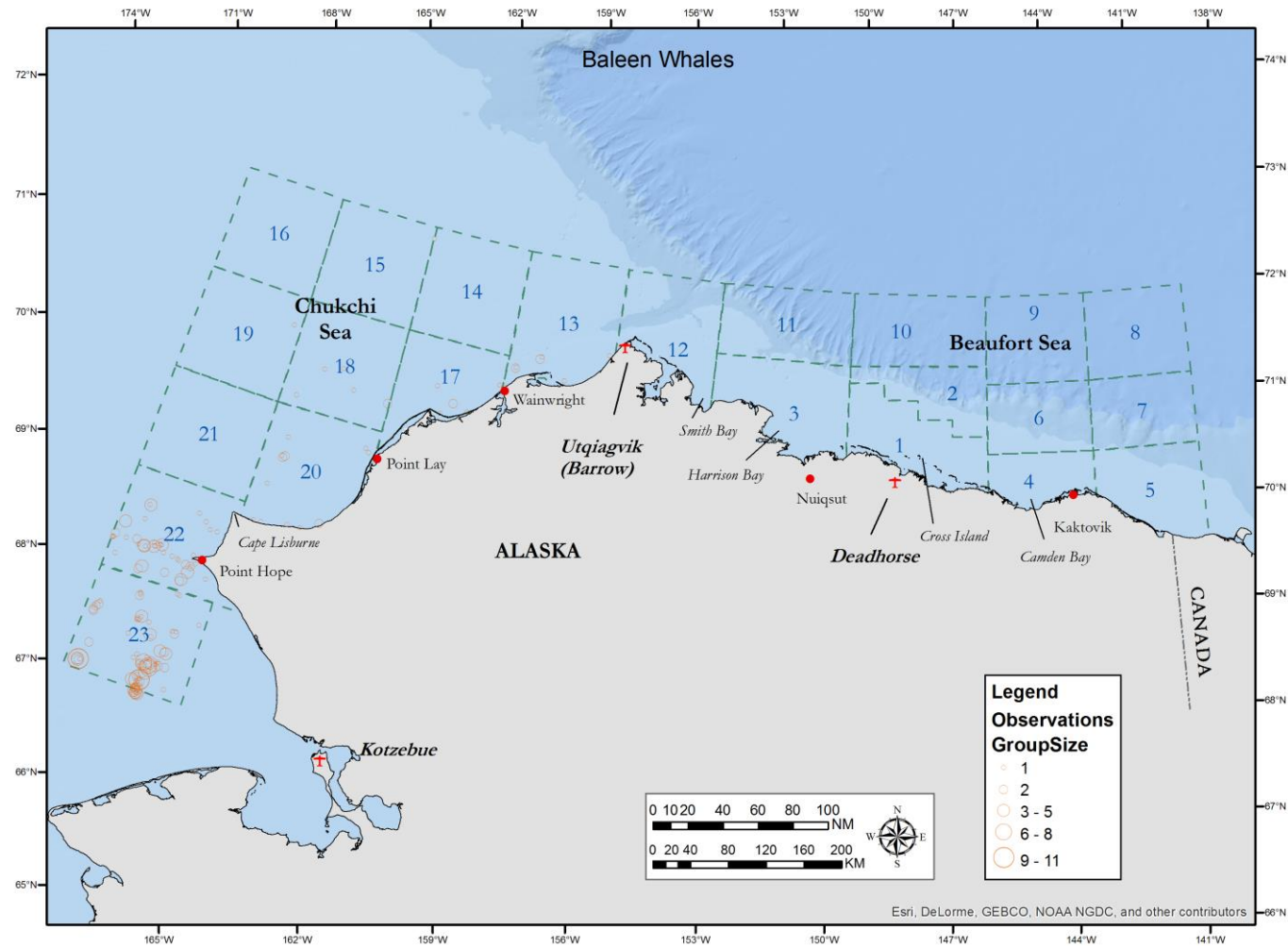


Figure 9. All on-transect sightings of the three species that comprise the baleen whale guild--fin whales (*Balaenoptera physalus*), humpback whales (*Megaptera novaeangliae*), and minke whales (*Balaenoptera acutorostrata*). There were no sightings of these sub-Arctic migrants in the Alaskan Beaufort Sea; most whales were seen in the southern Chukchi Sea near Point Hope.

Data Cleaning

The data provided by our collaborators at MML were in very good condition. However, to be consistent with previously established workflows for density products delivered to the U.S. Navy, we followed the process outlined in (Roberts et al. 2016). In particular, we used a custom-built ArcMap interface that allowed for screening of the ASAMM data at a daily level. This interface allows us to load one day's worth of survey effort, along with the sightings, and check and flag errors on a transect-by-transect basis. Most errors were small, and included such things as going off-effort late, or resuming a transect early. For example, when the plane breaks the transect to circle a group of large whales, they make the breakpoint with a time- and location-stamp. This is critical for meeting the Distance sampling assumptions of each individual transect. In most cases, these “break-transect” and “resume-transect” points are consistently noted; however in some small instances we detected fixable anomalies. These were edited in ArcMap, and custom Python code was run to update the sightings.

Throughout the data editing and cleaning phase, Schick and Roberts reviewed the events that had been flagged and resolved them. When more complicated events arose, we met with MML collaborators to review them and incorporate their suggested changes. An example of a more complicated edit/instance often arose when the plane broke survey to circle a sighted group. We kept detailed [processing notes](#) that described the steps we used to work through the data. Depending on the size of the group, and the time spent circling, the observers can often detect and observe new sightings while circling. Based on how far the group was from the initial sighting that led to breaking transect, and whether the species were similar or different, we encountered potentially ambiguous instances that required more input and consultation from data providers. While going through this process, we kept the original raw data file (a Microsoft Access database) as we received it from MML, and then worked with and produced edited working versions of the database. The final database we are using will be sent back to MML for their record-keeping.

Data Modeling -- Detection Functions

Once the data were cleaned and edited, we fitted detection functions. We followed standard Distance sampling approaches (Buckland et al. 2015) to the data:

1. We generated a histogram of perpendicular distance of on-transect sightings from the trackline.
2. We inspected these for initial outliers, quality assurance and quality control (see below for details).
3. We fitted initial detection functions to these data to check if left and right truncations were needed.
4. We incorporated the sighting-level covariates (**Table 7**) and using custom-Python code (Roberts et al. 2016), we applied multiple-covariate distance sampling techniques to iterate over all possible combinations of detection function models.
5. We reviewed the output from each model, and kept a final model (see below).

*Table 7. Summary table highlighting the final model for the detection function we chose for each species.**

Species	Platform	Key	Covariates
Bowhead Whales	MMS Otter	HR	Beaufort, Ice % Observed, Log Group Size, Observer
	MML Otter	HR	Group Size
	Commander	HR	Beaufort, Log Group Size, Glare
Beluga Whales	MMS Otter	HN	Depth Observed, Max Visibility
	MML Otter	HN	Max Visibility
	Commander	HR	Beaufort, Depth Observed, Longitude, Max Visibility, Glare
Gray Whales	MMS & MML Otter	HN	Max Visibility
	Commander	HR	Depth Observed, Group Size, Glare
Walrus	MML Otter	HR	Beaufort, Group Size
	Commander	HN	Beaufort, Group Size, Longitude, Glare
Bearded Seals	MML Otter	HN	Depth Observed
	Commander	HR	Longitude
Small Pinnipeds	MML Otter	HN	Glare
	Commander	HR	Beaufort, Ice % Observed, Log Group Size, Longitude, Glare
Unidentified Pinnipeds	MML Otter	HR	Beaufort
	Commander	HN	Max Visibility, Glare
Baleen Whales	Commander	HN	Common Name

*Definition of Terms: MMS = Minerals Management Service; MML = Marine Mammal Laboratory; HR = hazard rate; HN = half-normal; Beaufort = Beaufort Sea State in the field of view; Observer = which observer was in the plane; Depth Observed = bathymetric value of the sighting; Max Visibility = how far the observers can see; Glare = presence/absence of glare on the ocean surface; Ice % observed = % ice cover on the ocean surface; and Common Name = factor covariate for species (fin whale, humpback whale, and minke whale)

As with the data cleaning component, all of this work is supported with a custom Python library (Roberts et al. 2016). The library facilitated iterating over all possible combinations of models and covariates, occasionally leading to hundreds of possible detection functions to choose from. In our workflow we chose and then used, one “best” detection function,

which typically had the lowest Akaike information criterion (AIC) value. Because there were up to several hundred candidate models, this implies that not all of the uncertainty in detection is fully accounted for in subsequent modeling stages. We will return to the exploration and ramification of this in the Discussion section; this issue will be more fully explored in the DenMod working group (Funded by Living Marine Resources program, under the Broad Agency Announcement (BAA), solicitation N39430-16-R-7201).

Sighting Hierarchies by Platform

During steps one and two, we used a detection hierarchy to build up the fitting of the detection functions. This was built on software originally meant for displaying and interacting with phylogenetic data (<http://etetoolkit.org/>). In lieu of phylogenies, we had detection hierarchies built for the three different platforms: 1) MML Aero Commander; 2) MML Twin Otter; and 3) MMS Twin Otter. Within each survey platform, we had different numbers of survey years; within each year we had different numbers of sighted individuals **Figure 10**. (Note that we build one of these hierarchies for each species; the remaining plots are shown in **Appendix A**.) Using this approach, we interactively assigned covariates and truncation patterns to each of the three nodes/platforms. With color-coding available at the node and leaf level, we could also quickly see if a given platform or species had too few sightings and were highlighted in red. In these cases, the leaves may be aggregated up one platform level, e.g. lumping both Otters together, or lumping a few species together, e.g. lumping the minke, humpback, and fin whales together. While we lumped across the Otter platform, we did not lump the Otters in with the Commander, owing to their very different sighting configurations, i.e. different bubble windows. These differing configurations lead to different detection functions (Ferguson and Clarke 2013). Thus, for all species/guild combinations we were able to fit detection functions.

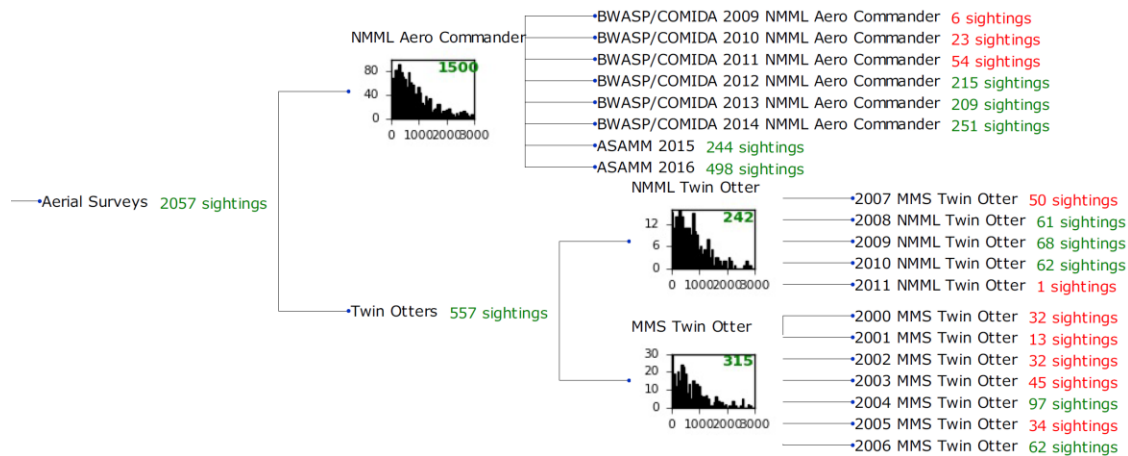


Figure 10. Hierarchical structure of the number of bowhead whale sightings by year and by platform. Sightings colored in red are below the 60 sighting group threshold suggested in Buckland et al. (2001) as the threshold needed to fit a detection function.

Multiple Covariate Distance Sampling

In steps one and two, we could view the histograms together with the phylogenies to arrive at a cohesive set of possible detection functions to be fit to the observed data. For example, in cases where there were relatively few sightings within a species, we chose to fit multiple covariate Distance sampling (MCDS) models limited to one covariate at a time. We were also able to restrict the observations used in the fitting process (e.g., excluding walrus seen hauled-out on-land, or excluding observations seen in very high Beaufort Sea State). These threshold values were species-specific. For example, we had a higher Beaufort Sea State cutoff for bowhead whales than for beluga whales. These decisions were made in consultation with Megan Ferguson (MML) and Janet Clarke (Leidos Corporation).

During the detection-function-fitting stage, we started with the candidate set of MCDS sighting covariates outlined by Ferguson and Clarke (2013). After initial fitting, we reviewed plots of observed distances against these covariate values, and in many cases revised the candidate set in a few different ways. This was done in an effort to capture different expected types of behavior in different areas. For example, in trying to fit depth as a sighting covariate; we initially tried the untransformed depth values, but also experimented with different categorical implementations of depth (e.g. nearshore, shelf, basin). We performed a similar task with longitude, using the longitude at the sighting, and using binned versions of longitude, e.g. east/west of Point Barrow. An additional way we iterated through the model-fitting process, was to explore the use of different binning levels (e.g., four longitude bins versus two). Finally, in a few cases, typically those with lower numbers of sightings and/or from older survey platforms, we found that the model with the lowest AIC value was not always the best-fit model in aggregate. In summary, we used several criteria to select the best model, including: the number of sightings, covariates that may impact sightability, survey platform, AIC, tests of goodness of fit, and visual observation of the fit of the detection function to data.

Availability Bias— $g(0)$

Unfortunately, there are no ASAMM-study-specific estimates of availability bias. However, there are some smaller-scale studies within the Beaufort Sea for bowhead whales (Robertson et al. 2015). For the other AMM species that had estimates from the published literature, we used those. For some species, no published values exist. The species-specific summaries are in **Table 8**.

Table 8. Species-specific availability bias values used to correct the observed group size estimates into final abundance values used in modeling. If no correction was available, we used a g(0) estimate of 1.

Species	Group Size	g(0) Estimate	Source
Bowhead Whale	1	0.211375	(Robertson et al. 2015)
	2-4	0.281	(Robertson et al. 2015)
	>4	1	(Robertson et al. 2015)
Beluga Whale	Any	0.5405	Lowry et al. (Janet Clarke, Leidos Corporation, <i>pers. comm.</i>)
Gray Whale	Any	0.95	(Forney and Barlow 1998)
Walrus	1	0.365	(Heide-Jørgensen et al. 2014)
Bearded Seal	Any	1	No Source
Small Pinniped	Any	1	No Source
Unidentified Pinniped	Any	1	No Source
Baleen Whale	Any	0.95	(Forney and Barlow 1998)

Data Modeling -- Processing and Preparation of Environmental Covariates

We sought to explain the observed abundance on a species-by-species level. We did this with a combination of static and dynamic predictors thought to influence the distribution of the different species (**Tables 9, 10**). This predictive relationship was quantified, not at the sightings level, but at the segment level. Segments are sub-sections or portions of an individual transect leg. Custom-written Python code (Roberts et al. 2016) was used to partition the tracks into 10-kilometer segment lengths. Each segment had from 0 to many sightings of different AMMs, each with an estimate of group size. From the entire segment database, we made copies corresponding to the number of species/guilds we modeled. For example, starting with one set of segments with observed abundance of bowhead whales, beluga whales, and gray whales, we created three separate copies, one for each of the three species. Then we incorporated information from the species-specific detection functions to effort-correct the observed abundance values for each species (Miller et al. 2013, Hedley and Buckland 2004). At the end of this process, we had eight different sets of segments for each of the eight AMM species or guilds we modeled. In each of these datasets, each segment had the original observations along with an effort-corrected/adjusted final abundance value for the entire segment.

In addition to correcting the abundance, we used ArcGIS to spatially and temporally co-locate the values of different environmental covariates (expressed as static or dynamic raster grids) to the centroid of each segment. We used a combination of static and temporally dynamic rasters (**Tables 9, 10**). All of the covariate rasters were projected to a common Albers equal area projection at a cell size of 10 square kilometers.

*Table 9. Summary of the static covariates used in the density surface prediction.**

Covariate Name	Measurement Units	Source
Depth	Meters	SRTM 30
Slope	% rise in degrees	Derived from Depth, SRTM 30
Distance to Coast Line	Meters	Derived from ESRI Basemap
Distance to 200m Isobath	Meters	SRTM 30
Distance from Barrow Canyon	Meters	Lat/Long Derived from ESRI Base Map
x raster	Projected Eastings (meters)	MGET Toolbox using spatial extent of study area
y raster	Projected Northings (meters)	MGET Toolbox using spatial extent of study area

*Acronyms are as follows. SRTM refers to Shuttle Radar Topography Mission. ESRI refers to Environmental Systems Research Institute. MGET refers to the Marine Geospatial Ecology Toolbox.

Table 10. Summary of the dynamic environmental predictors used in the GAM analysis.

Covariate Name	Measurement Units	Source
Ice Concentration	% ice cover/cell (0-100)	NSIDC*
Distance to Ice Edge	Meters	NSIDC

*National Snow and Ice Data Center

For the dynamic ice covariates, we started with raw monthly GeoTIFFs from the National Snow and Ice Data Center (NSIDC). The ice concentration required a few minimal map algebra processing steps to convert the GeoTIFFs into a usable ice concentration raster. We created the distance to ice-edge raster by starting with the raw ice-extent GeoTIFF from NSIDC. These rasters have three values: land, ice, and no-data. We masked the land, and used the Euclidean Distance algorithm to create monthly rasters that represented the distance to the ice edge.

For all static or dynamic rasters, we used the Extract by Mask tool in ArcGIS with a snap raster in order to assure a common spatial extent. With the rasters prepared, we then sampled all of the environmental data onto the species-specific segments. This final step prepared us for modeling the observed abundance as a function of the environmental predictors.

Data Modeling -- Generalized Additive Models

We used GAMs to build the quantitative relationship that explains the observed abundance at the segment level. The workflow was consistent across each species, and proceeded as follows. Once the environmental predictors were sampled and associated with each segment, we began fitting exploratory models. The full model we started with for each species related abundance to the environmental variables using the candidate set of predictors outlined above. We used a bivariate spatial smooth for the x and y rasters, and for each of the smooths we started with a thin plate spline. For the spatial smooth, we also explored using a soap film smoother, but will address that when we discuss the bowhead models. We used the R package `mgcv`, and an initial model setup could be fit using this *example* R code:

```
dsm_nb_Full <- gam(Abundance ~ offset(log(Area)) +
  s(x, y, bs = 'ts') +
  s(Depth, bs = 'ts') +
  s(Slope, bs = "ts") +
  s(d200m, bs = "ts") +
  s(d2coast, bs = "ts") +
  s(d2barrowCanyon, bs = 'ts') +
  s(d2iceEdge, bs = 'ts') +
  s(iceConcentration, bs = "ts"),
  data = obs, family = nb())
```

In this *example* code, the first six predictor variables are static, while the last two ice-related variables are dynamic at a monthly temporal resolution. The offset term accounts for the fact that not all of the segments are equal length. We used a Negative Binomial family throughout based on input from MML collaborators.

Prior to model fitting, we constructed an exploratory data analysis to determine the levels of correlation among the explanatory predictor variables. The covariates representing spatial values, i.e. the x and y rasters, exhibited correlation with some of the individual static predictors. Despite this, we included them in the model as we wanted to account for spatial structure, and because the canonical base model to experiment with is one with only a spatial smooth (Buckland et al. 2015). Two additional high correlations ($> \text{abs}[0.5]$) were between the Depth and Slope covariates, and the two ice rasters. Based on this exploratory analysis, we excluded Slope from the models; however, we chose to keep both ice covariates in the model. We did this because the rasters are dynamic, and because while related, the rasters do express two different characteristics/representations of ice as a possible explanatory covariate.

Following the exploratory analysis, the modeling workflow continued with examining the initial output for model fit, significance and shape of individual smooth terms, percent deviance explained, and the REML (Restricted Maximum Likelihood) score. At this point, we dropped predictor terms that were insignificant, and refit a model of reduced dimensionality. We iterated through this procedure on a species by species until we reached a final model. Typically this final model only contained significant smooth terms (though there were exceptions).

Following an initial review of the models by regional and taxonomic experts in May 2017, we noted a few issues to explore further. First, and foremost, experts noted that for bowheads in particular, there were a few embayments (Smith Bay and Harrison Bay) where the predicted density for bowheads was high, even when few sightings had been noted. To address this, we followed Wood, Bravington, and Hedley (2008) and built a soap film smoother to replace the bivariate spatial smooth from the initial model $s(x, y, bs = 'ts')$. We then took the final model, and replaced the bivariate smoother with the soap film smoother.

Final model selection for all species was based on these criteria:

- the known biology of the species
- the significance of the smooth terms
- AIC, and relative AIC score
- REML scores
- the percent deviance explained by the model.

Data Modeling -- Density Prediction

Entering this phase of the analysis, we had two primary results - the detection function models fit to each species/guild/platform combination, and the GAM fit for each species and/or taxonomic grouping. The final phase of the modeling process was to use the GAM output to predict species density across both space and time.

Temporal Dimensions

We used 17 years of data to do the model fitting. This 17-year dataset was combined across years to produce a climatology, or densitology (Redfern et al. 2006). In addition, we produced density surfaces for July, August, September, and October. These densitologies represent the modern day density surface for each of the eight species/guild combinations. Though the climate has undergone significant changes across that period (Jeffries, Overland, and Perovich 2013), the year-to-year variation is being explored separately (Megan Ferguson, MML, *pers. comm.*).

Spatial Dimensions

To create these dynamic predictions, we use the fitted relationships between species abundance and the predictor variables to predict smooth density surfaces across specific extent(s). We predict these values on a 10 by 10 kilometer grid, the extent of which corresponds to the spatial extent of the ASAMM study area (**Figure 1**). For most species included herein this area is a subset of their entire range. After an initial expert review meeting in May of 2017, we agreed to extend the northern prediction boundaries for two species - bowhead whales and beluga whales. For the northern boundary of each area, we used published northernmost occurrences of tagged individuals: (74 °N) for bowheads (Citta et al. 2015) and (81 °N) for beluga whales (Suydam, Lowry, and Frost 2005, Suydam et al. (2001)).

Results

Here we document the three main classes of results for each of the eight species/guild combinations. We start with the detection functions, then discuss the results from the abundance-environment relationships, and end with the predicted density surfaces. While the structure of the data, modeling, and results is the same in each of the three subsections, the combination of biology and different significant predictors yields a changing pattern.

Detection Functions

We chose a final working model that was typically the one with the lowest AIC value. We include detailed summaries of the detection functions in Appendix A. For some species there were several detection function models within two AIC units of the ‘best’ model (not shown). Though we chose one ‘best’ model, we acknowledge several plausible models exist for several species. As noted previously, the best way to capture and represent all of the uncertainty in the modeling process remains an active area of research.

In cases with simpler model forms, i.e. one covariate, we can easily interpret the influence of the covariate on the detection function. As the complexity of the model increases, this becomes more difficult. In each species/platform combination, we have depicted the best detection function, along with the Q-Q plot indicating fit. This metric can be combined with the tabular values for an indication of overall fit. Details are provided in **Appendix A**.

Generalized Additive Model

The final models chosen to use for density-surface modeling for each species are summarized in **Table 11**. We have not included any of the intermediate modeling results. As with the detection functions, while we chose a final working model, there is model uncertainty. The following sections provide an overview of the results; details on species-specific results are provided in Appendix B.

Table 11. Summary table highlighting the final covariates included in each species or guild-specific GAM. Further details given in each summary section.

Species	Final Predictive GAM Formula	Deviance Explained
Bowhead Whales	Soap Film Spatial Smooth, Distance to 200m Isobath, Distance to Ice Edge, Ice Concentration	19.6%
Beluga Whales	Spatial Smooth, Depth, Distance to 200m Isobath, Ice Concentration	23.4%
Gray Whales	Soap Film Spatial Smooth, Distance to 200m Isobath, Distance to Ice Edge, Ice Concentration	71.9%
Walrus	Soap Film Spatial Smooth, Distance to 200m Isobath, Ice Concentration	48.2%
Bearded Seals	Soap Film Spatial Smooth, Depth	3.03%
Small Pinnipeds	Soap Film Spatial Smooth, Depth, Distance to Ice Edge, Ice Concentration	6.62%
Unid. Pinnipeds	Soap Film Spatial Smooth, Depth, Ice Concentration	10.1%
Baleen Whales	Soap Film Spatial Smooth	69.4%

Detailed graphical and numerical summaries of the GAM fits for each species are shown in **Appendix B**.

Predicted Density—Surfaces & Total Abundance

Here we show the densitology for each species/guild combination. For the species whose final GAM model included a dynamic covariate, the monthly rasters for July, August, September, and October are also included. We also include the abundance values for each species/month combination (**Table 12**).

Table 12. Predicted abundances and CV, overall and by month. Two groups only contain the total abundance (bearded seals, and baleen whales).

Species	All Months	July	August	September	October
Bowhead Whales	488 (0.149)	216 (0.193)	576 (0.131)	754 (0.138)	405 (0.135)
Beluga Whales	20,170 (1.463)	16,975 (1.494)	21,626 (1.471)	23,312 (1.475)	18,766 (1.412)
Gray Whales	138 (0.21)	138 (0.253)	149 (0.186)	109 (0.209)	158 (0.194)
Walrus	9,164 (0.252)	11,481 (0.31)	9,521 (0.225)	8,276 (0.225)	7,376 (0.248)
Bearded Seals	395 (0.124)	395 (0.124)	395 (0.124)	395 (0.124)	395 (0.124)
Small Pinnipeds	9,641 (0.058)	7,428 (0.068)	10,454 (0.051)	10,856 (0.055)	9,825 (0.058)
Unidentified Pinnipeds	1,112 (0.16)	809 (0.15)	1,200 (0.156)	1,300 (0.166)	1,138 (0.17)
Baleen Whales	46 (0.48)	46 (0.48)	46 (0.48)	46 (0.48)	46 (0.48)

Bowhead Whales

For bowheads, the vast majority of sightings were well shoreward of the 200-m isobath with peak density near Point Barrow (**Figure 11 A**). Estimates of uncertainty were lowest (**Figure 11 B**) where density estimates were highest (**Figure 11 A**), which indicates good fit. Despite the slight northward extrapolation for bowheads, very few whales were predicted north of 72 °N

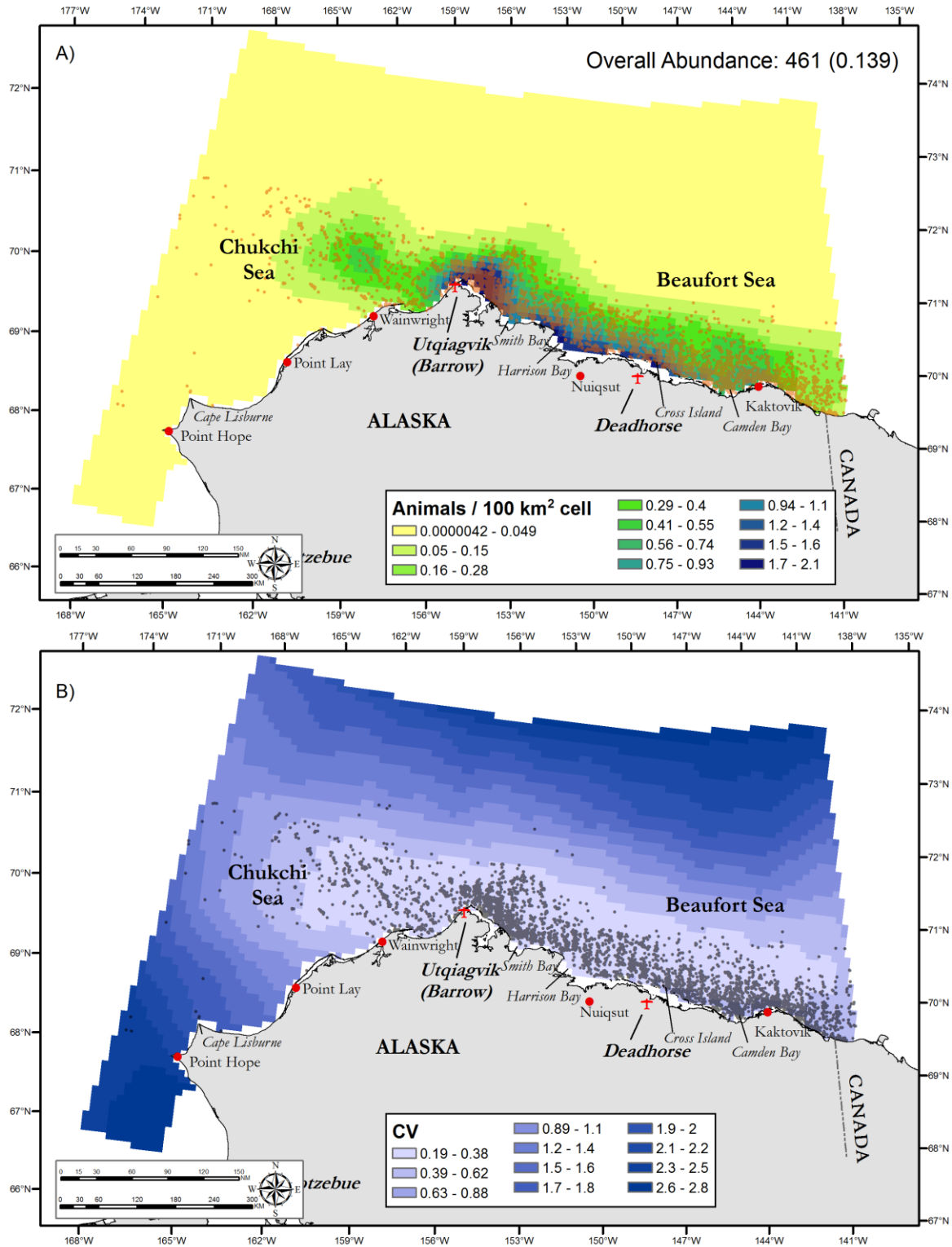


Figure 11. (A) Predicted densitology for bowhead whales (2000-2016). Bowheads observed on-transect are shown with orange dots. (B) Predicted CV surface.

Next, we depict the monthly summary of density and uncertainty (coefficient of variation). Because a spatial smooth was included in the final model, it appears that certain months had predictions in areas where/when fewer bowheads were seen (e.g., August west of Point Barrow) (**Figure 13 A**). The higher predicted densities for Smith Bay and Harrison Bay are in September (**Figure 14**). In all months, the highest densities corresponded with low estimates of uncertainty (e.g., **Figure 11 B**).

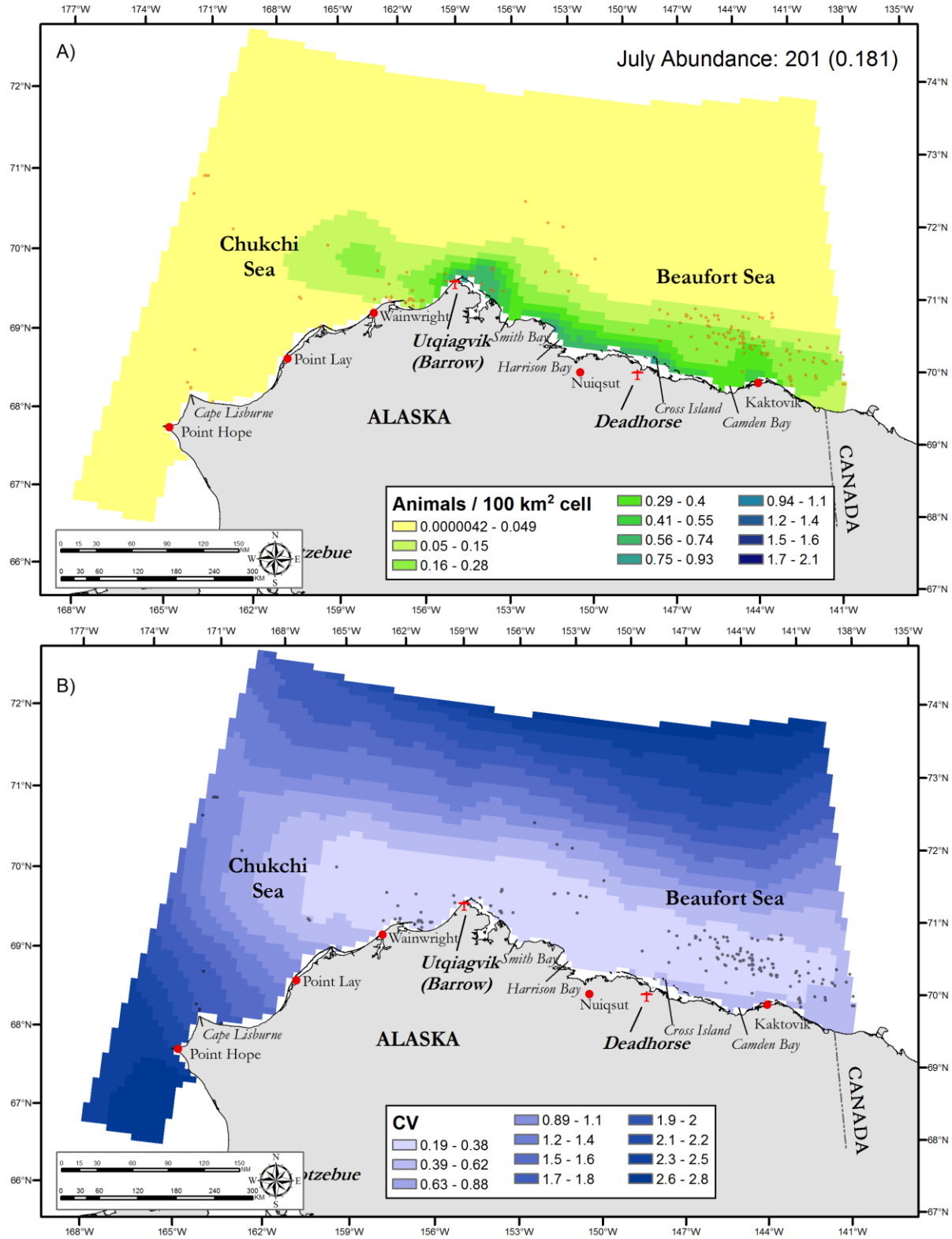


Figure 12. (A) Predicted density for bowhead whales in July (2000-2016). Bowheads observed on-transect are shown with orange dots. (B) Predicted CV surface.

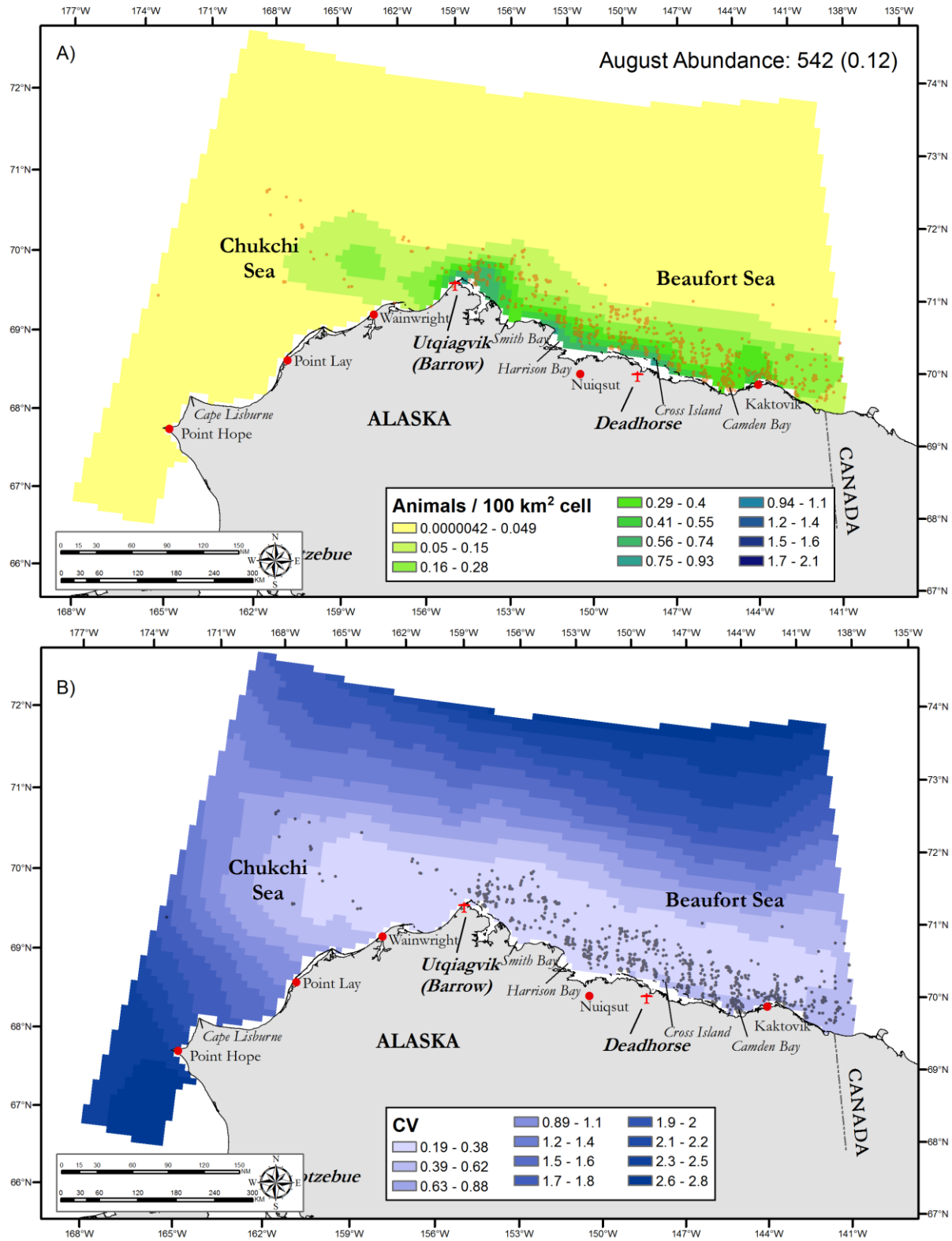


Figure 13. (A) Predicted density for bowhead whales in August (2000-2016). Bowheads observed on-transect are shown with orange dots. (B) Predicted CV surface.

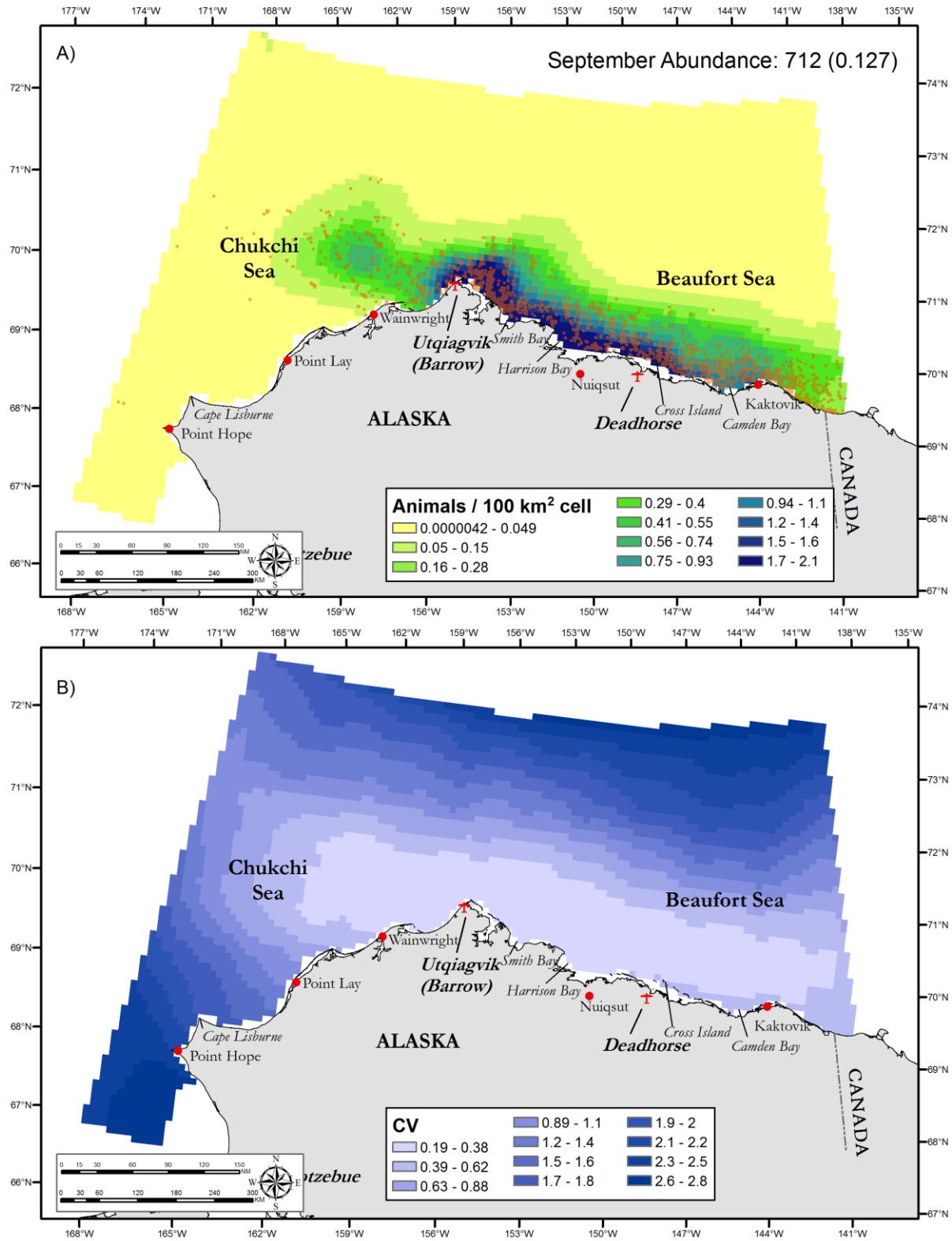


Figure 14. (A) Predicted density for bowhead whales in September (2000-2016). Bowheads observed on-transect are shown with orange dots. (B) Predicted CV surface.

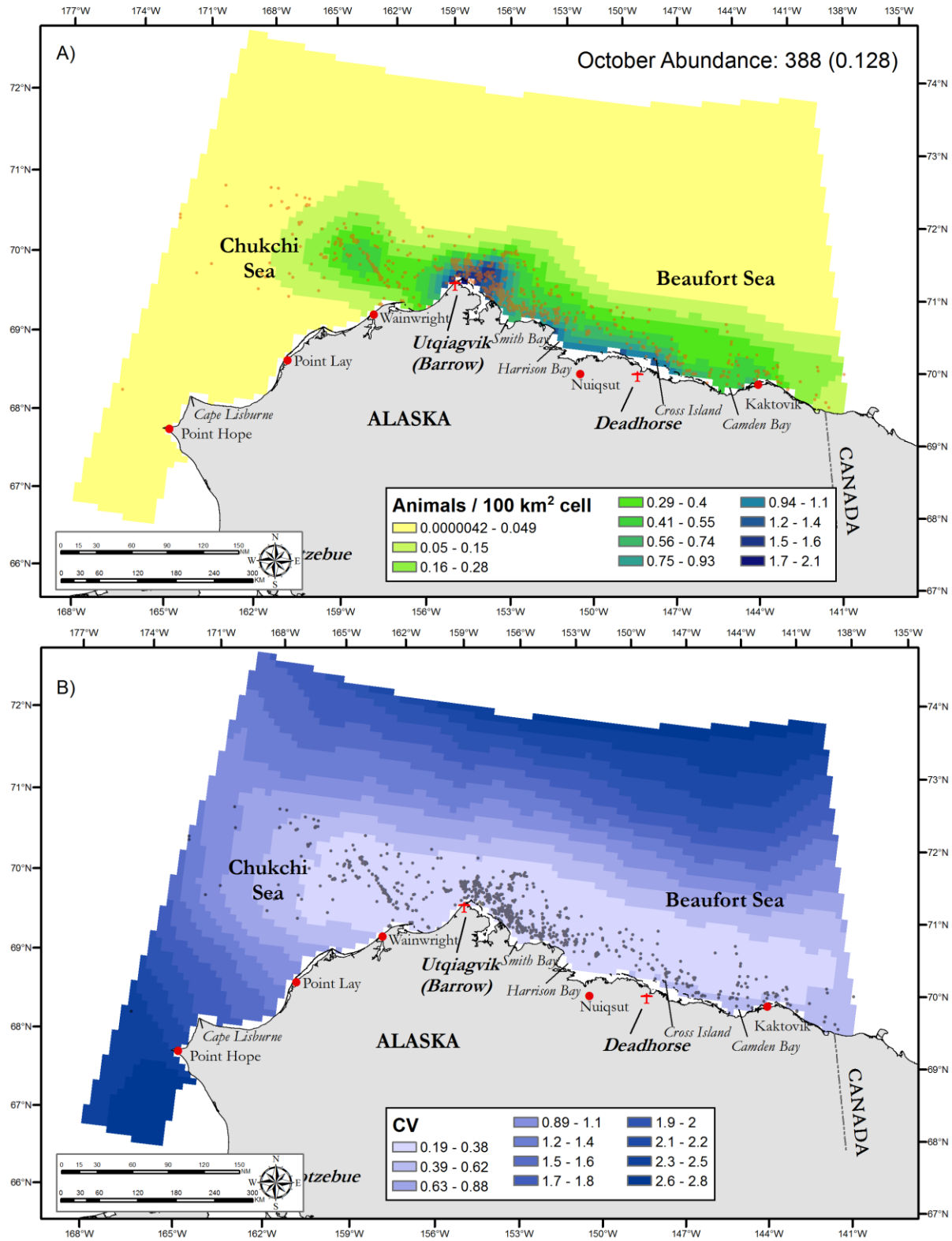


Figure 15. (A) Predicted density for bowhead whales in October (2000-2016). Bowheads observed on-transect are shown with orange dots. (B) Predicted CV surface.

Beluga Whales

Below are the predicted density and CV surfaces. Note that for beluga whales we have predicted/extrapolated to a much farther northern extent - 81 °N, and in contrast to the bowheads, we do see a large number of whales being predicted between 73 and 77 °N (**Figure 16**). These higher predictions are also made with higher uncertainty - though not as high as the predictions within and immediately north of the ASAMM study area (**Figures 16 A, 16 B**). Within the ASAMM study area, peak densities are predicted much farther offshore than bowheads - typically occurring along the shelf-break (**Figure 16 A**).

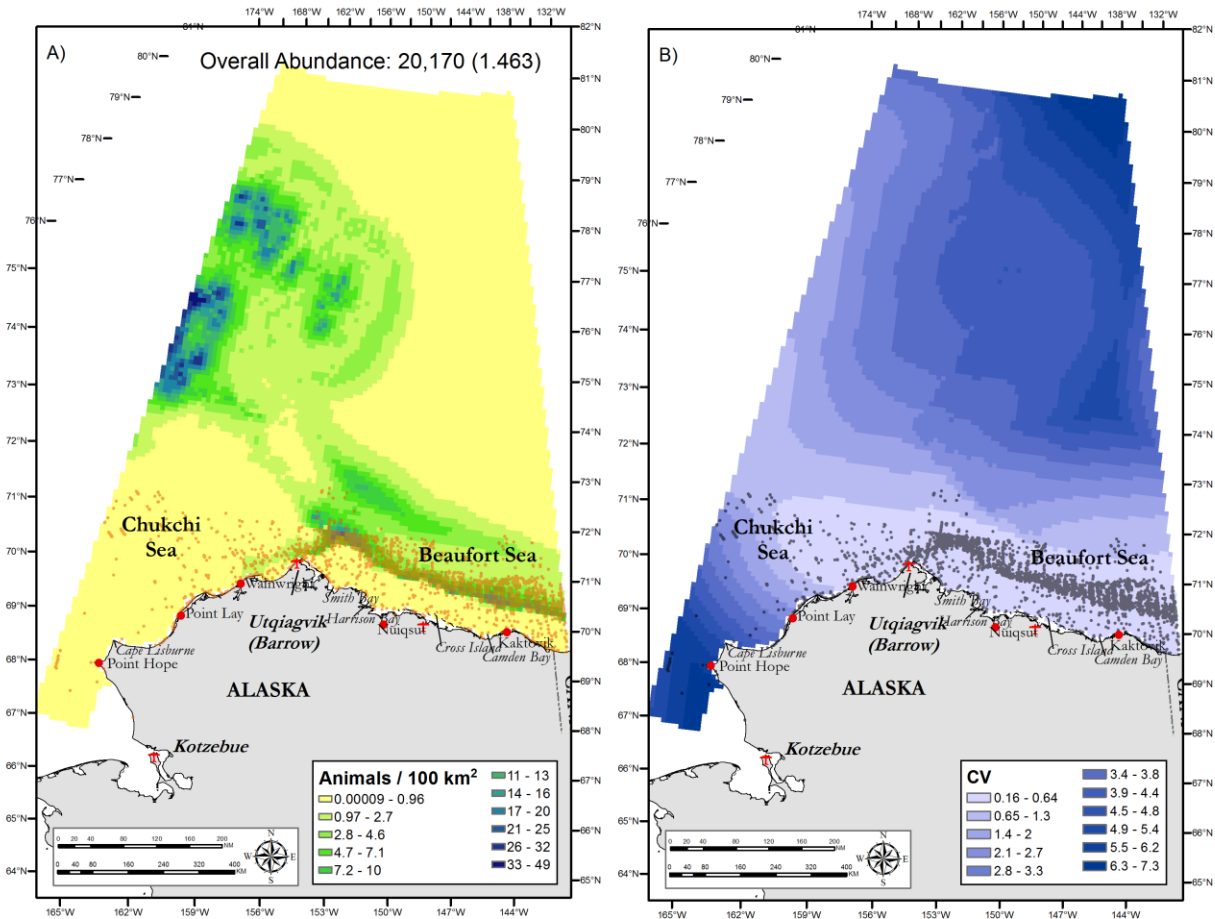


Figure 16. (A) Predicted densitology for beluga whales (2000-2016). Belugas observed on-transect are shown with orange dots. (B) Predicted CV surface.

In all months, the northerly predicted densities, i.e. those outside of the ASAMM study area, are all higher than those predicted within the study area.

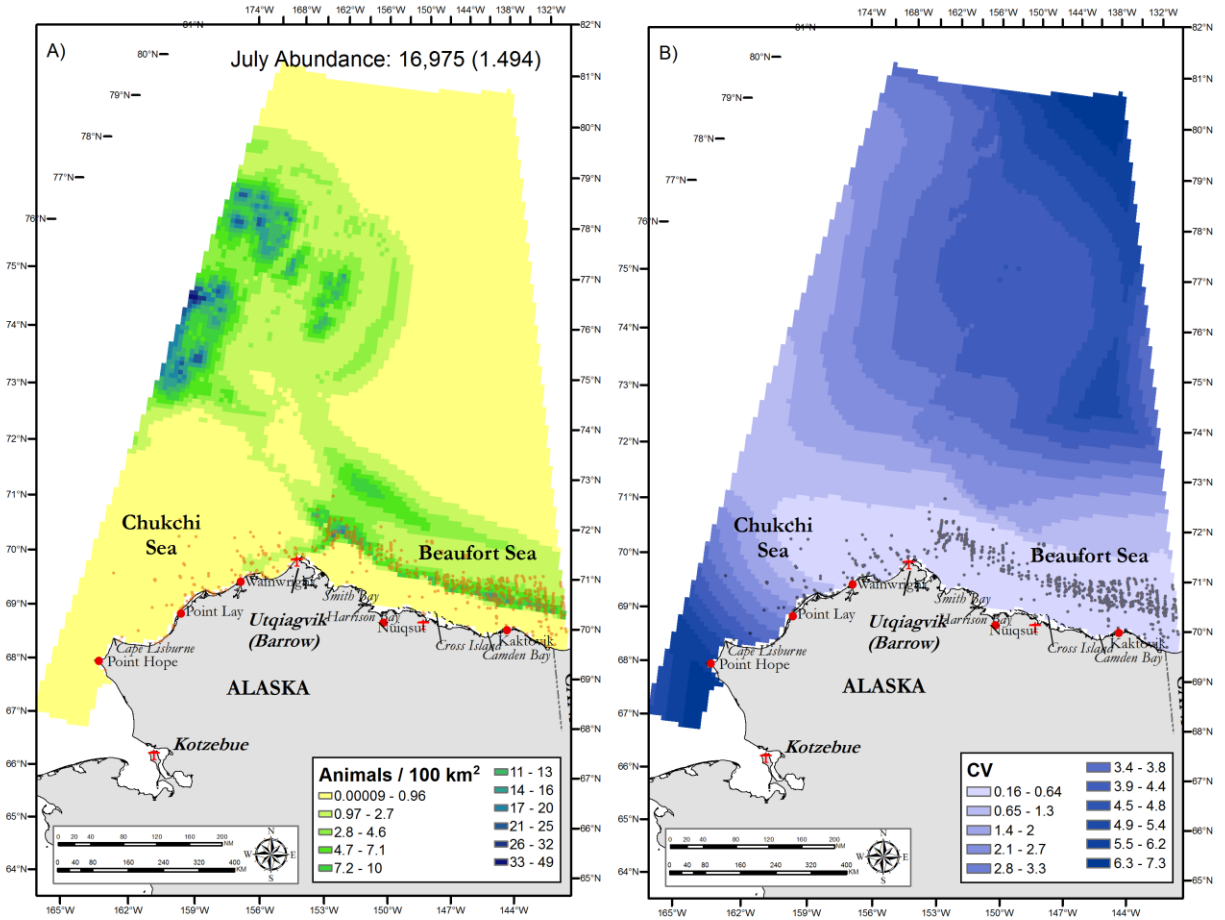


Figure 17. (A) Predicted density for beluga whales in July (2000-2016). Belugas observed on-transect are shown with orange dots. (B) Predicted CV surface.

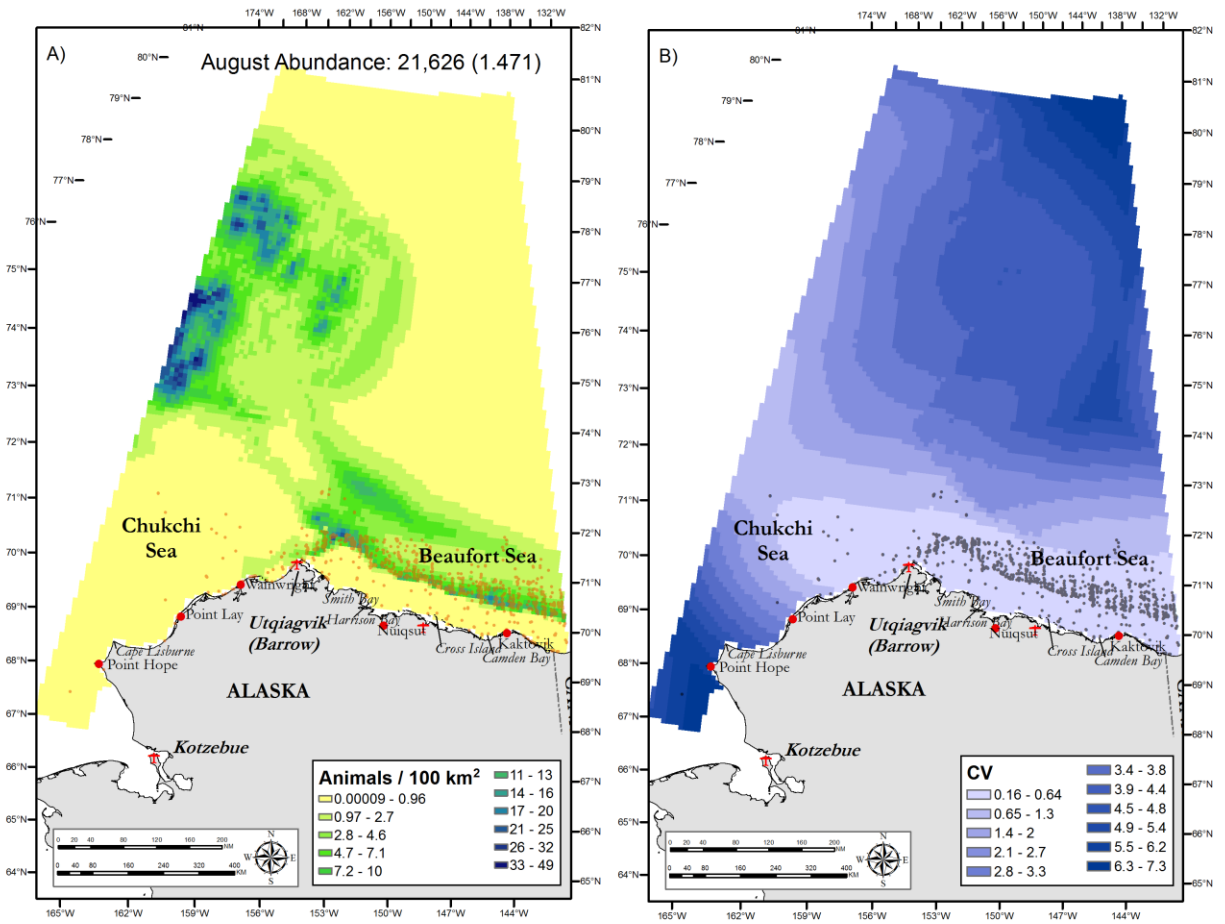


Figure 18. (A) Predicted density for beluga whales in August (2000-2016). Belugas observed on-transect are shown with orange dots. (B) Predicted CV surface.

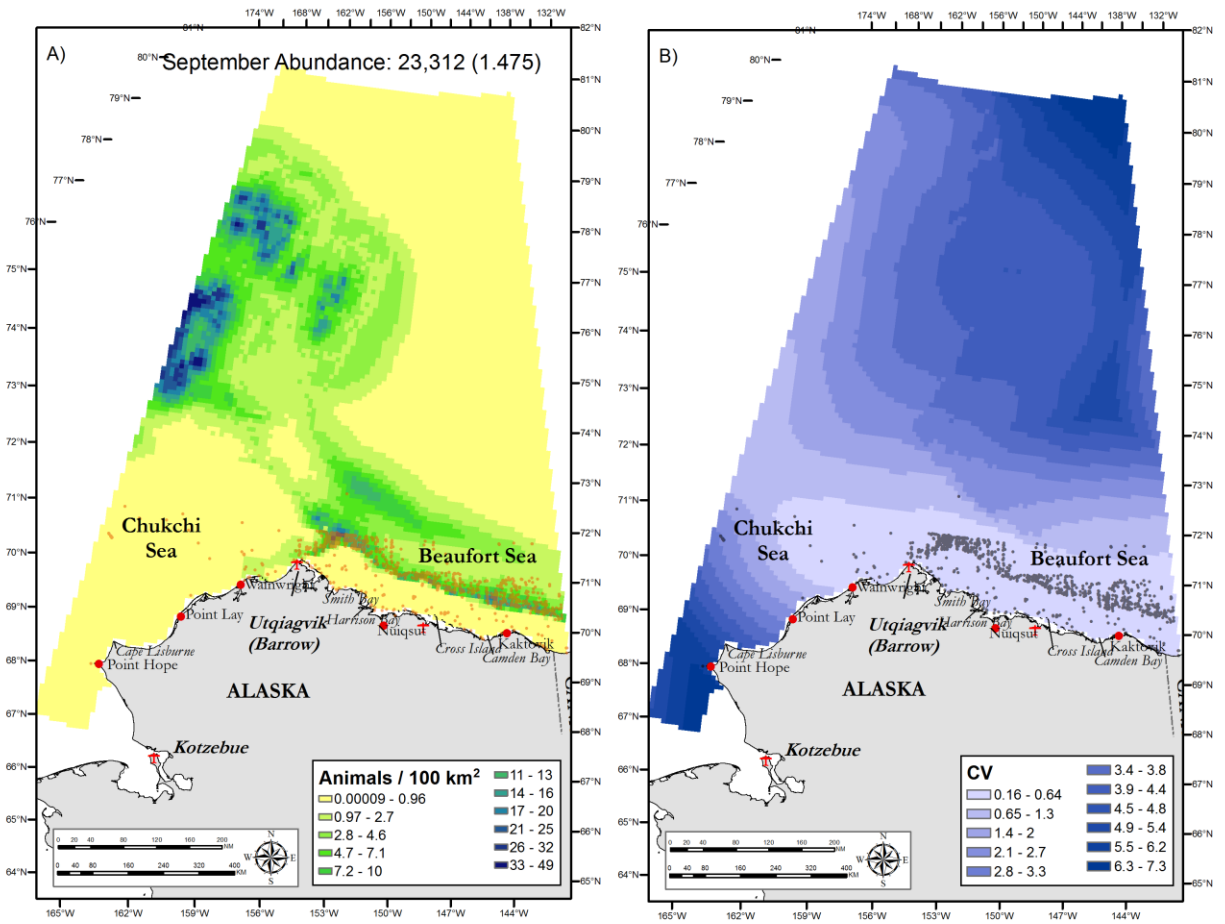


Figure 19. (A) Predicted density for beluga whales in September (2000-2016). Belugas observed on-transect are shown with orange dots. (B) Predicted CV surface.

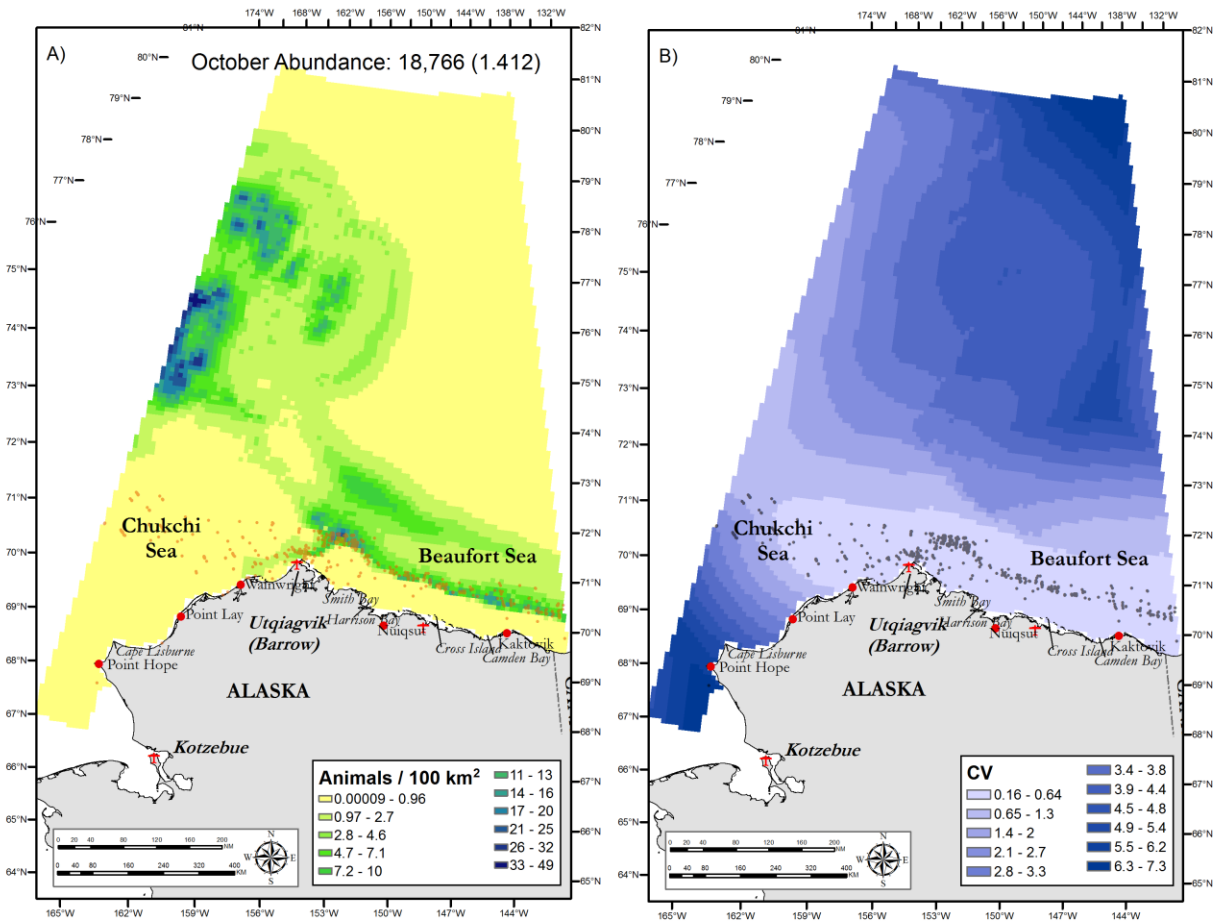


Figure 20. (A) Predicted density for beluga whales in October (2000-2016). Belugas observed on-transect are shown with orange dots. (B) Predicted CV surface.

Gray Whales

Below are the predicted density and CV surfaces. As with bowheads, the areas of higher density (**Figure 21 A**) correspond with lower predicted uncertainty (**Figure 21 B**) with one exception. This is in the southwest corner of the ASAMM study area (**Figure 21**). Here we observed a large number of gray whales, but have low predicted density with higher uncertainty. We suspect this is owing to the inclusion of the static spatial smooth, and suspect fit may be improved by including the interaction between time and the spatial smooth.

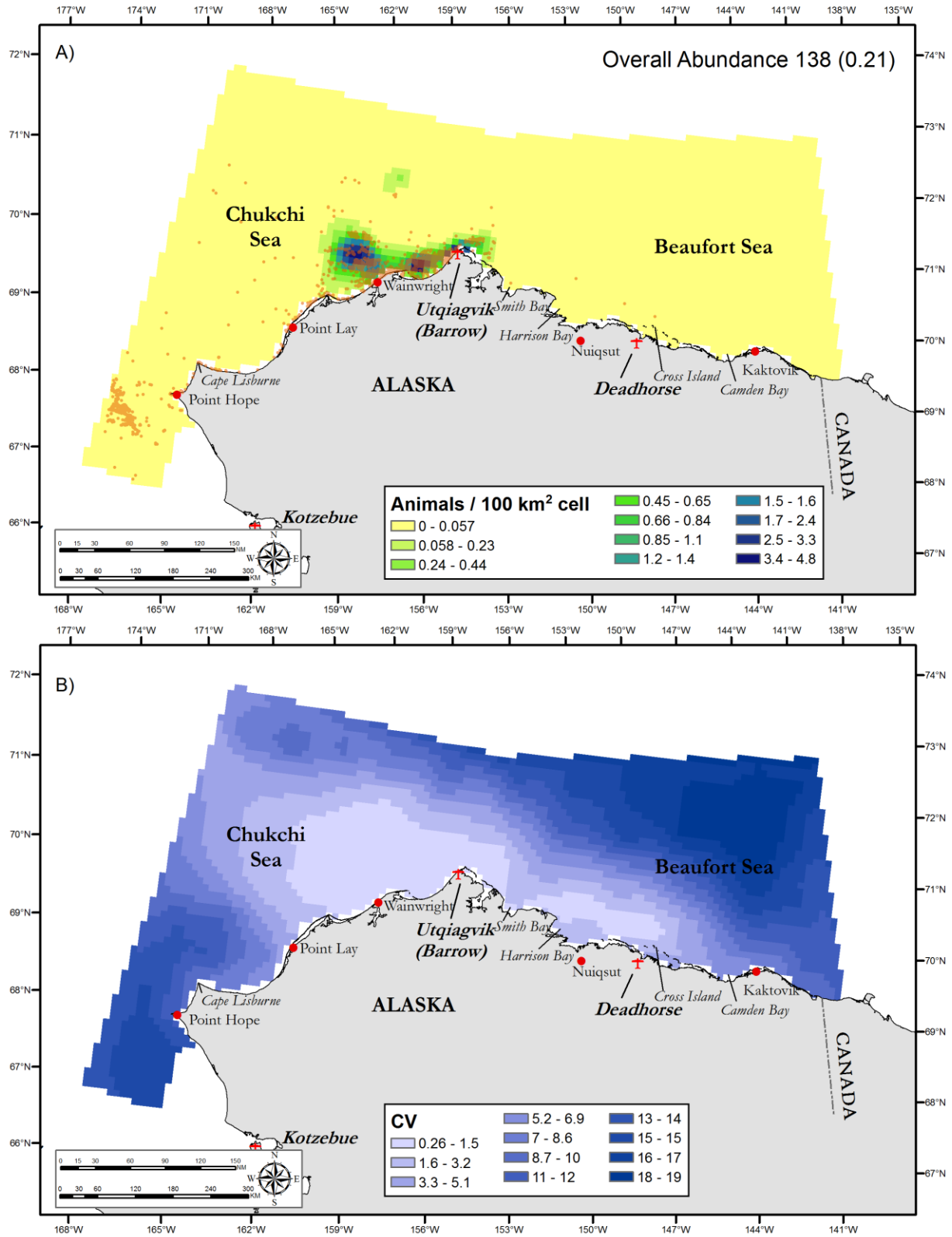


Figure 21. (A) Predicted densitology for gray whales (2000-2016). Gray whales observed on-transect are shown with orange dots. (B) Predicted CV surface.

The spatial patterns are consistent month to month, with highest predicted densities in October (**Figure 25 A**).

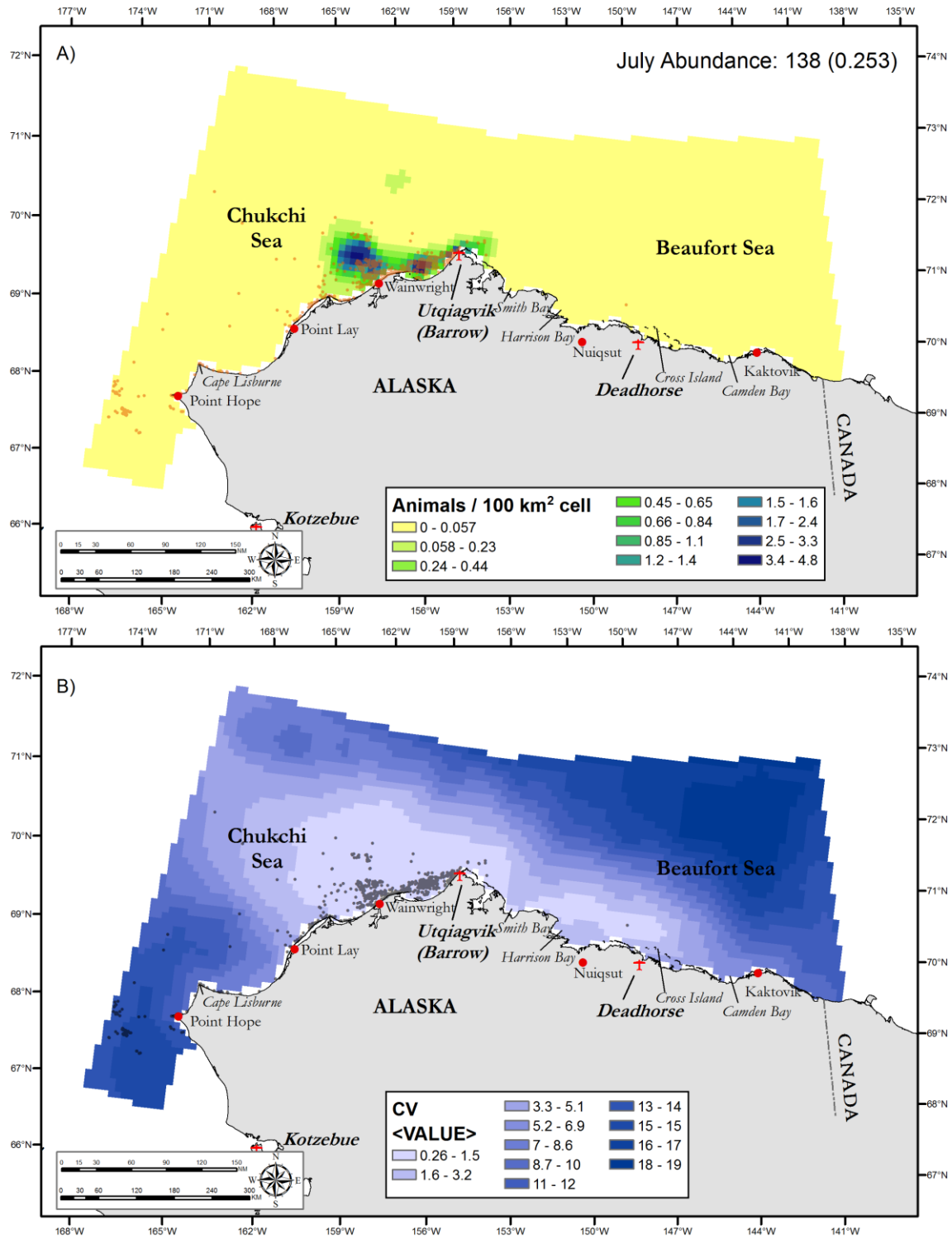


Figure 22. (A) Predicted density for gray whales in July (2000-2016). Gray whales observed on-transect are shown with orange dots. (B) Predicted CV surface.

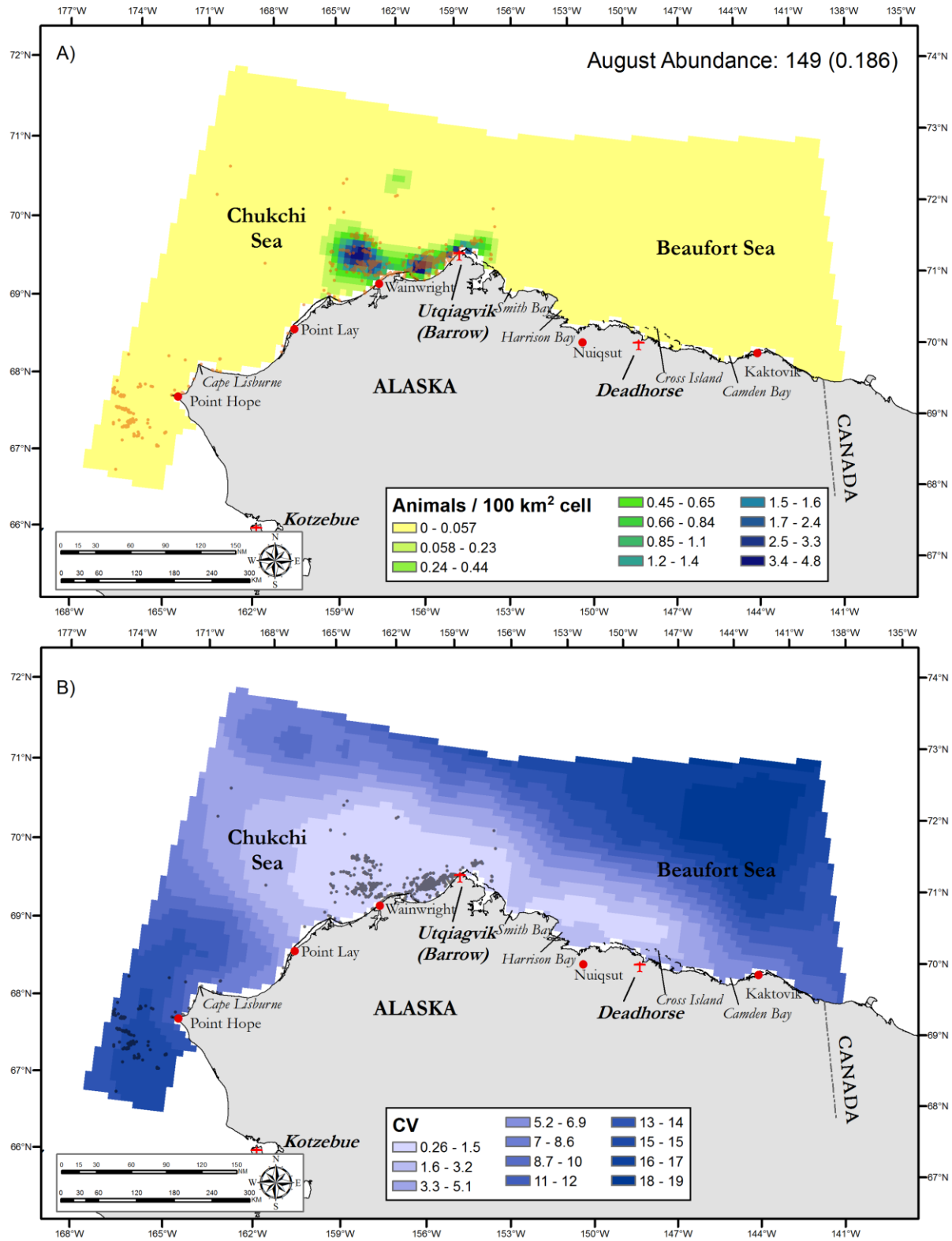


Figure 23. (A) Predicted density for gray whales in August (2000-2016). Gray whales observed on-transect are shown with orange dots. (B) Predicted CV surface.

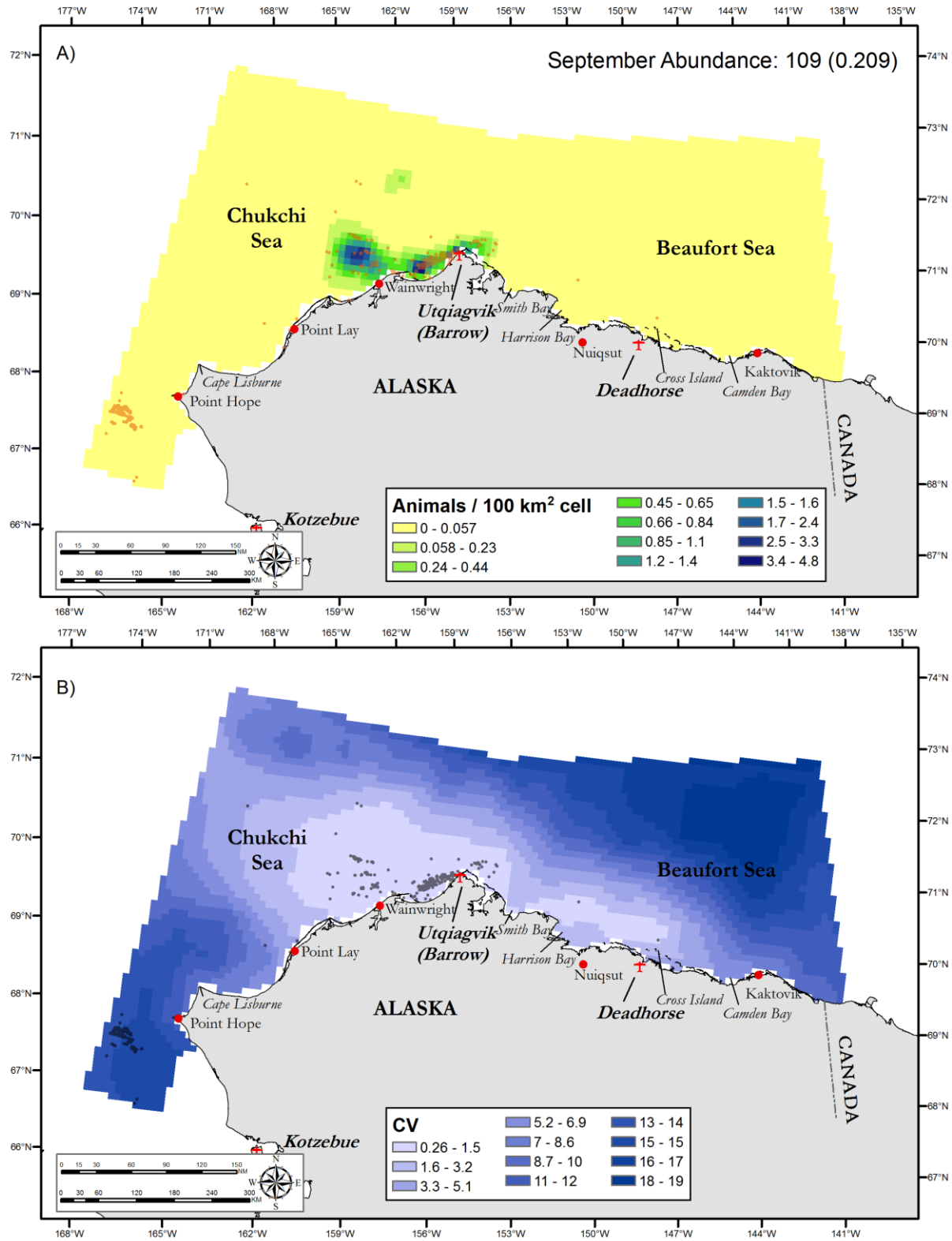


Figure 24. (A) Predicted density for gray whales in September (2000-2016). Gray whales observed on-transect are shown with orange dots. (B) Predicted CV surface.

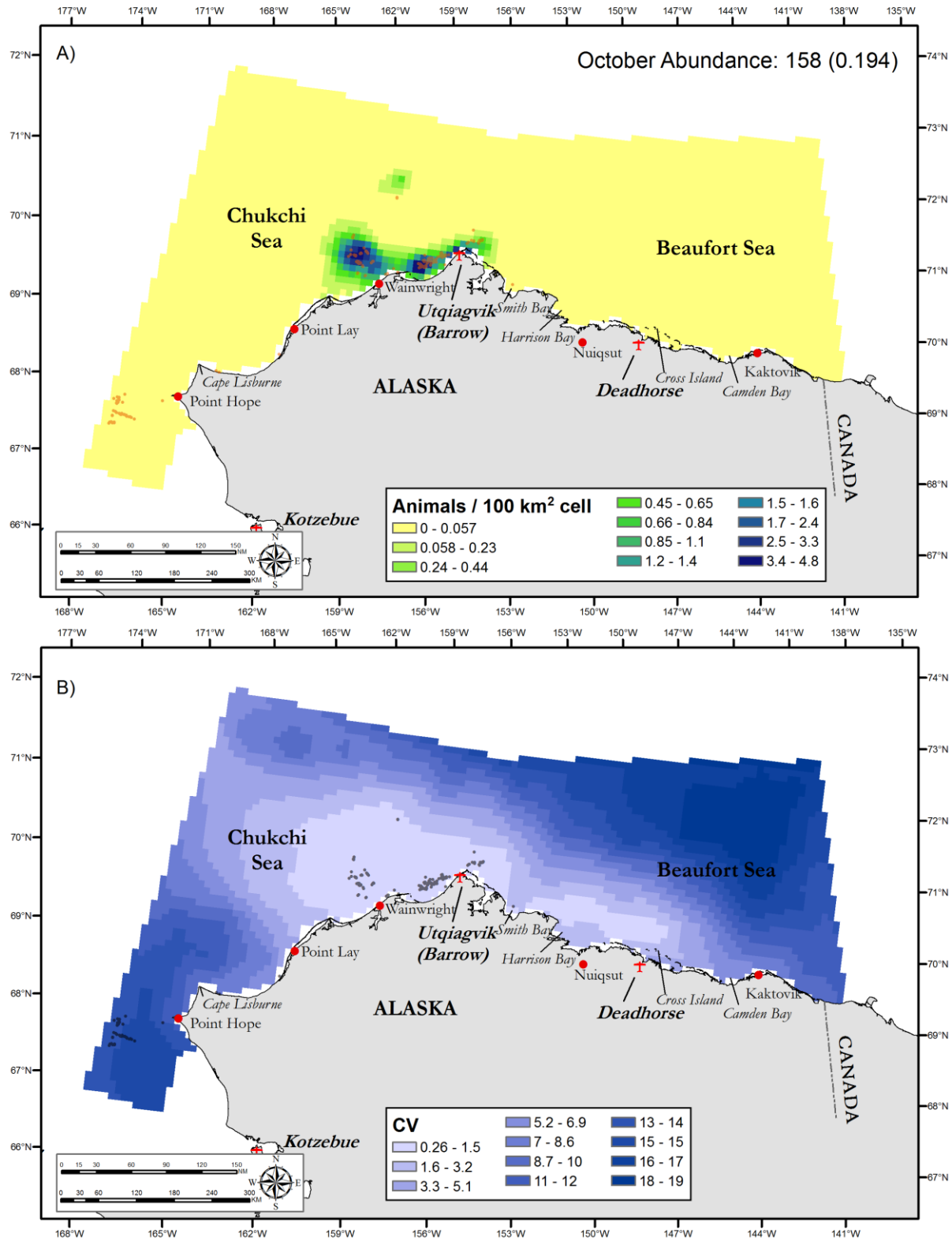


Figure 25. (A) Predicted density for gray whales in October (2000-2016). Gray whales observed on-transect are shown with orange dots. (B) Predicted CV surface.

Walrus

Highest predicted values were in July, declining as the summer progresses. Highest values are predicted offshore in the Hannah Shoal region of the northeast Chukchi Sea (**Figure 26 A**); as with previous species, these predicted densities also correspond to areas of low predicted uncertainty (**Figure 26 B**).

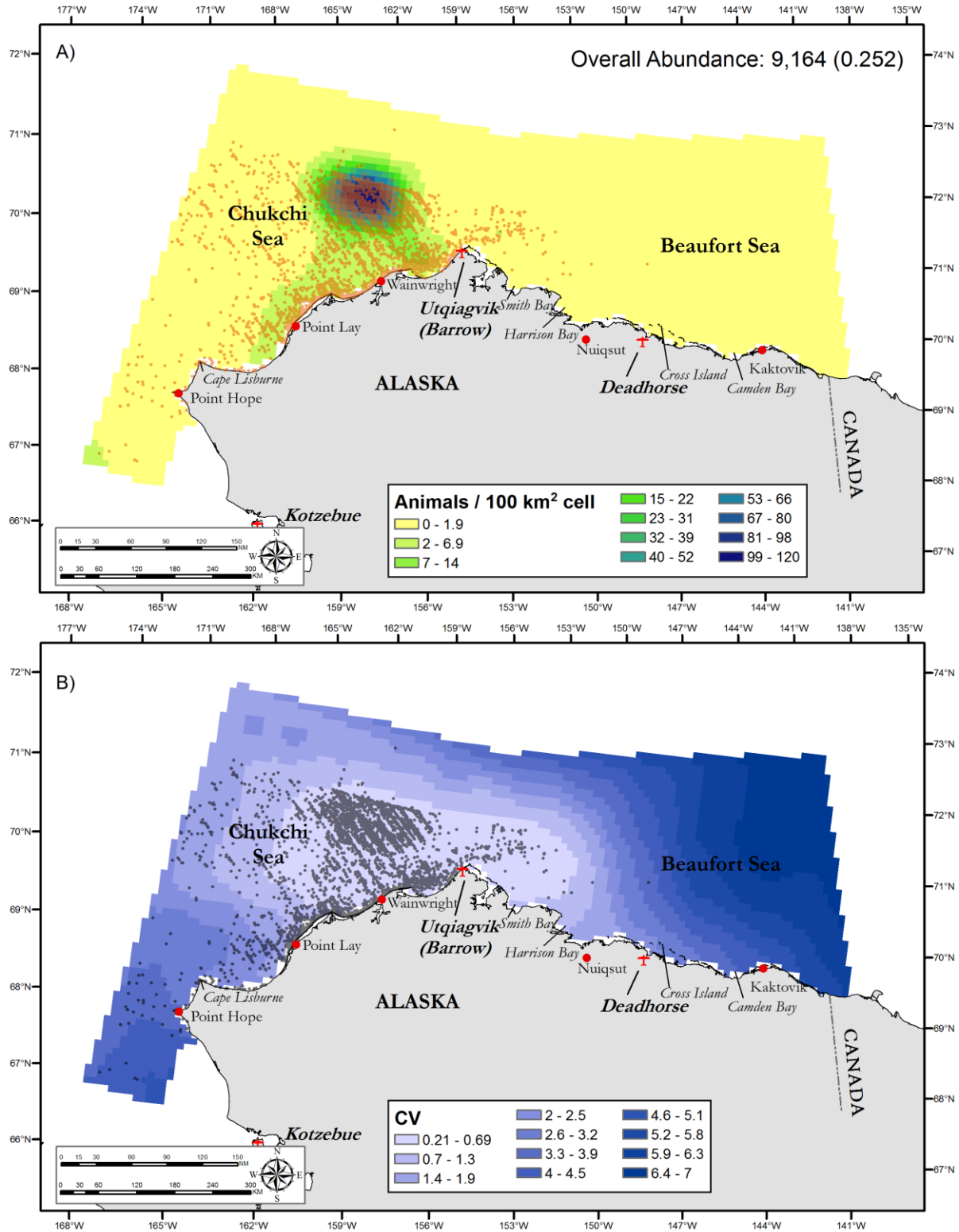


Figure 26. (A) Predicted densitology for walrus (2000-2016). Walrus observed on-transect are shown with orange dots. (B) Predicted CV surface.

The spatial pattern of the monthly predictions do not change drastically month to month. Though the peak of the monthly surfaces is in the Hannah Shoal region, the spatial predictions closer to shore (e.g. between Point Lay and Point Barrow, do change month to month). For example, compare September distributions to October. In October (**Figure 30 A**), the predicted densities are lower, though smoother in space than those in September (**Figure 29 A**).

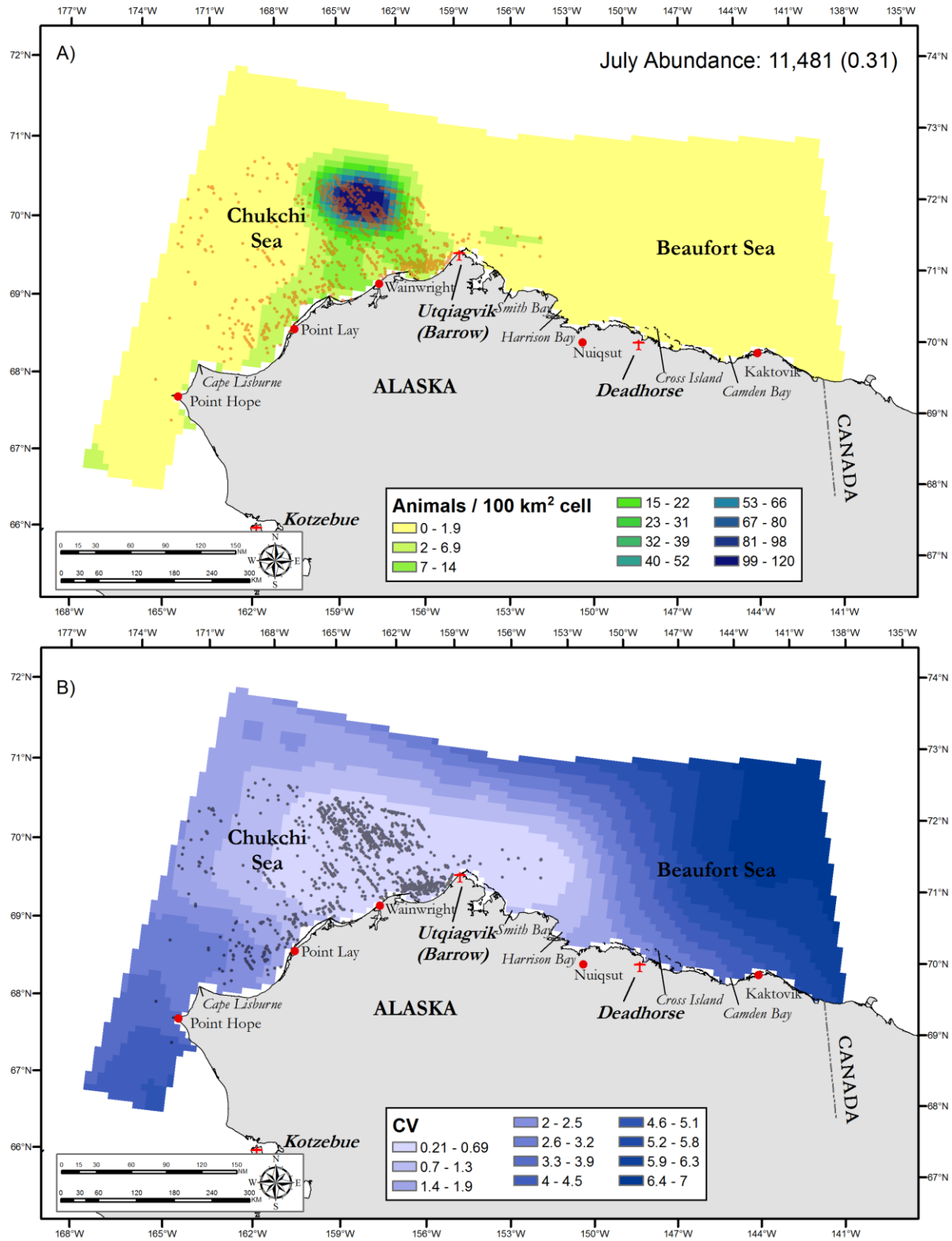


Figure 27. (A) Predicted density for walrus in July (2000-2016). Walrus observed on-transect are shown with orange dots. (B) Predicted CV surface.

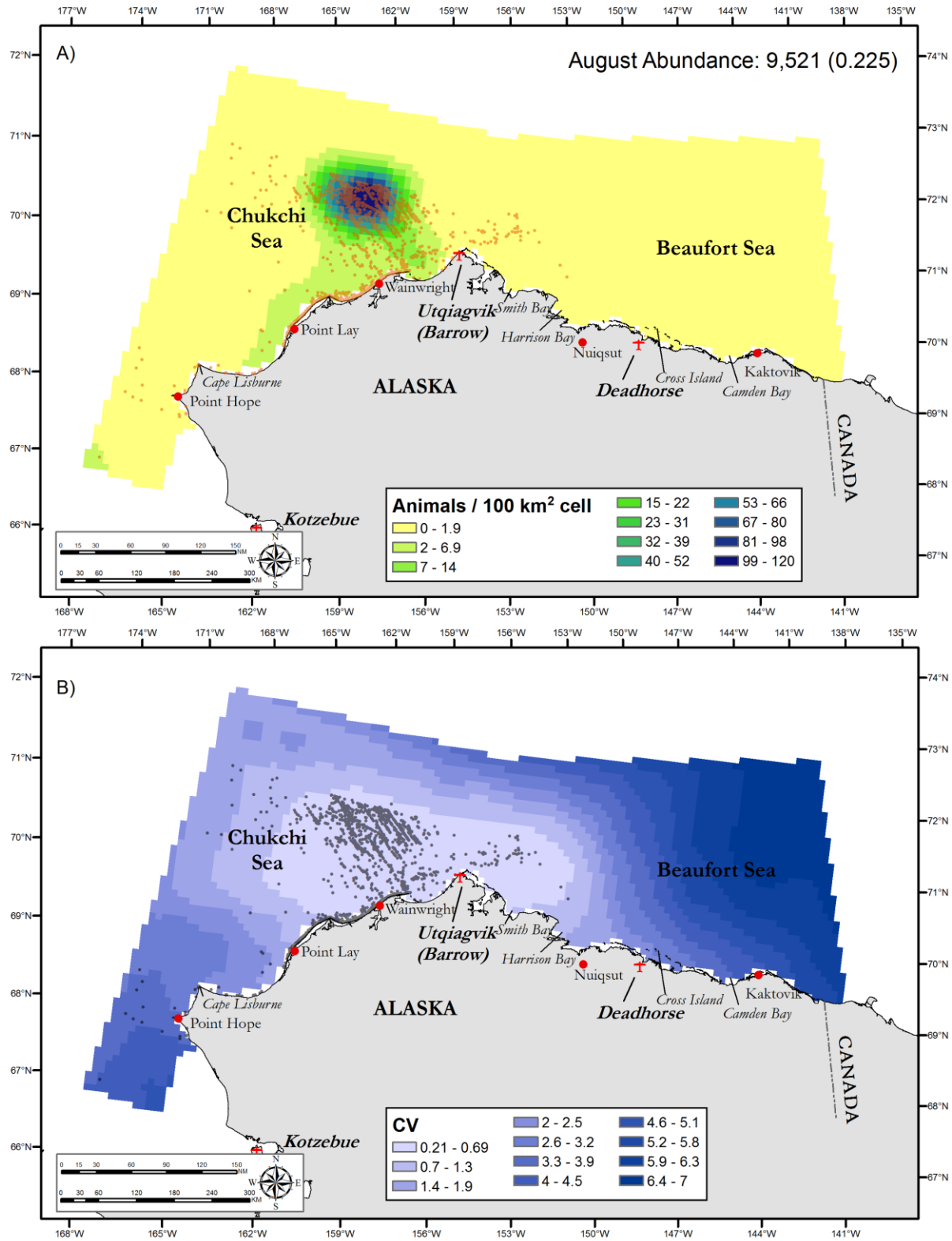


Figure 28. (A) Predicted density for walrus in August (2000-2016). Walrus observed on-transect are shown with orange dots. (B) Predicted CV surface.

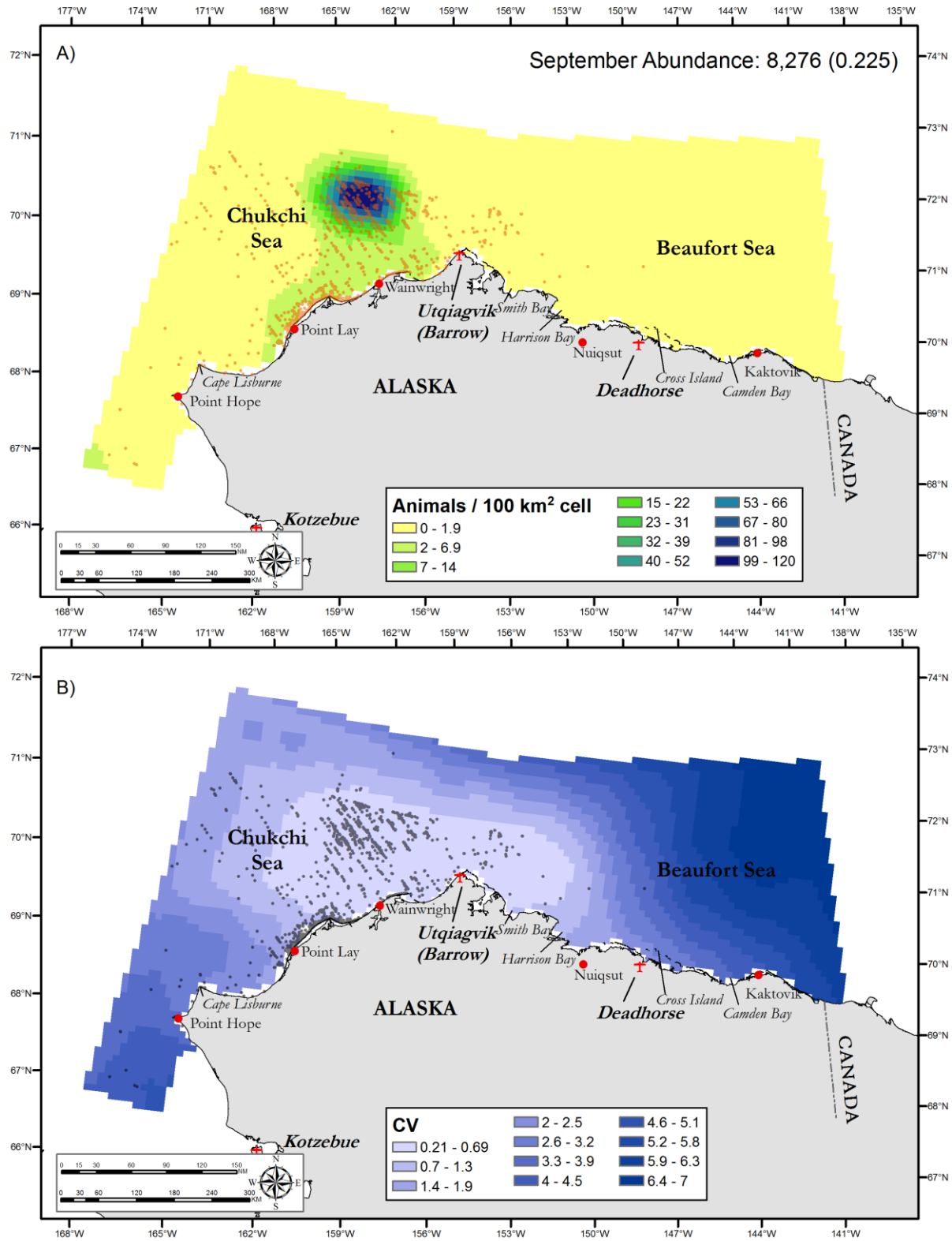


Figure 29. (A) Predicted density for walrus in September (2000-2016). Walrus observed on-transect are shown with orange dots. (B) Predicted CV surface.

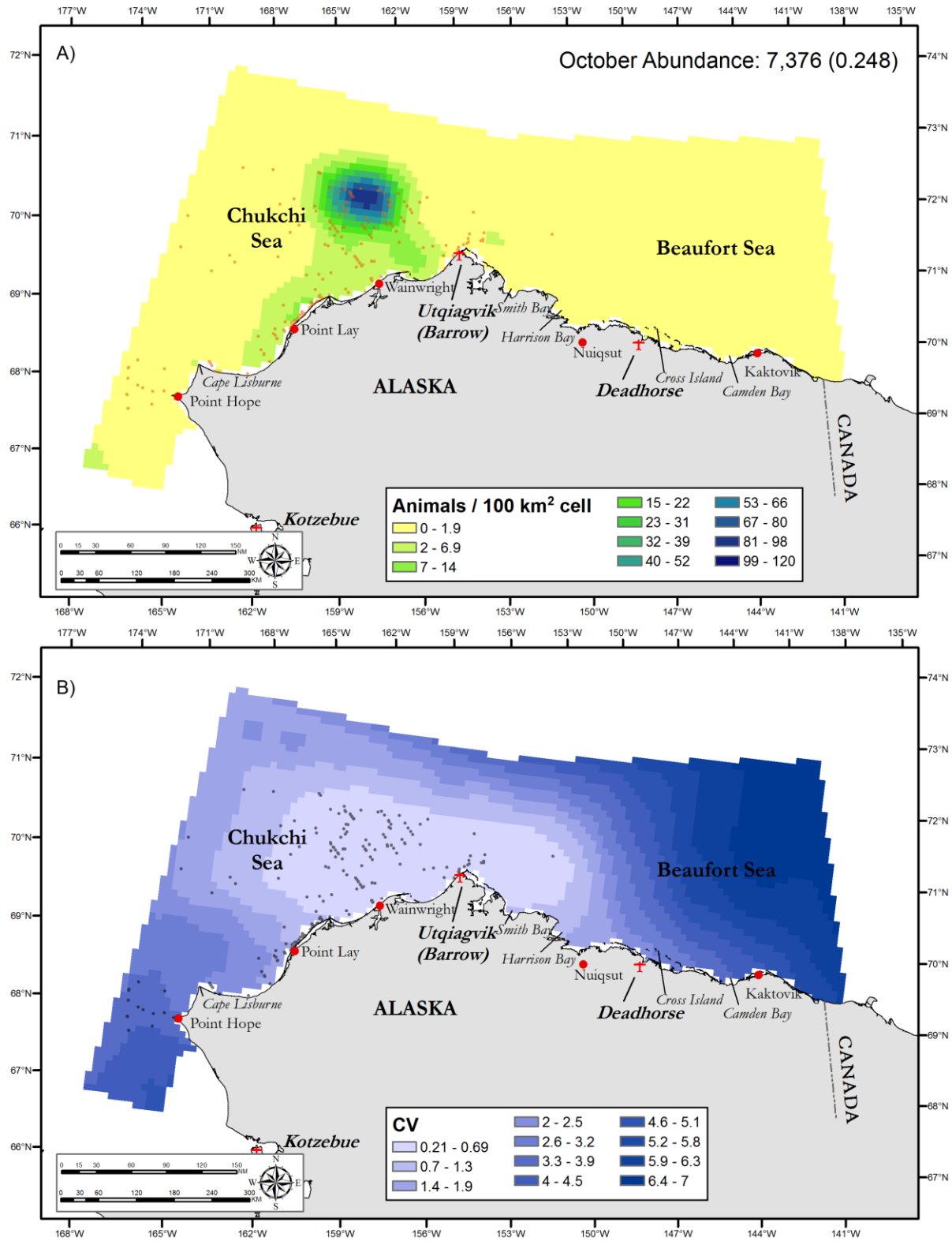


Figure 30. (A) Predicted density for walrus in October (2000-2016). Walrus observed on-transect are shown with orange dots. (B) Predicted CV surface.

Bearded Seals

Below are the predicted density and CV surfaces. Note that since no dynamic covariates were included in the final GAM, we only show predicted results for the densitology and accompanying coefficient of variation surface.

Highest predicted values were observed near the shelf break in the Alaskan Beaufort Sea (**Figure 31 A**). Significant numbers of seals were also predicted near shore in the Chukchi Sea. Note that in contrast to previous species, the uncertainty is not uniformly lower in areas with predicted higher densities (**Figure 31 B**). For example, the band of high predicted density east of Barrow and west of Kaktovik has higher uncertainty (**Figure 31 B**).

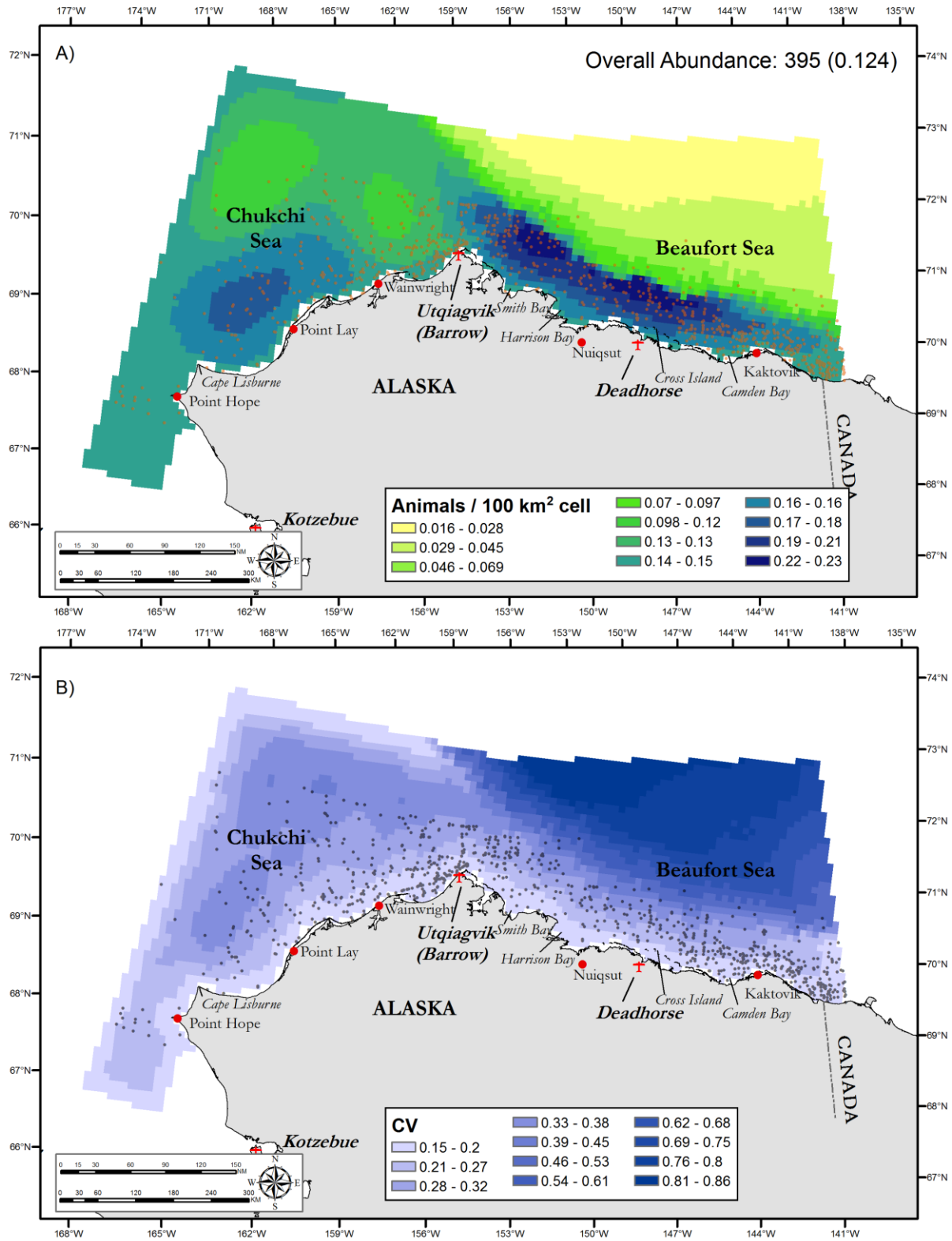


Figure 31. (A) Predicted densitology for bearded seals (2000-2016). Bearded seals observed on-transect are shown with orange dots. (B) Predicted CV surface.

Small Pinnipeds

Below are the predicted density and CV surfaces. Peak densities are northeast of Smith Bay - east of Point Barrow (**Figure 32 A**); other high density areas are coastal waters at the Alaska/Canada border, and between Point Lay and Wainwright. In all areas of high predicted density, uncertainty is low (**Figure 32 B**).

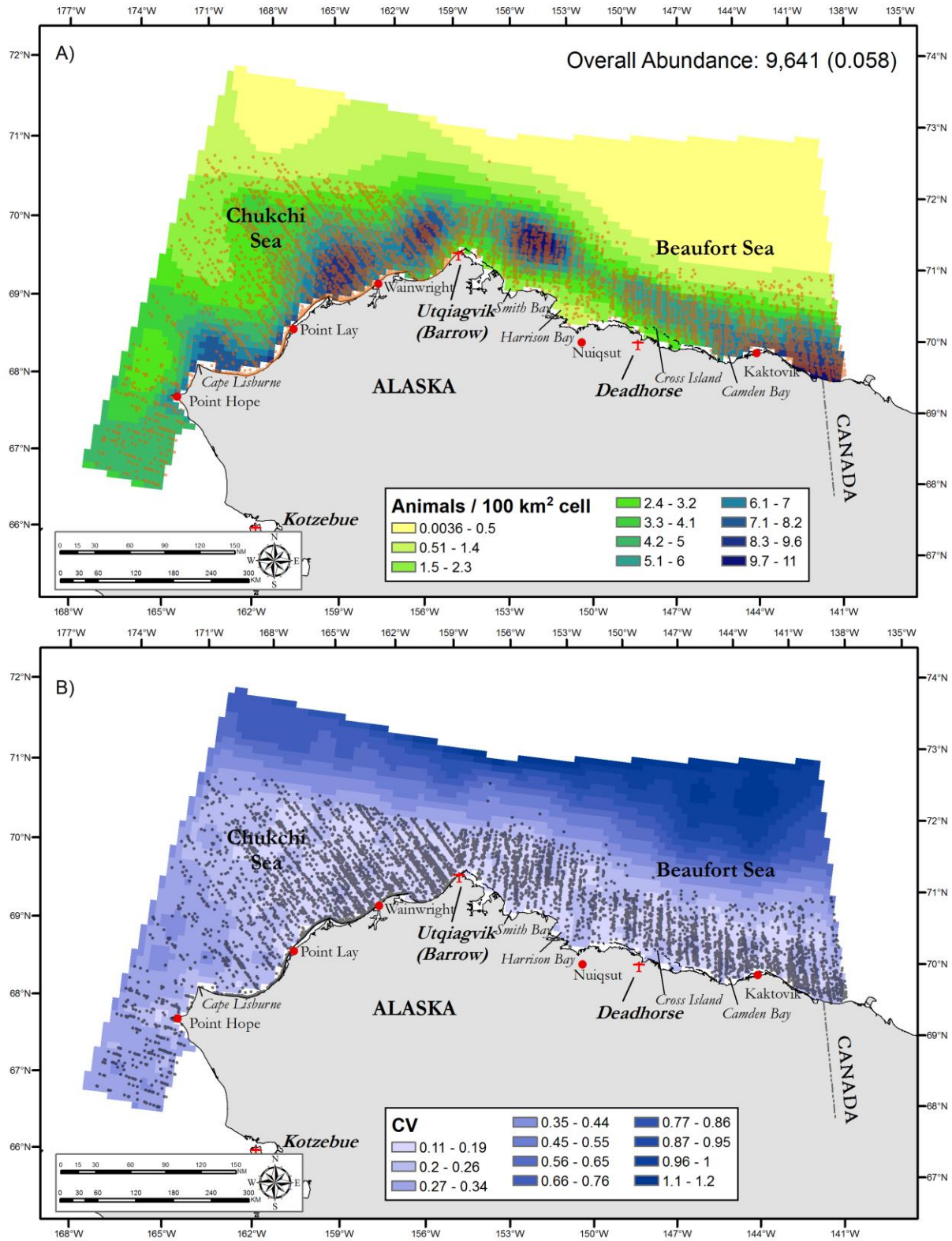


Figure 32. (A) Predicted densitology for small pinnipeds (2000-2016). Small pinnipeds observed on-transect are shown with orange dots. (B) Predicted CV surface.

Numbers are lower in July, and higher densities are seen around Point Lay (Figure 33). As the year progresses, higher densities are observed north of Smith Bay (Figure 34).

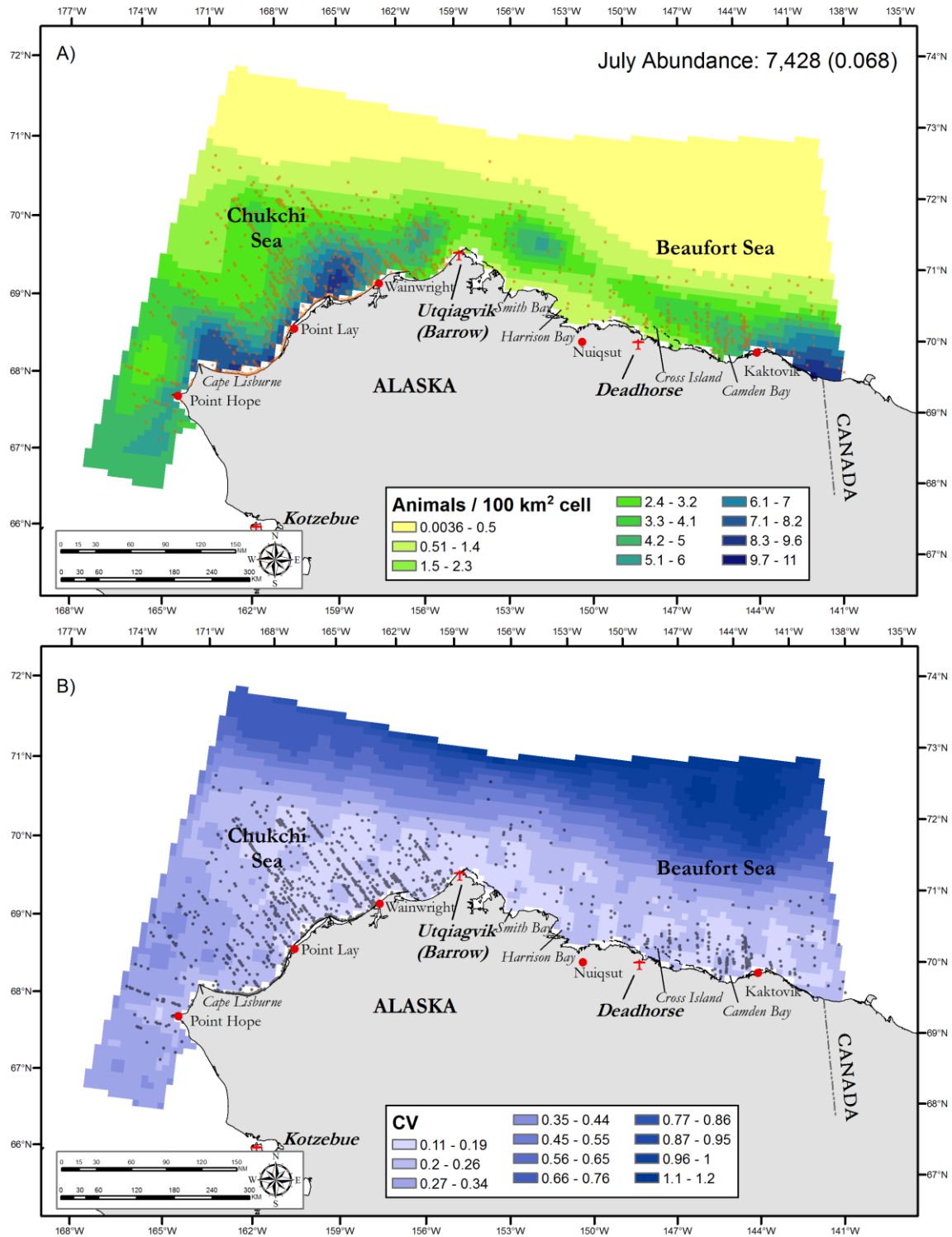


Figure 33. (A) Predicted densitology for small pinnipeds in July (2000-2016). Small pinnipeds observed on-transect are shown with orange dots. (B) Predicted CV surface.

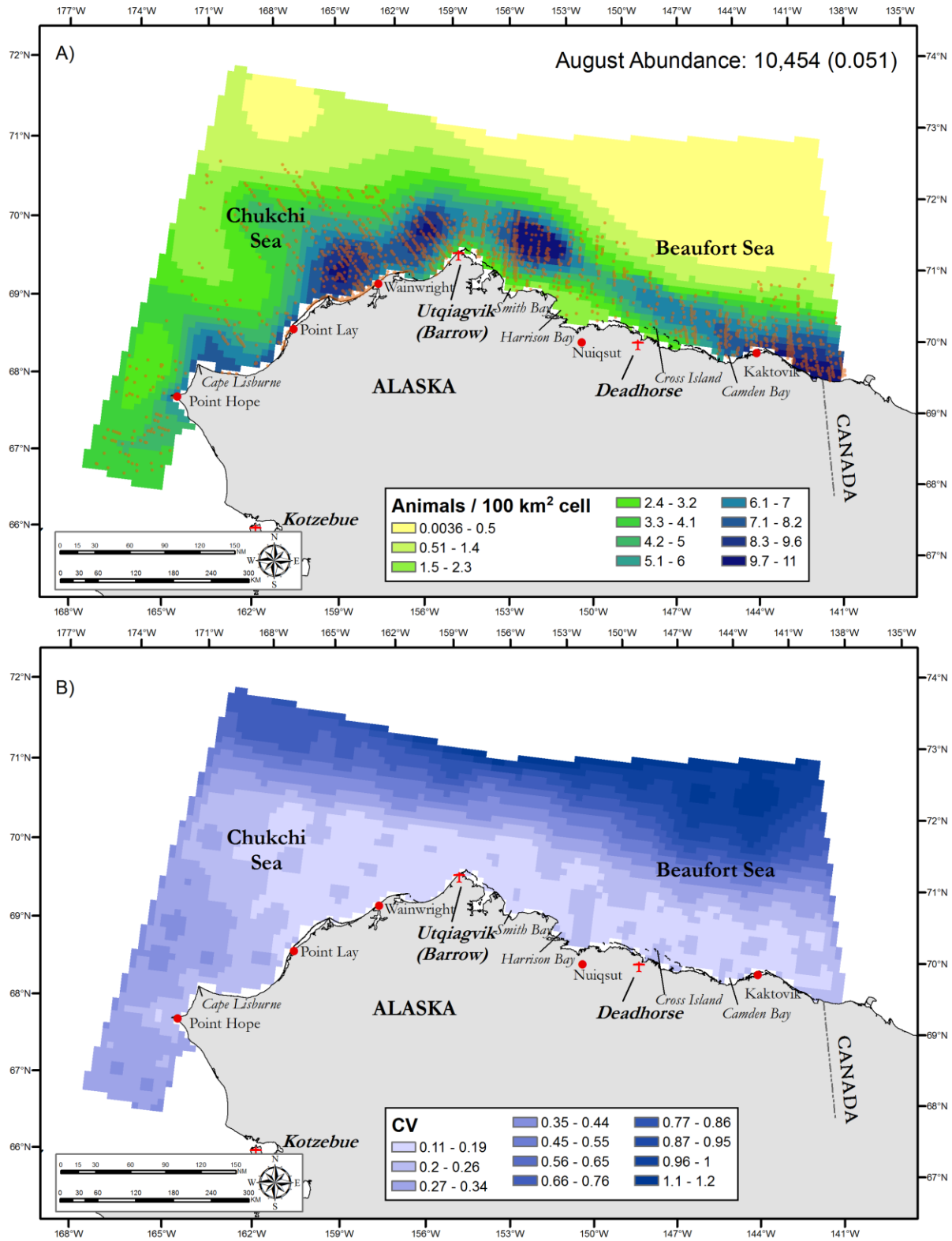


Figure 34. (A) Predicted densitology for small pinnipeds in August (2000-2016). Small pinnipeds observed on-transect are shown with orange dots. (B) Predicted CV surface.

Peak density near the Alaska/Canada border is highest in August (**Figure 34**) and September (**Figure 35**) - falling off in October (**Figure 36**).

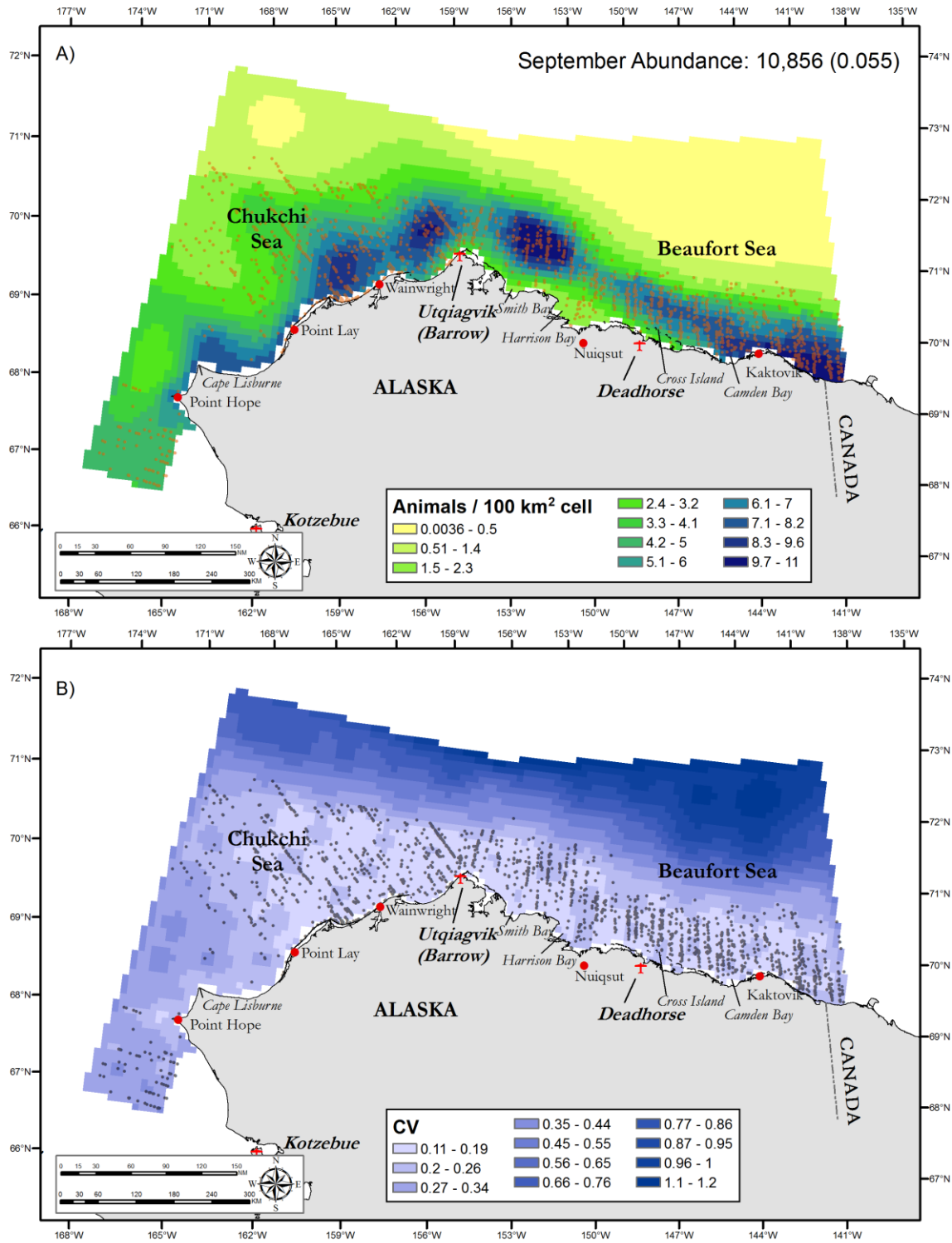


Figure 35. (A) Predicted densitology for small pinnipeds in September (2000-2016). Small pinnipeds observed on-transect are shown with orange dots. (B) Predicted CV surface.

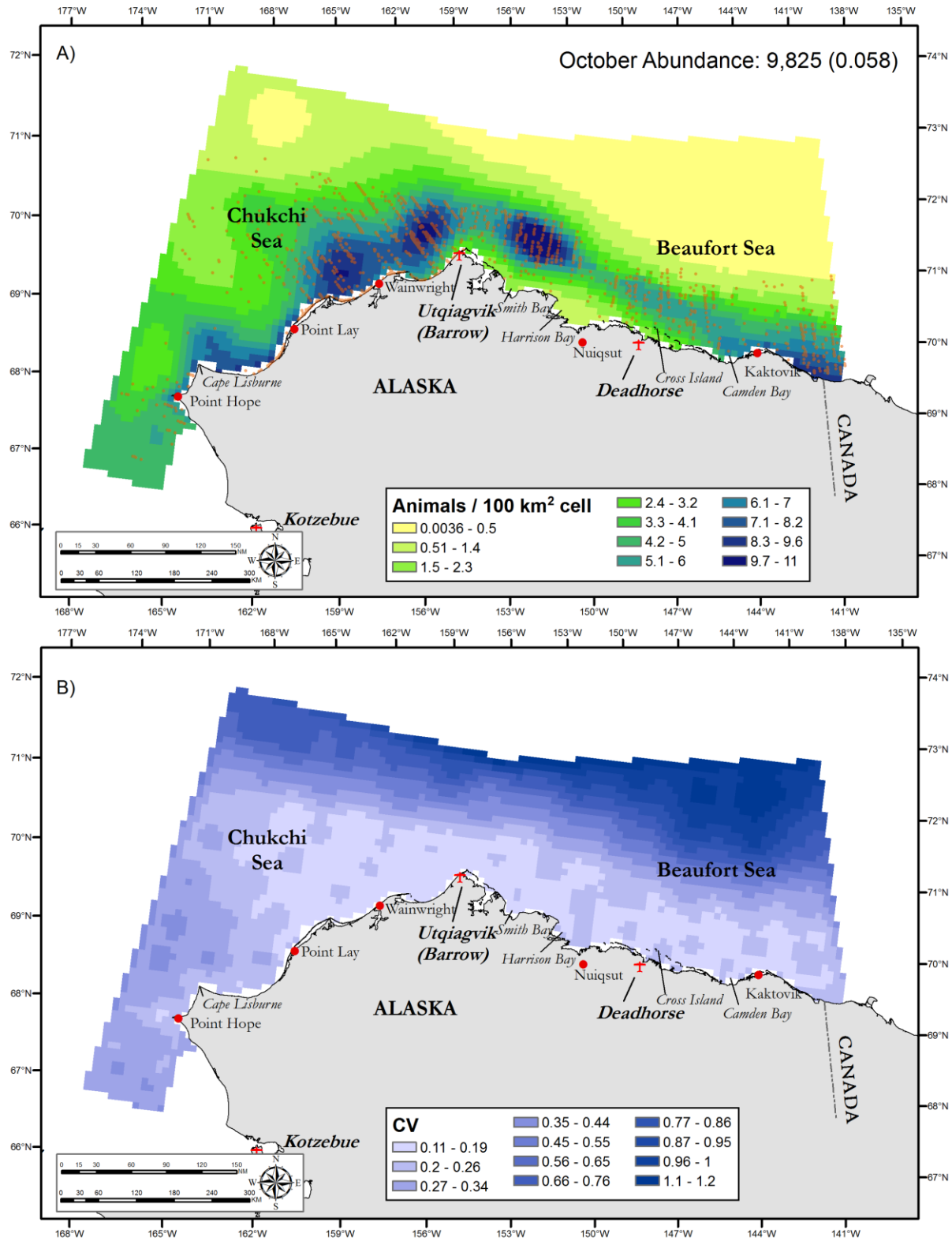


Figure 36. (A) Predicted densitology for small pinnipeds in October (2000-2016). Small pinnipeds observed on-transect are shown with orange dots. (B) Predicted CV surface.

Unidentified Pinnipeds

Predicted density patterns for the unidentified pinnipeds category (**Figure 37 A**) are strikingly different from the small pinnipeds category (**Figure 32 A**). While the highest densities are seen in Canadian waters, it appears that this is a combination of some sightings in specific months (especially August and October) as well as the static spatial smooth.

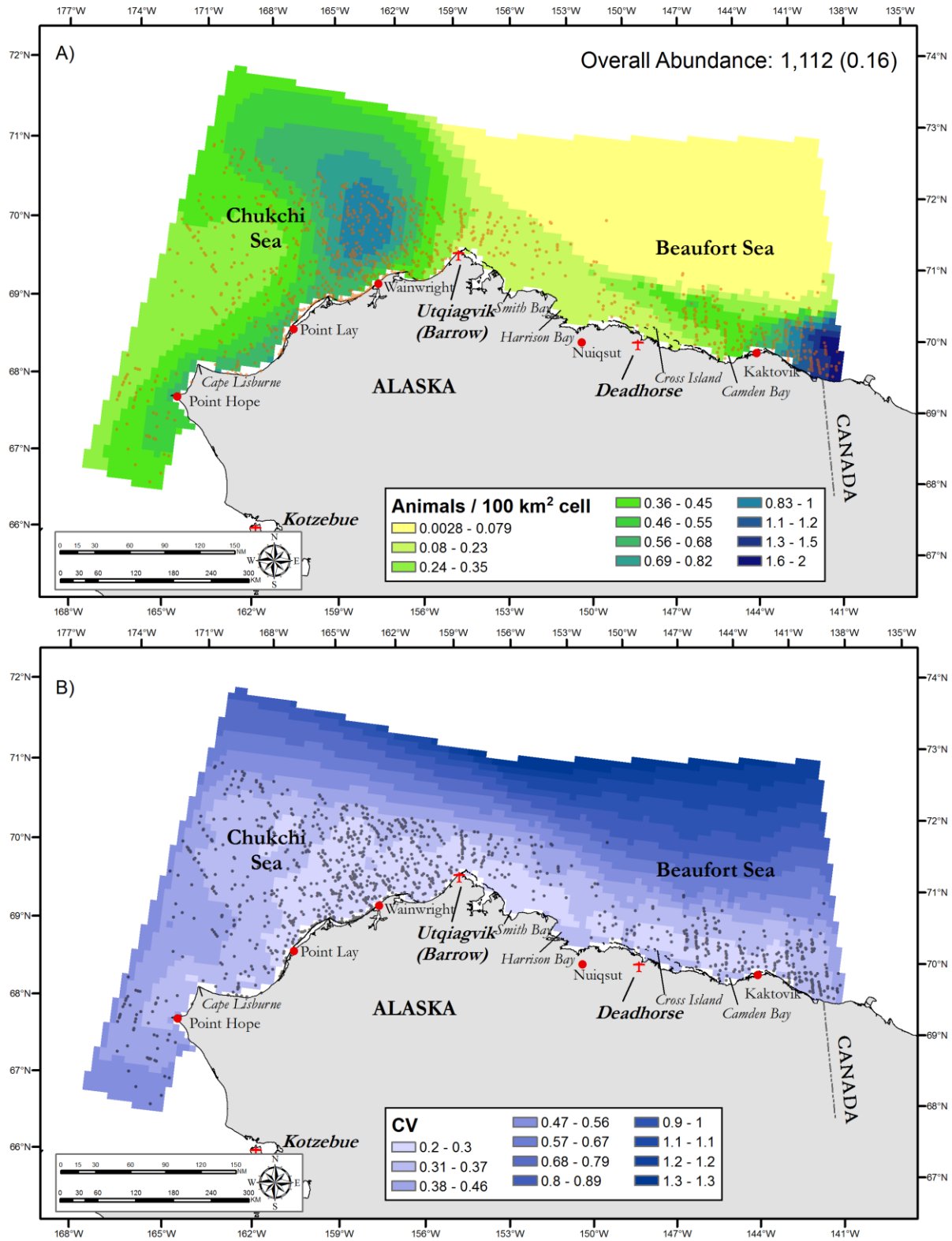


Figure 37. (A) Predicted densitology for unidentified pinnipeds (2000-2016). Unidentified pinnipeds observed on-transect are shown with orange dots. (B) Predicted CV surface.

The spatial pattern for monthly density is similar month to month, building toward a peak density in the Hannah Shoal region (northwest of Wainwright) in September (**Figures 38, 39, 40, 41**). The edge effect seen in Canadian waters in certain months is likely owing to the spatial smooth (e.g., **Figure 38 B**).

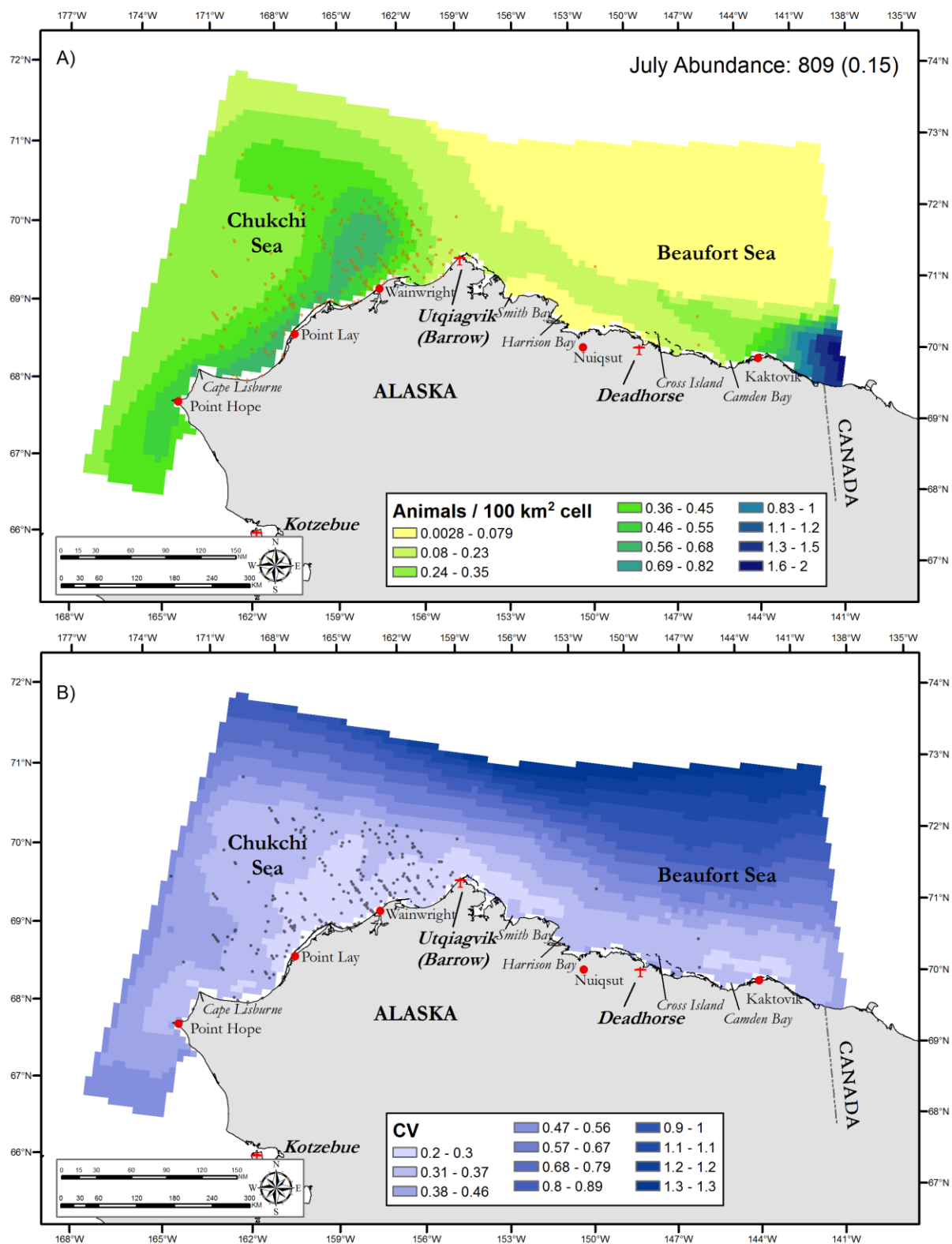


Figure 38. (A) Predicted densitology for unidentified pinnipeds in July (2000-2016). Unidentified pinnipeds observed on-transect are shown with orange dots. (B) Predicted CV surface.

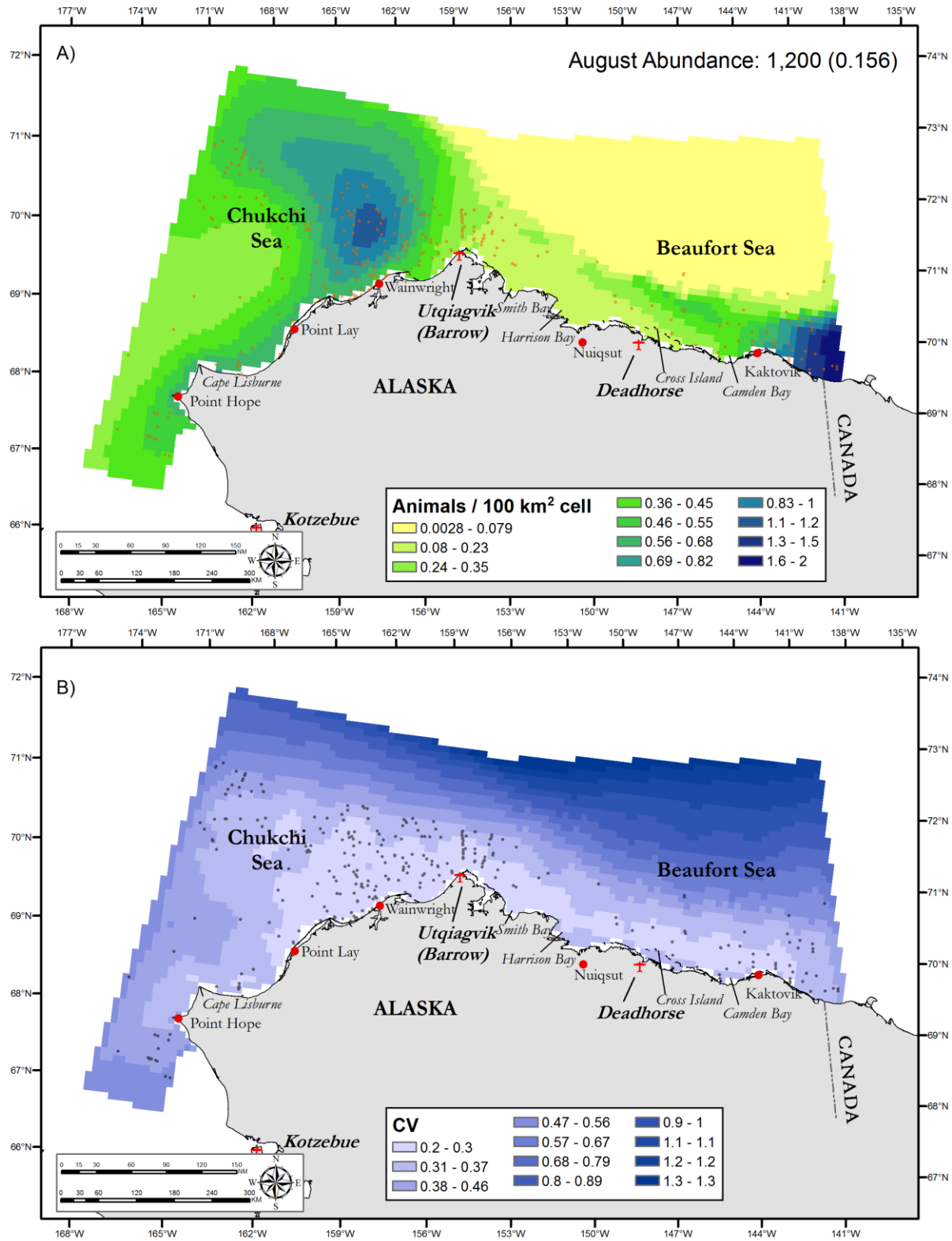


Figure 39. (A) Predicted densitology for unidentified pinnipeds in August (2000-2016). Unidentified pinnipeds observed on-transect are shown with orange dots. (B) Predicted CV surface.

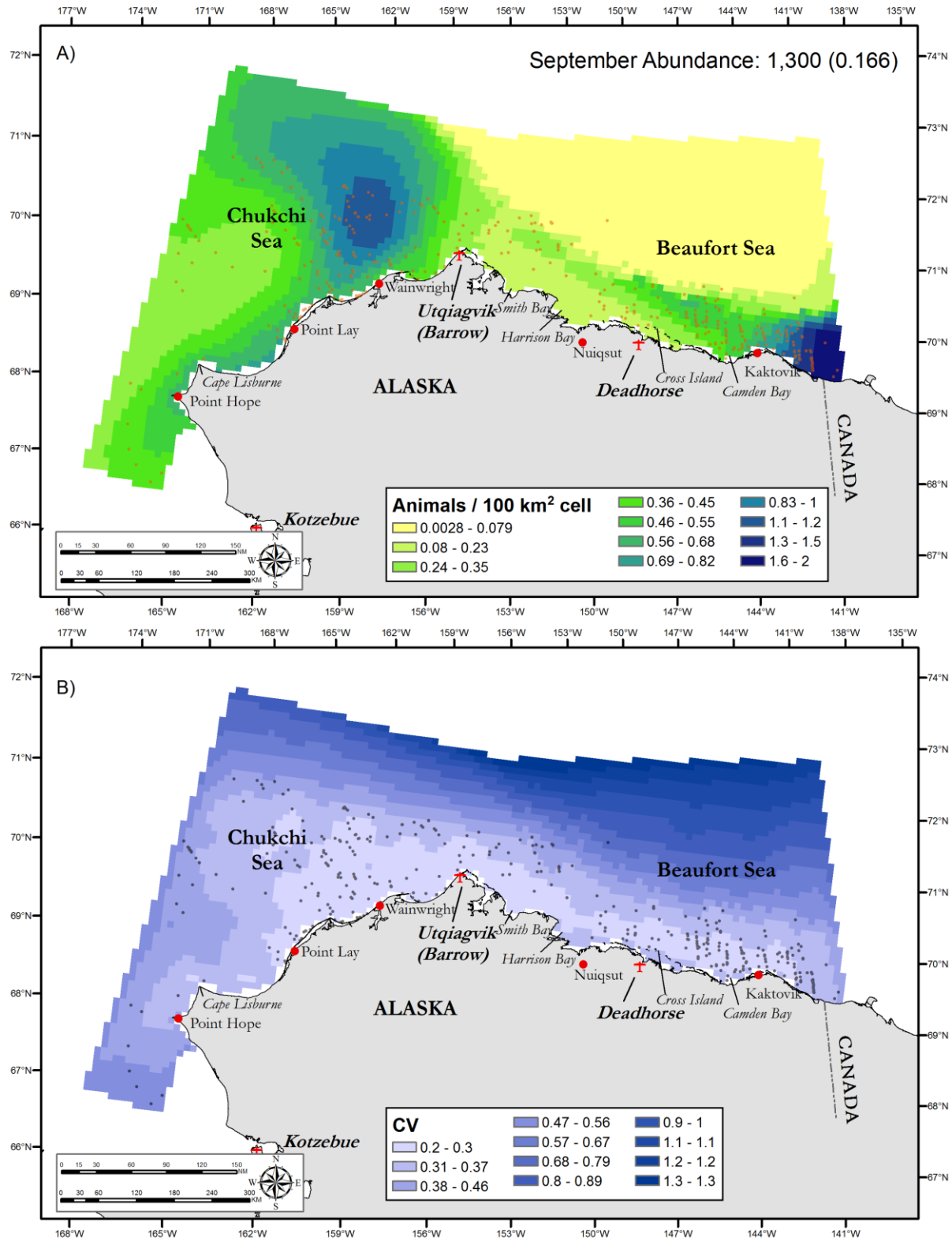


Figure 40. (A) Predicted densitology for unidentified pinnipeds in September (2000-2016). Unidentified pinnipeds observed on-transect are shown with orange dots. (B) Predicted CV surface.

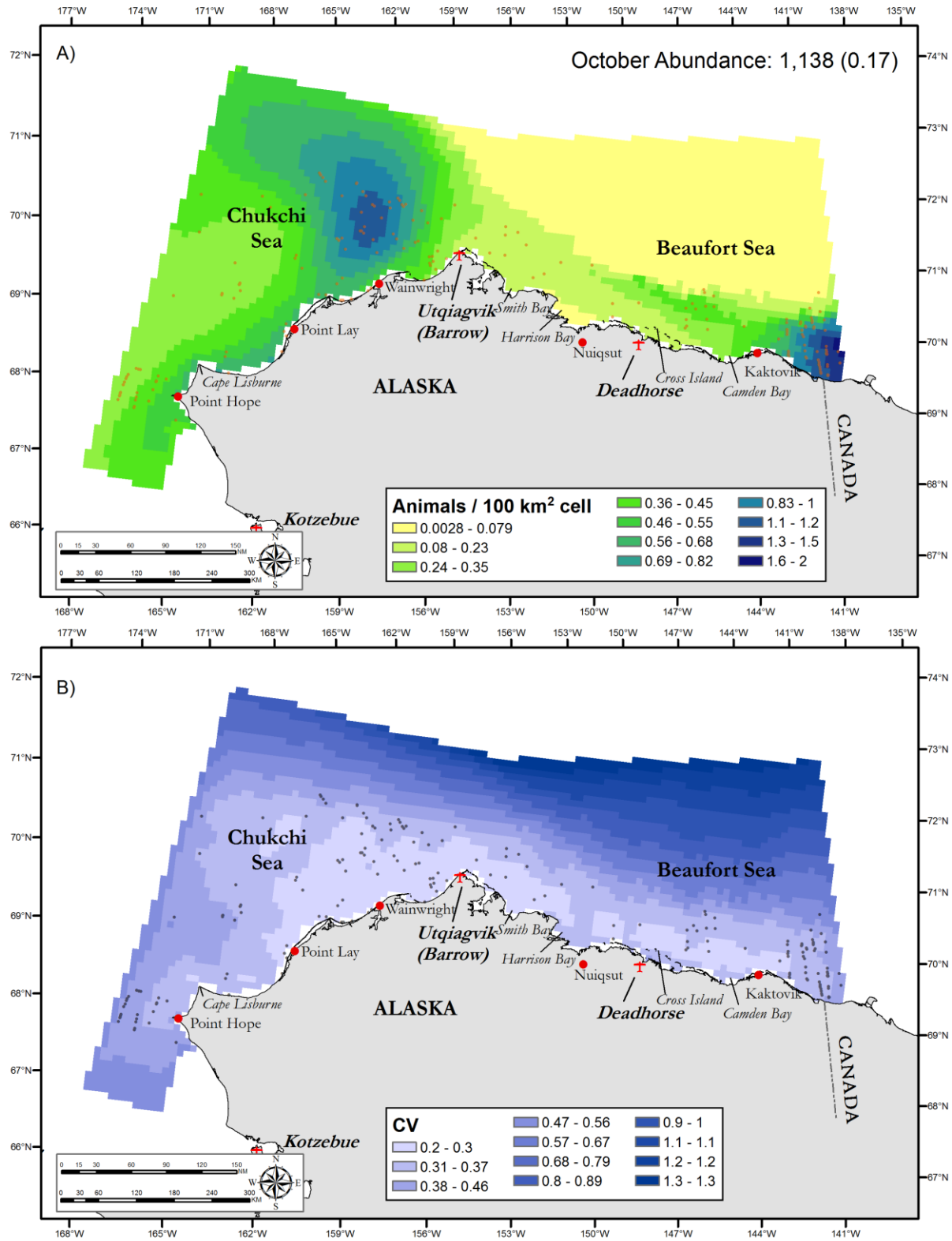


Figure 41. (A) Predicted densitology for unidentified pinnipeds in October (2000-2016). Unidentified pinnipeds observed on-transect are shown with orange dots. (B) Predicted CV surface.

Baleen Whales

Here we chose to use a simple model with only a spatial smooth predictor term. The reason is that when we include other dynamic covariates, we end up losing any spatial terms. The ones remaining in the model are Distance to Ice Edge, and Distance to 200-m Isobath. As a result the bottom corner of the map is high for both of those terms, and we end up with wildly erroneous predictions (e.g., 800,000 baleen whales in one month).

Below are the predicted density and CV surfaces for the baleen whale group. As with bearded seals, since there are no dynamic rasters, we only show the densitology. Highest densities (**Figure 42 A**) are in the areas of lowest predicted uncertainty (**Figure 42 B**). Highest densities are in the farthest south area of ASAMM (**Figure 42**).

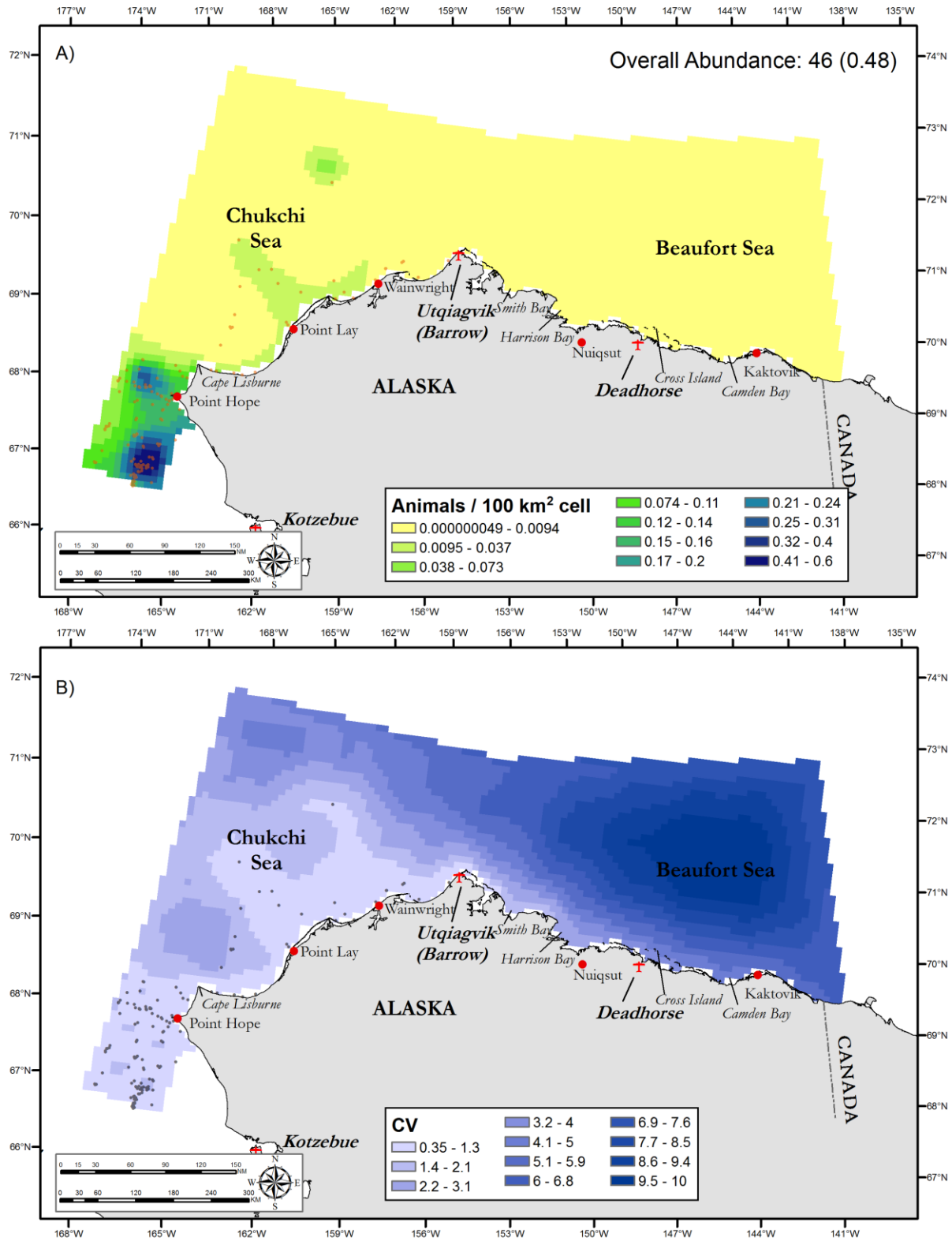


Figure 42. (A) Predicted densitology for baleen whales (2000-2016). Baleen whales observed on-transect are shown with orange dots. (B) Predicted CV surface.

Discussion

We have documented the distribution, abundance, and predicted density of eight different species and marine mammal guilds across the eastern Chukchi and Alaskan Beaufort seas. This represents an important first milestone to synoptically understand distribution patterns in this area. As the climate changes, we presume that a) species distribution patterns may change, and b) new areas will be available for anthropogenic use. Having a baseline for reference in future years will allow us to quantify the changes that may be observed. In addition, because we have predictive distribution patterns with uncertainty, we have the ability to estimate how many AMMs may be impacted by anthropogenic activity. Here we discuss species-specific predictions, issues that arose during modeling, and suggestions for future research.

Species-level Predictions

We have generated spatial predictions for eight species and species groups. The first four species - bowheads, belugas, gray whales, and walrus - have a large number of sightings over the years. With the exception of high abundances predicted in the initial run in three embayments for bowheads, results were favorably reviewed by AMM experts in May 2017. We have made significant changes since that meeting, incorporating expert feedback to improve the models, and also to extend predictions farther north for bowheads and belugas. In contrast to these four, the other four groups (bearded seal, baleen whales, small pinnipeds, and unidentified pinnipeds) have fewer sightings, and the pinniped data were collected under sub-optimal conditions (i.e. higher than optimal survey altitudes). Despite these limitations, the predictions represent an important first step.

Bowhead Whales

The predicted density--both the spatial patterns (**Figure 11**) and the timing of the number(s) of whales in each month (**Table 12**)--highlights the importance of nearshore waters in the Alaskan Beaufort, and how the numbers of whales changes over the season. Even with the northward extrapolation essentially no bowheads are predicted north of approximately 72.5 °N (**Figure 11**). We know, however, from tagging data that bowheads do migrate farther north, e.g., Citta et al. (2015). The spatial smooth plays a strong role in these predictions, therefore incorporating more dynamic covariates that may predict the near- and offshore habitat more closely may improve these estimates. Alternatively, incorporating an interaction between the spatial smooth and a month term, may account for spatial variation over time. Lastly, there exist no double platform surveys in the ASAMM data that would allow us to use a more refined estimate of $g(0)$ for the availability bias. It is plausible that a better value for this parameter would increase the accuracy of the population size estimates.

Beluga Whales

The estimated abundance of belugas in the ASAMM and extrapolated area is substantially higher than the bowheads (**Table 12**). In contrast to bowheads, belugas are seen consistently farther offshore (**Figure 16**) - responding apparently to the depth gradients

associated with the shelf break. One area of future research is to examine the predicted area at 74 °N at the western side of the extrapolated area. Specifically, to examine the environmental characteristics of the area and co-locate known records of satellite-tagged belugas to see if individuals have made use of this area in the past. As with bowheads, while the dynamic covariates improved model fit, the ice covariates were not strong predictors (**Appendix B**); rather the (static) Depth and Distance to 200m Isobath covariates were much stronger patterning variables. We envision the Regional Ocean Modeling System (ROMS) covariates (see Future Work section in the discussion) to possibly predict beluga habitat with greater predictive power.

Gray Whales

The distribution of gray whales is captured well in and around the area north of Wainwright, and west of Point Barrow (**Figure 21**). However, the observations in the northwestern corner of block 23 are not adequately captured (**Figure 21**), and the uncertainty is higher in this block (**Figure 21B**). The highest number(s) of sightings in block 23 appear to be in October (**Figure 25**). What appears to be happening is that for gray whales, the strongest predictor after the spatial smooth is the Distance to 200-m Isobath (**Figure 43**), with higher distances yielding lower predicted abundances (**Appendix B**). If we examine this covariate, it is clear that this area in block 23 is far from this isobath; hence the lower predicted abundances, even though a lot of gray whales are sighted in this area. Having a model that accounted for a spatially varying response to covariates likely would improve predictions in this situation. A different way to address this would be to include a time-specific smooth.

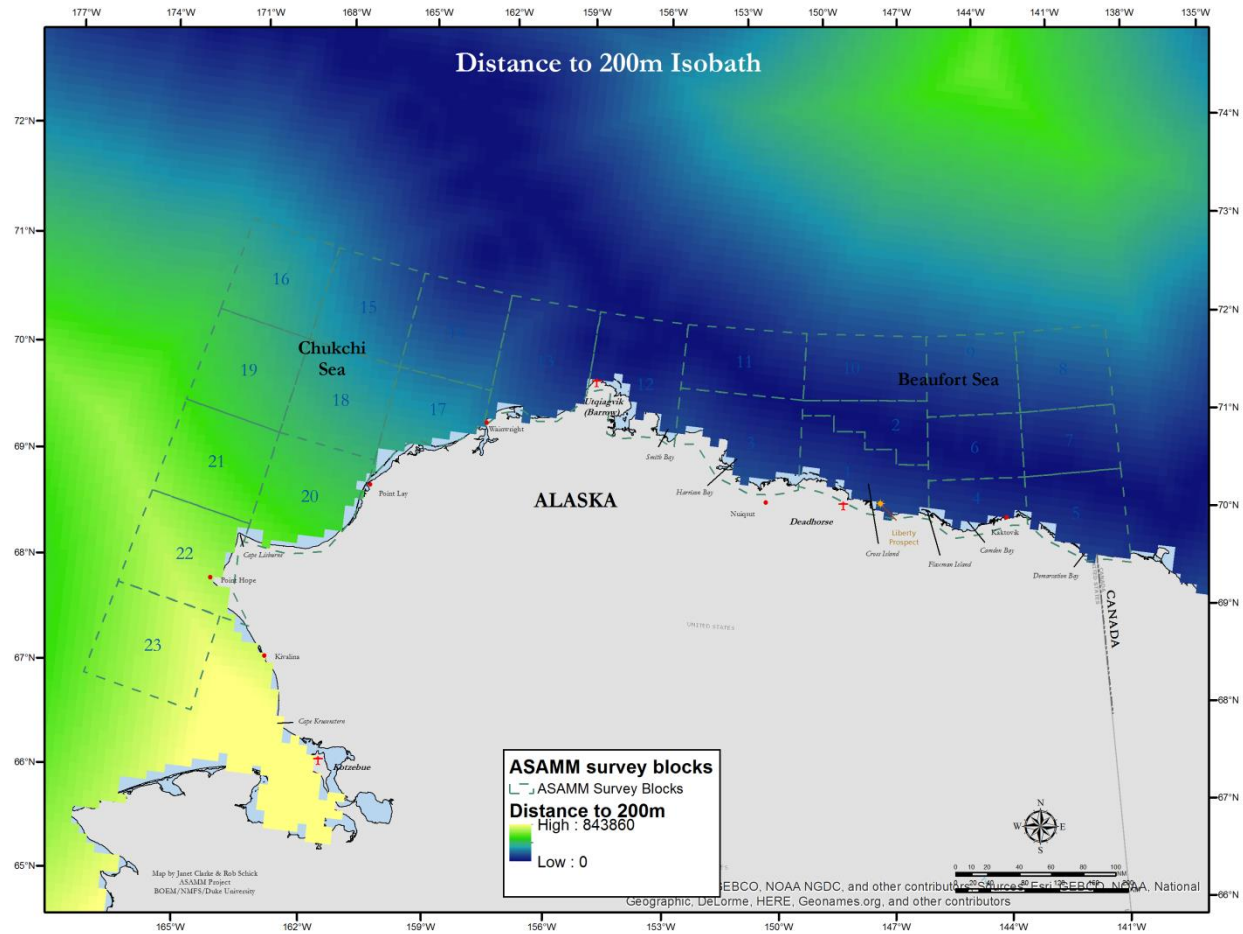


Figure 43. Plot of the Distance to 200-m Isobath covariate. Note how far areas in block 23 are from the 200-m isobath covariate (i.e., they have high distance values).

Walrus

Across all months, predicted walrus densities were highest in the Hannah Shoal region northwest of Point Barrow (**Figures 27, 28, 29, 30**). These high density areas were also areas of consistently low uncertainty. The walrus model outputs indicated a strong effect of ice concentration, although the spatial smooth had a strong relationship as well (**Appendix B**). Accordingly, it will be interesting to explore the relationship with more benthic data, as well as perhaps some dynamic "distance to ice floe" representations of the larger floes that walrus use for haulouts, which might show more fine-grained spatial response.

Bearded Seals

Though we have a decent number of sightings of bearded seals (**Figure 31**), the high-density predictions come with higher uncertainty than for other species. Compared to the other Arctic seals, bearded seals are slightly easier to identify from the air, owing to their unique body shape (Janet Clarke, Leidos Corporation, *pers. comm.*); however survey altitudes are still higher than optimal for these smaller species. Therefore, it is not

surprising that the predictions are less certain. There is evidence in the literature that competitive exclusion exists between walrus and bearded seals (Simpkins et al. (2003)). While it appears this may be true at first glance (**Figures 26, 31**), we did test this quantitatively and found no significant (negative) relationship between walrus density and bearded seal abundance (results not shown).

Small Pinnipeds & Unidentified Pinnipeds

Though we have generated predicted density surfaces for these two groups, there does not exist much in the literature about pinniped distribution in the open-water period. As noted earlier, most of the extensive research has been done at the haulout locations during the ice period. Because the planes fly at higher altitudes during the ASAMM study, this makes species level identification a challenge. Further work, possibly with informed priors in a Bayesian setting, may elucidate some of the species-level differences. However, the lack of data during the open-water period, which could be compared with our predictions, will make such an analysis difficult. The small-pinnipeds surfaces look more realistic, but it will be worth exploring how these patterns might change with the inclusion of additional covariates. A final challenge with the pinniped data is that the data collection has been uneven over the years of the survey (Janet Clarke, Leidos Corporation, *pers. comm.*). This is not surprising, because ASAMM has always been a large whale survey, but we mention it to highlight the differential survey effort paid to the species and species-groups herein.

Baleen Whales

While the model results appear to be quite consistent with the observations, we note two issues that bear further examination. First, the predicted model included no dynamic or static covariates aside from the spatial smooth. Second, we chose a set of covariates for all of the core AMMs and Arctic migrants (gray whales). However, from ecological first principles, we would not expect these different species to respond to the same set of covariates. The sub-Arctic migrants like fin and minke whales, are no doubt using this habitat to feed. Accordingly, if we can acquire covariates that represent their prey, or a proxy for prey, then the explanatory and predictive power should increase.

Modeling and Analytical Caveats

We followed a standard Distance and density surface modeling (Miller et al. (2013)) approach in this analysis, and while we included dynamic covariates, in all cases the spatial smooth was the dominant predictor variable (**Appendix B**). In some cases, e.g., bowhead whales, this led to predictions whose spatial patterns changed little across the months. We will discuss this further in the Future Work section, but we note that there is likely a spatial and temporal mismatch between some of the covariates and some of the predicted species distributions. Refining some of the abundance models to include a dynamic response in time to specific covariates may prove beneficial.

There are a few features of the ASAMM data that violate some of the strictures of Distance sampling methodology. Once such is the presence of a coastal transect, which extends from Point Barrow to Point Hope. We did not treat this transect differently from other transects,

which were typically oriented perpendicular to the shore and the bathymetry (**Figure 1**). Because this transect parallels the shore, it is possible that detection probabilities and species density are not equal on each side. One possible fix would be to use only the sightings from the ocean side of the plane, and/or further right truncating the shoreward sightings.

Although management decisions need to be made on the species level, we chose to group some of the species. This was done for different reasons, though the grouping has similar problems in each case. For pinnipeds, there are four primary ice-associated seal species in the region. However, few of these are identifiable to the species level at the altitudes flown during the ASAMM study (Peter Boveng, MML, *pers. comm.*). As a result of this lumping, the species-specific patterns and responses to covariates are likely blurred out. Though there have been attempts at using Bayesian statistics to impute species identification (Conn et al. (2013)), these required auxiliary information like double observer trials, which do not exist for the ASAMM study. With the baleen whale group, comprised of fin whales, humpback whales, and minke whales, we chose to lump them together to increase sample size (see **Appendix A, Figure 51**). Even though we can readily identify each of these three species, the lumping likely leads to blurring of species-specific responses.

We predicted beluga whale density to the northernmost boundary and saw high predicted densities well outside of the sampled area (**Figure 16**). Two beluga stocks are known to be in this area - the Eastern Chukchi Stock and the Beaufort Sea Stock (Allen and Angliss 2015). It is not clear how these stocks may overlap in this area, nor if they respond to the same covariates in the same fashion. While this will be difficult to tease apart, it is worth considering. For example, it is possible that belugas seen west of Point Barrow in areas like the Kasegaluk Lagoon may be responding to a different set of covariates than those seen east of Point Barrow.

Based on feedback in our expert review meeting in May, 2017, we implemented the soap film smoother to address the over-prediction of bowheads in two bays with few sightings (**Figure 44**). The inclusion of the soap film smoother has improved predictions, especially in Smith Bay and Camden Bay (**Figure 11**). However, in some areas predictions are high when few whales were seen, e.g. Harrison Bay in **Figure 14**. It is possible that with different covariates some of these predictions close to shore may change.

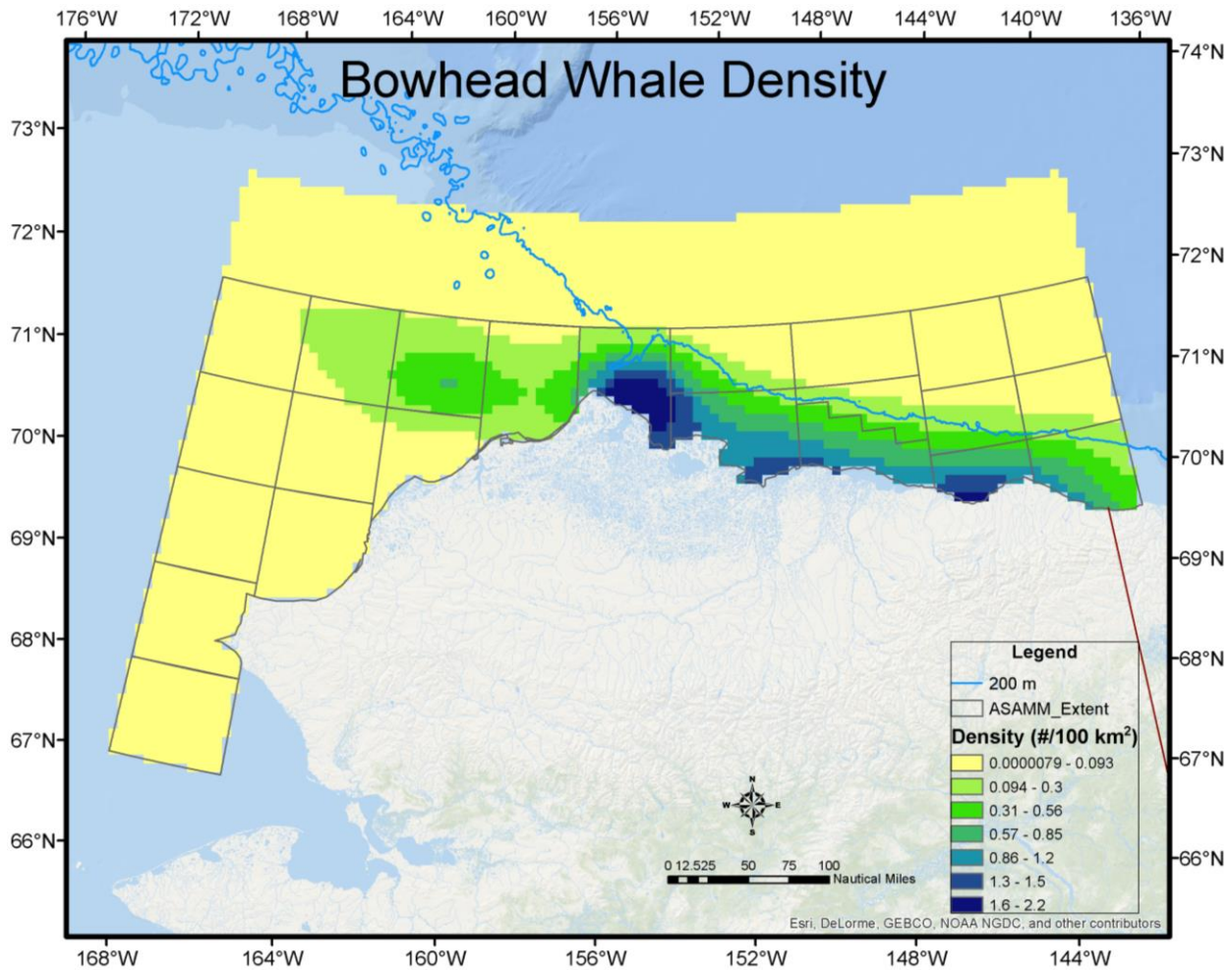


Figure 44. Initial predicted density for bowhead whales in the ASAMM study area prior to inclusion of the soap smoother.

Future Work

Though we have generated predicted density models for these eight groups--including six of which had dynamic monthly predictions--there is scope for improvement and expansion of the analysis. These include exploring additional dynamic covariates, including additional data, and exploring methods of modeling the species jointly.

Covariates

Our initial models included all static covariates. For example, in May 2017 at the expert review meeting, we presented the modeled relationships between abundance and three static covariates: 1) Depth, 2) Slope, and 3) a spatial smooth. We incorporated feedback from AMM experts, and built on the models through the inclusion of additional static and new dynamic covariates (**Tables 9, 10**). While these led to improved models in terms of deviance explained, there were still some final models that require additional refinement. We suspect that this refinement may benefit from the inclusion of new predictor

covariates. For example, with bowheads, the final model, though improved with the inclusion of dynamic covariates, still explained relatively little deviance (**Table 11**). In addition, if you compare the monthly predictions (**Figures 12, 13, 14, 15**), it is apparent that the impact of the spatial smooth is driving much of the observed patterns. Research into the distribution of bowhead whales has suggested a very dynamic and specific response to the presence of krill (Ashjian et al. 2010). These responses likely occur at very short time scales, much shorter than the monthly resolution at which we are modeling. However, it is clear that, while ice concentration may play an explanatory role in the timing of migration into the area, this covariate is likely not a good predictor of fine-scale distribution and abundance near the coast. The reason(s) for this are that the ice has largely receded from coastal areas in summer and fall. This means that we need better covariates to try and explain the patterns we are observing and predicting, including an interaction between time and the spatial smooth. To address this, we have obtained a pan-Arctic ROMS model that we will incorporate in the next round of analysis (Danielson et al. (2014), Danielson et al. (2017)).

We have worked with this type of covariate data previously (Schick et al. (2013)), and they have been used successfully in similar density-modeling efforts on the U.S. West Coast (Becker et al. (2016)). One of the primary advantages of using ROMS data is that we avoid the issue of clouds obscuring remotely sensed products. A second advantage is that we can examine covariates at depth (Schick et al. (2013)). Because marine mammals must regularly return to the surface to breathe, and because remotely sensed covariates offer surface-level predictors, this is often the first correlation that can be examined. However, biological and physical oceanographic factors occur at depth as well. Locating features at depth (Citta et al. (2015), Ashjian et al. (2010)) that may predict AMM distribution should improve model fit.

Additional Data Sources

While we had a rich database to work with in the ASAMM data, the dataset is limited in spatial extent. This needs to be addressed in the next phase of modeling. Specifically, we will explore the use of datasets on bowhead and beluga whales that were collected in the Canadian Beaufort Sea (Lois Harwood, DFO, *pers. comm.*) to broaden predictions across the entire Beaufort Sea. We will also include data gathered in the Bering Sea, although a pan-Arctic approach to modeling may prove difficult, because the Bering and Chukchi seas represent drastically different ecosystems. We may end up with separate predictions for the Bering Sea and for the Chukchi Sea.

In addition to the data analyzed herein, we will include another year's worth of the ASAMM data in future efforts. Also, MML conducted aerial surveys for beluga whales in a region just south of the ASAMM study area, Kotzebue Sound, Alaska. We will incorporate these data as well, which should augment and improve the predictions for the Chukchi Sea.

We stress that there are many different types of marine mammal data in this area, from standard line-transect data we have analyzed here (Ferguson and Clarke (2013)), to acoustics data (Moore et al. (2006)), and telemetry data (Citta et al. (2015), Jay, Fischbach, and Kochnev (2012), Suydam, Lowry, and Frost (2005)). Clearly, not all of these types fit

into a standard Distance-based density-surface approach. However, they can still be useful in at least two ways. First, we can use them to validate model predictions from the line-transect data. Second, they can be used as part of different analytical techniques (e.g. joint species modeling in a Bayesian framework) (see next section).

Modeling Species Jointly

Recent Bayesian species-distribution modeling efforts have highlighted the utility of jointly modeling all species within a community (Clark et al. (2017), Ovaskainen et al. (2017)). Although these represent a significant departure from standard Distance-based methods, they also represent an interesting potential avenue of exploration, if for no other reason than capturing and modeling species interactions at the same time. Specifically, by incorporating a covariance matrix for all the species involved in the analysis, we can parameterize the degree to which certain species in the Arctic respond to each other. This is especially true as new sub-Arctic migrants increasingly forage in the Arctic. Their presence may cause core Arctic species to respond in ways not yet understood.

One additional benefit to this approach is that, because we would be modeling the species jointly, we can borrow strength across the species. Specifically, inference about the distribution and abundance of rarer species could be made stronger with more data. Of course, extremely rare species will always be challenging, but there is promise in this avenue of research. As new models and new data become available, there will be the challenge of figuring out which model is best to use within a management and regulatory setting---a non-trivial task. However, we argue that the more analytical approaches that are brought to bear on different datasets, the more inference we will draw.

Summary

We have presented a synoptic, dynamic depiction of predicted density for AMMs in the Chukchi and Alaskan Beaufort seas. Though preliminary, the results for the better-studied species are consistent with the current literature. For the less-well studied species, e.g. ice-associated seals during the open-water period, our results offer some of the first density predictions for these species in these areas. These results offer a baseline going forward. First, by going through this initial exercise, we have learned more about several species that were not the main focus of the ASAMM aerial surveys. We have also realized what needs to be explored further in terms of introducing new covariates, as well as incorporating additional datasets, which should improve the model fits, and expand the spatial scope of our understanding of AMM distribution. Finally, and perhaps of highest importance, this snapshot provides an up-to-date summary of AMM distribution as the Arctic continues to change.

Literature Cited

- Aerts, L.A.M., A.E. McFarland, B.H. Watts, K.S. Lomac-MacNair, P.E. Seiser, S.S. Wisdom, A.V. Kirk, and C.A. Schudel. 2013. "Marine Mammal Distribution and Abundance in an Offshore Sub-Region of the Northeastern Chukchi Sea during the Open-Water Season." *Cont. Shelf Res.* 67: 116–26.
- Allen, B.M., and R.P. Angliss. 2015. *Alaska Mammal Stock Assessments, 2014*. NOAA Tech Memo NMFS-AFSC-301. National Marine Fisheries Service, Seattle, Washington.
- Ashjian, C.J., S.R. Braund, R.G. Campbell, J.C. George, J. Kruse, W. Maslowski, S.E. Moore, et al. 2010. "Climate Variability, Oceanography, Bowhead Whale Distribution, and Iñupiat Subsistence Whaling Near Barrow, Alaska." *Arctic* 63 (2): 179–94.
- Becker, E.A., K.A. Forney, P.C. Fiedler, J. Barlow, S.J. Chivers, C.A. Edwards, A.M. Moore, and J.V. Redfern. 2016. "Moving Towards Dynamic Ocean Management: How Well Do Modeled Ocean Products Predict Species Distributions?" *Remote Sens.* 8 (2): 149. doi:10.3390/rs8020149.
- Bengtson, J.L., L.M. Hiruki-Raring, M.A. Simpkins, and P.L. Boveng. 2005. "Ringed and Bearded Seal Densities in the Eastern Chukchi Sea, 1999–2000." *Polar Biol.* 28 (11): 833–45.
- Buckland, S.T., D.R. Anderson, K.P. Burnham, J.L. Laake, D.L. Borchers, and L. Thomas. 2001. *Introduction to Distance Sampling: Estimating Abundance of Biological Populations*. Oxford University Press, New York.
- Buckland, S.T., E.A. Rexstad, T.A. Marques, and C.S. Oedekoven. 2015. *Distance Sampling: Methods and Applications*. Springer International Publishing, Cham, Switzerland.
- Burns, J.J., and S.J. Harbo. 1972. "An Aerial Census of Ringed Seals, Northern Coast of Alaska." *Arctic* 25 (4): 279–90.
- Burns, J.J., L.H. Shapiro, and F.H. Fay. 1981. "Ice as Marine Mammal Habitat in the Bering Sea." Pages 781–97 in *The Eastern Bering Sea Shelf: Oceanography and Resources. Volume 2*. (J.A. Calder, and D.W. Hood, eds.) University of Washington Press, Seattle, Washington.
- Burns, J.J., J.J. Montague, and C.J. Cowles, eds. 1993. *The Bowhead Whale*. Society for Marine Mammalogy, Lawrence, Kansas.
- Citta, J.J., L.T. Quakenbush, S.R. Okkonen, M.L. Druckenmiller, W. Maslowski, J. Clement-Kinney, J.C. George, et al. 2015. "Ecological Characteristics of Core-Use Areas Used by Bering-Chukchi-Beaufort (BCB) Bowhead Whales, 2006–2012." *Prog. Oceanogr.* 136: 201–22.
- Clark, J.S., D. Nemergut, B. Seyednasrollah, P.J. Turner, and S. Zhang. 2017. "Generalized Joint Attribute Modeling for Biodiversity Analysis: Median-Zero, Multivariate, Multifarious Data." *Ecol. Monogr.* 87 (1): 34–56.

- Clarke, J.T., A.S. Kennedy, and M.C. Ferguson. 2016. "Bowhead and Gray Whale Distributions, Sighting Rates, and Habitat Associations in the Eastern Chukchi Sea, Summer and Fall 2009–15, with a Retrospective Comparison to 1982–91." *Arctic* 69 (4): 359–77.
- Conn, P.B., B.T. McClintock, M.F. Cameron, D.S. Johnson, E.E. Moreland, and P.L. Boveng. 2013. "Accommodating Species Identification Errors in Transect Surveys." *Ecology* 94 (11): 2607–18.
- Conn, P.B., J.M. Ver Hoef, B.T. McClintock, E.E. Moreland, J.M. London, M.F. Cameron, S.P. Dahle, and P.L. Boveng. 2014. "Estimating Multispecies Abundance Using Automated Detection Systems: Ice-Associated Seals in the Bering Sea." *Methods Ecol. Evol.* 5 (12): 1280–93.
- Danielson, S.L., T.J. Weingartner, K.S. Hedstrom, K. Aagaard, R. Woodgate, E. Curchitser, and P.J. Stabenro. 2014. "Coupled Wind-Forced Controls of the Bering–Chukchi Shelf Circulation and the Bering Strait Throughflow: Ekman Transport, Continental Shelf Waves, and Variations of the Pacific–Arctic Sea Surface Height Gradient." *Prog. Oceanogr.* 125: 40–61.
- Danielson, S.L., L. Eisner, C.Ladd, C. Mordy, L. Sousa, and T.J. Weingartner. 2017. "A Comparison Between Late Summer 2012 and 2013 Water Masses, Macronutrients, and Phytoplankton Standing Crops in the Northern Bering and Chukchi Seas." *Deep Sea Res. Part 2 Top. Stud. Oceanogr.* 135: 7–26.
- Dunton, K.H., J.L. Goodall, S.V. Schonberg, J.M. Grebmeier, and D.R. Maidment. 2005. "Multi-Decadal Synthesis of Benthic–Pelagic Coupling in the Western Arctic: Role of Cross-Shelf Advective Processes." *Deep Sea Res. Part 2 Top. Stud. Oceanogr.* 52 (24): 3462–77.
- Fay, F.H. 1982. *Ecology and Biology of the Pacific Walrus, Odobenus rosmarus divergens Illiger*. North American Fauna No. 74 US Fish & Wildlife Service, Washington, DC.
- Ferguson, M.C., and J.T. Clarke. 2013. *Estimates of Detection Probability for BWASP Bowhead Whale, Gray Whale, and Beluga Sightings Collected from Twin Otter and Aero Commander Aircraft, 1989 to 2007 and 2008 to 2011*. NOAA Tech Memo NMFS-AFSC-261. National Marine Fisheries Service, Seattle, Washington.
- Forney, K.A., and J. Barlow. 1998. "Seasonal Patterns in the Abundance and Distribution of California Cetaceans, 1991–1992." *Mar. Mamm. Sci.* 14 (3): 460–89.
- George, J.C., J. Zeh, R. Suydam, and C. Clark. 2004. "Abundance and Population Trend (1978–2001) of Western Arctic Bowhead Whales Surveyed near Barrow, Alaska." *Mar. Mamm. Sci.* 20 (4): 755–73.
- Grebmeier, J.M., L.W. Cooper, H.M. Feder, and B.I. Sirenko. 2006. "Ecosystem Dynamics of the Pacific-Influenced Northern Bering and Chukchi Seas in the Amerasian Arctic." *Prog. Oceanogr.* 71 (2-4): 331–61.
- Harwood, L.A., J. Auld, A. Joynt, and S.E. Moore. 2009. *Distribution of Bowhead Whales in the SE Beaufort Sea during Late Summer, 2007–2009*. DFO Can. Sci. Advis. Sec. Res. Doc 2009/111.

- Harwood, L.A., T.G. Smith, J.C. Auld, H. Melling, and D.J. Yurkowski. 2015. "Seasonal Movements and Diving of Ringed Seals, *Pusa hispida*, in the Western Canadian Arctic, 1999–2001 and 2010–11." *Arctic* 68 (2): 193–209.
- Hauser, D.W., K.L. Laidre, H.L. Stern, S.E. Moore, R.S. Suydam, and P.R. Richard. 2017. "Habitat Selection by Two Beluga Whale Populations in the Chukchi and Beaufort Seas." *PLoS One* 12 (2): e0172755. <https://doi.org/10.1371/journal.pone.0172755>
- Hedley, S.L., and S.T. Buckland. 2004. "Spatial Models for Line Transect Sampling." *JABES* 9 (2): 181–99.
- Heide-Jørgensen, M.P., K.L. Laidre, S. Fossette, M. Rasmussen, N.H. Nielsen, and R.G. Hansen. 2014. "Abundance of Walruses in Eastern Baffin Bay and Davis Strait." *NAMMCO Sci. Publ.* 9: 159–71.
- Jay, C.V., A.S. Fischbach, and A.A. Kochnev. 2012. "Walrus Areas of Use in the Chukchi Sea during Sparse Sea Ice Cover." *Mar. Ecol. Prog. Ser.* 468: 1–13.
- Jay, C.V., R.L. Taylor, A.S. Fischbach, M.S. Udevitz, and W.S. Beatty. 2017. "Walrus Haul-out and in Water Activity Levels Relative to Sea Ice Availability in the Chukchi Sea." *J. Mammal.* 98 (2): 386–96.
- Jeffries, M.O., J.E. Overland, and D.K. Perovich. 2013. "The Arctic Shifts to a New Normal." *Phys. Today* 66 (10): 35–40.
- Kovacs, K.M., C. Lydersen, J.E. Overland, and S.E. Moore. 2011. "Impacts of Changing Sea-Ice Conditions on Arctic Marine Mammals." *Mar. Biodivers.* 41 (1): 181–94.
- Laidre, K.L., H. Stern, K.M. Kovacs, L. Lowry, S.E. Moore, E.V. Regehr, S.H. Ferguson, et al. 2015. "Arctic Marine Mammal Population Status, Sea Ice Habitat Loss, and Conservation Recommendations for the 21st Century." *Conserv. Biol.* 29 (3): 724–37.
- Laidre, K.L., I. Stirling, L.F. Lowry, Ø. Wiig, M.P. Heide-Jørgensen, and S.H. Ferguson. 2008. "Quantifying the Sensitivity of Arctic Marine Mammals to Climate-Induced Habitat Change." *Ecol. Appl.* 18 (supplement2): s97–125.
- Marques, T.A., S.T. Buckland, R. Bispo, and B. Howland. 2013. "Accounting for Animal Density Gradients Using Independent Information in Distance Sampling Surveys." *Stat. Methods Appl.* 22 (1): 67–80.
- Miller, D.L., M. L. Burt, E.A. Rexstad, and L. Thomas. 2013. "Spatial Models for Distance Sampling Data: Recent Developments and Future Directions." *Methods Ecol. Evol.* 4 (11): 1001–10.
- Moore, S.E. 2016. "Is It 'Boom Times' for Baleen Whales in the Pacific Arctic Region?" *Biol. Lett.* 12 (9). doi: 10.1098/rsbl.2016.0251.
- Moore, S.E., and H.P. Huntington. 2008. "Arctic Marine Mammals and Climate Change: Impacts and Resilience." *Ecol. Appl.* 18 (supplement 2): s157–165.

- Moore, S.E., and R.R. Reeves. 1993. "Distribution and Movement." Pages 313–86 in *The Bowhead Whale*. (J.J. Burns, J.J. Montague, and C.J. Cowles, eds.) Society for Marine Mammalogy, Lawrence, Kansas.
- Moore, S.E., K.M. Stafford, D.K. Mellinger, and J.A. Hildebrand. 2006. "Listening for Large Whales in the Offshore Waters of Alaska." *Bioscience* 56 (1): 49–55.
- Ovaskainen, O., G. Tikhonov, A. Norberg, F.G. Blanchet, L. Duan, D. Dunson, T. Roslin, and N. Abrego. 2017. "How to Make More Out of Community Data? A Conceptual Framework and Its Implementation as Models and Software." *Ecol. Lett.* 20 (5): 561–76.
- Redfern, J.V., M.C. Ferguson, E.A. Becker, K.D. Hyrenbach, C. Good, J. Barlow, K. Kaschner, et al. 2006. "Techniques for Cetacean-Habitat Modeling." *Mar. Ecol. Prog. Ser.* 310: 271–95.
- Roberts, J.J., B.D. Best, L. Mannocci, E. Fujioka, P.N. Halpin, D.L. Palka, L.P. Garrison, et al. 2016. "Habitat-Based Cetacean Density Models for the U.S. Atlantic and Gulf of Mexico." *Sci. Rep.* 6: 22615. doi: 22610.21038/srep22615.
- Robertson, F.C., W.R. Koski, J.R. Brandon, T.A. Thomas, and A.W. Trites. 2015. "Correction Factors Account for the Availability of Bowhead Whales Exposed to Seismic Operations in the Beaufort Sea." *J. Cetac. Res. Manage.* 15 (1): 35–44.
- Schick, R.S., J.J. Roberts, S.A. Eckert, P.N. Halpin, H. Bailey, F. Chai, L. Shi, and J.S. Clark. 2013. "Pelagic Movements of Pacific Leatherback Turtles (*Dermochelys coriacea*) Highlight the Role of Prey and Ocean Currents." *Move. Ecol.* 1: 11. <https://doi.org/10.1186/2051-3933-1-11>
- Screen, J.A., and D. Williamson. 2017. "Ice-Free Arctic at 1.5°C?" *Nat. Clim. Change* 7:230-1.
- Simpkins, M.A., L.M. Hiruki-Raring, G. Sheffield, J.M. Grebmeier, and J.L. Bengtson. 2003. "Habitat Selection by Ice-Associated Pinnipeds Near St. Lawrence Island, Alaska in March 2001." *Polar Biol.* 26 (9): 577–86.
- Suydam, R.S., L.F. Lowry, K.J. Frost, G.M. O’Corry-Crowe, and D. Pikok. 2001. "Satellite Tracking of Eastern Chukchi Sea Beluga Whales into the Arctic Ocean." *Arctic* 54 (3): 237–43.
- Suydam, R.S., L.F. Lowry, and K.J. Frost. 2005. *Distribution and Movements of Beluga Whales from the Eastern Chukchi Sea Stock during Summer and Early Autumn*. OCS Study MMS 2005-035. Minerals Management Service, Anchorage, Alaska.
- Tynan, C.T., and D.P. DeMaster. 1997. "Observations and Predictions of Arctic Climatic Change: Potential Effects on Marine Mammals." *Arctic* 50 (4): 308–22.
- Ver Hoef, J.M., M.F. Cameron, P.L. Boveng, J.M. London, and E.E. Moreland. 2014. "A Spatial Hierarchical Model for Abundance of Three Ice-Associated Seal Species in the Eastern Bering Sea." *Stat. Methodol.* 17: 46–66.

Walsh, J.E. 2008. "Climate of the Arctic Marine Environment." *Ecol. Appl.* 18 (supplement2): s3–22.

Wood, S.N., M.V. Bravington, and S.L. Hedley. 2008. "Soap Film Smoothing." *J. R. Stat. Soc. Series B Stat. Methodol.* 70 (5): 931–55.

This page intentionally left blank.

Appendix A - Detection Functions

Sightings Hierarchies

Next we provide the graphical overview for each of the remaining seven species/guild combinations: beluga whales (**Figure 45**), gray whales (**Figure 46**), walrus (**Figure 47**), bearded seals (**Figure 48**), small pinnipeds (**Figure 49**), unidentified pinnipeds (**Figure 50**), and the baleen whale guild (**Figure 51**).

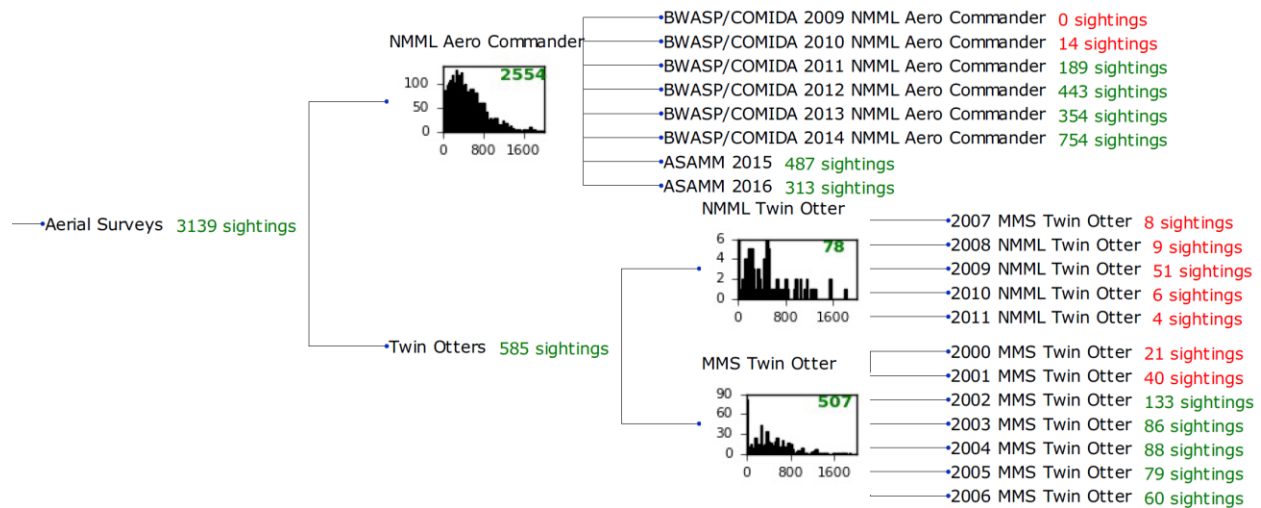


Figure 45. Beluga whale sightings/platform hierarchy.

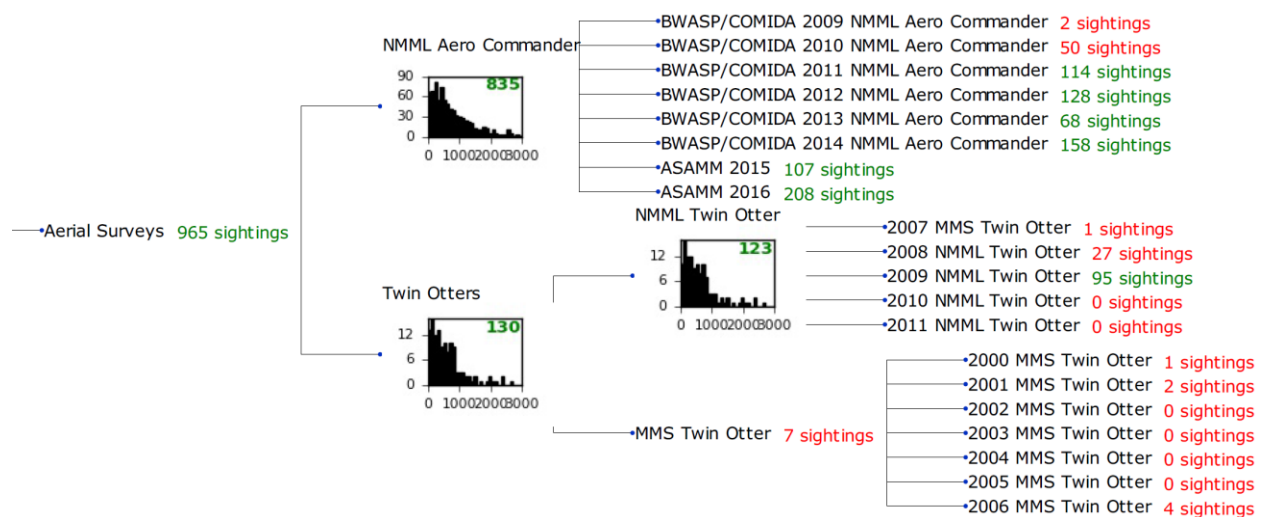


Figure 46. Gray whale sightings/platform hierarchy.

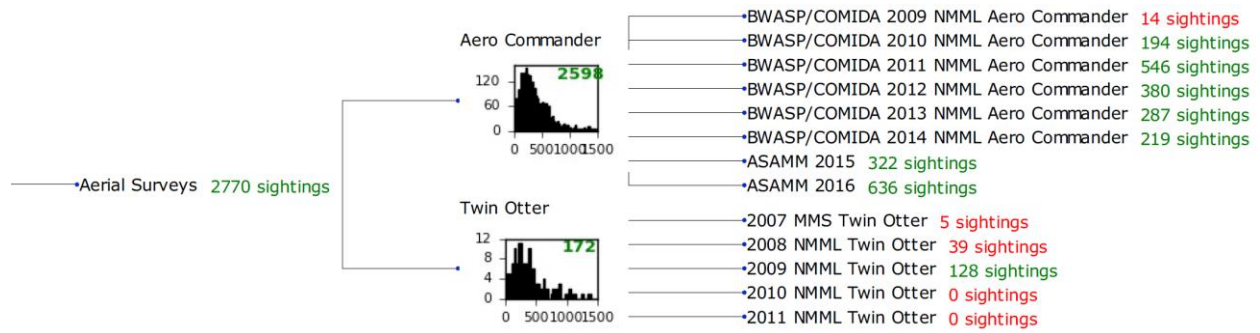


Figure 47. Walrus sightings/platform hierarchy.

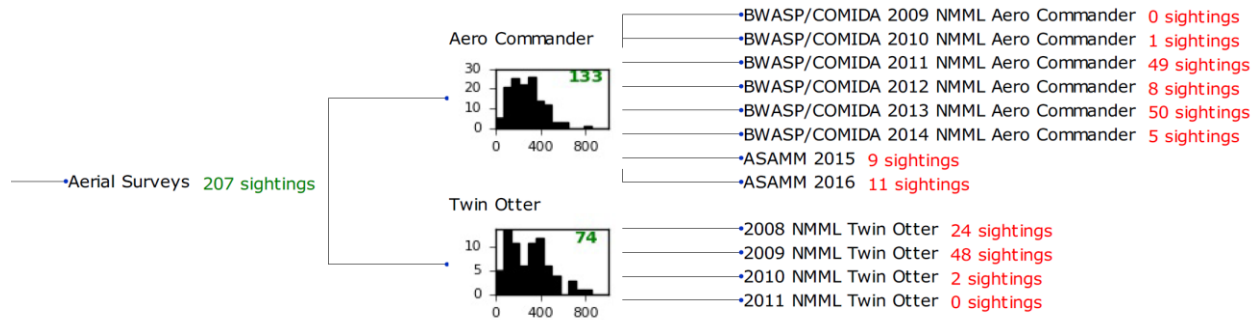


Figure 48. Bearded seal sightings/platform hierarchy.

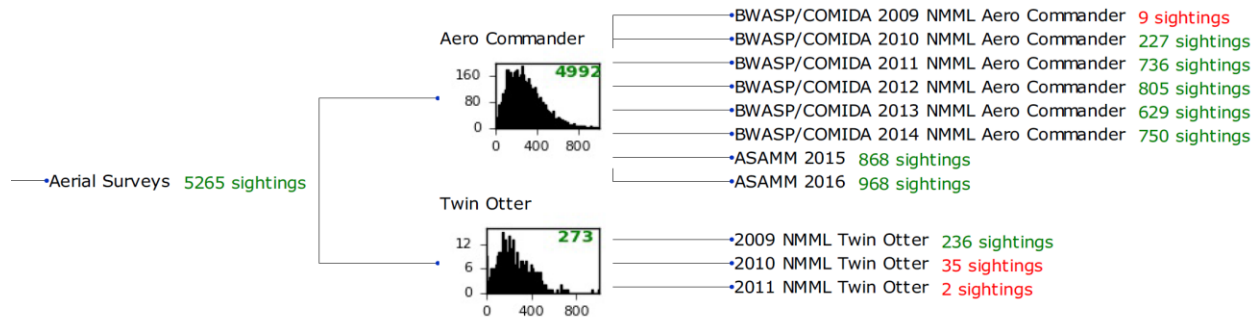


Figure 49. Small pinnipeds sightings/platform hierarchy.

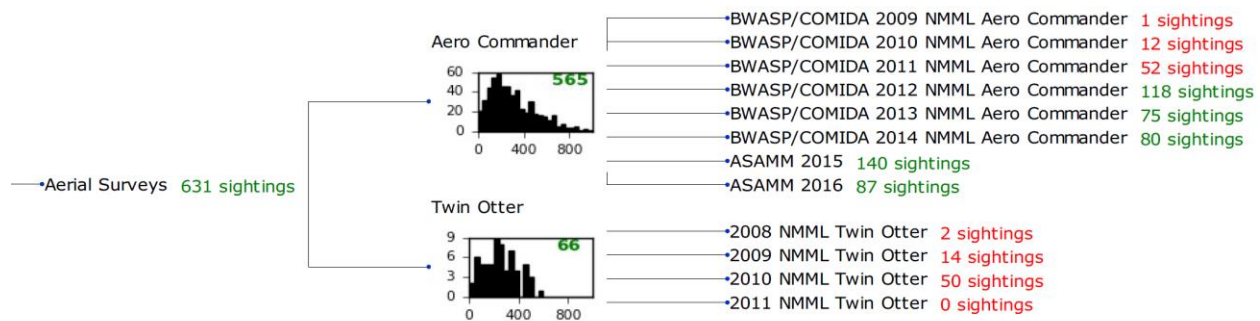


Figure 50. Small pinnipeds sightings/platform hierarchy.

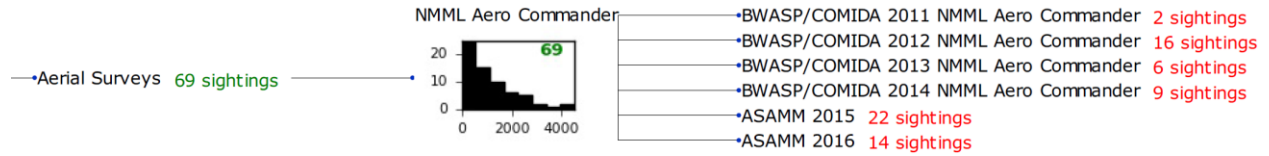


Figure 51. Baleen whale sightings/platform hierarchy.

Fitted Detection Functions

Bowhead Whales

The detection function fits improved with more sightings (**Figures 52, 53, 54**). In the Commander, we have both left and right truncated the observations, and effective strip half-width (ESHW) ranged from 1,005 to 1,314m. Though the poorest fit is in the MMS Otter (**Figure 52**), it is still a reasonably good detection function. There may be some evidence of trackline guarding in this platform (**Figure 52**). This has been noted in previous analysis of these data (Ferguson and Clarke 2013), and historically relate to one individual observer. This individual's observing tendencies have been accounted for with the Observer covariate in the formula for the detection function. In both the platforms operated by MML, we see the influence of group size - larger groups are easier to detect (**Figures 53, 54**).

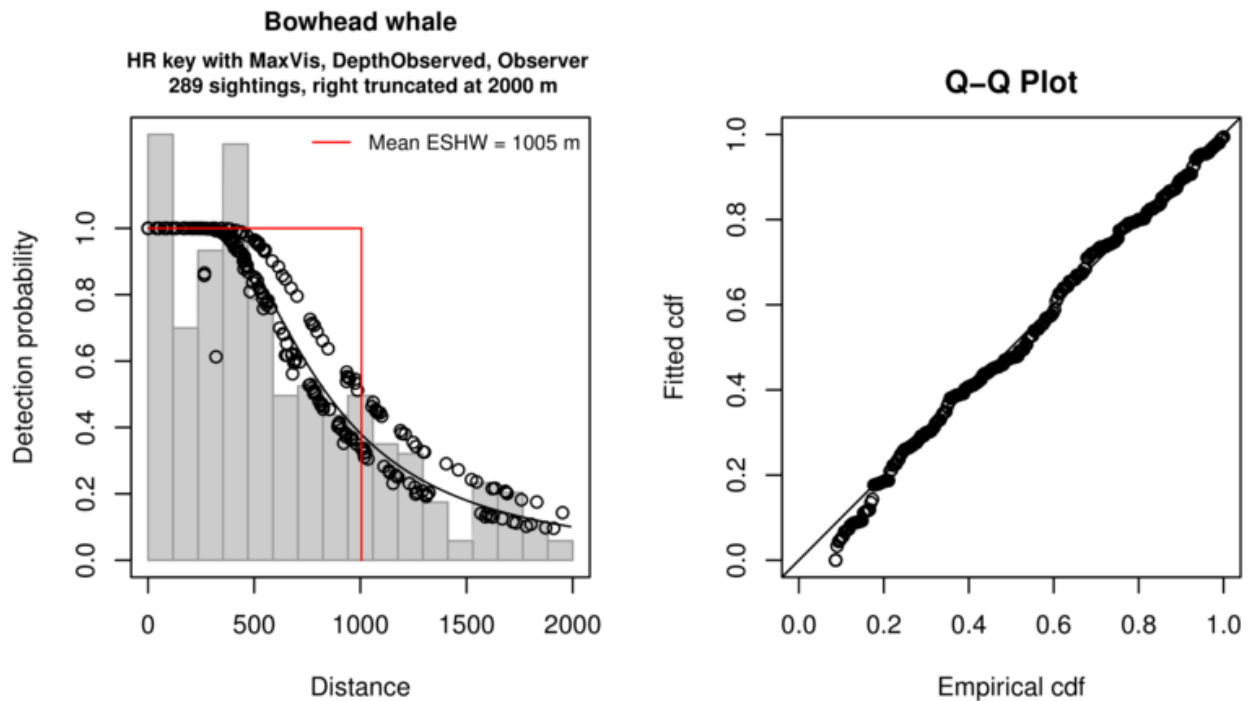


Figure 52. Final detection function chosen for the MMS Otter platform for bowhead whales shows a decent fit with three covariates included in the detection function model: 1) Maximum Visibility, 2) Depth Observed, and 3) Observer.

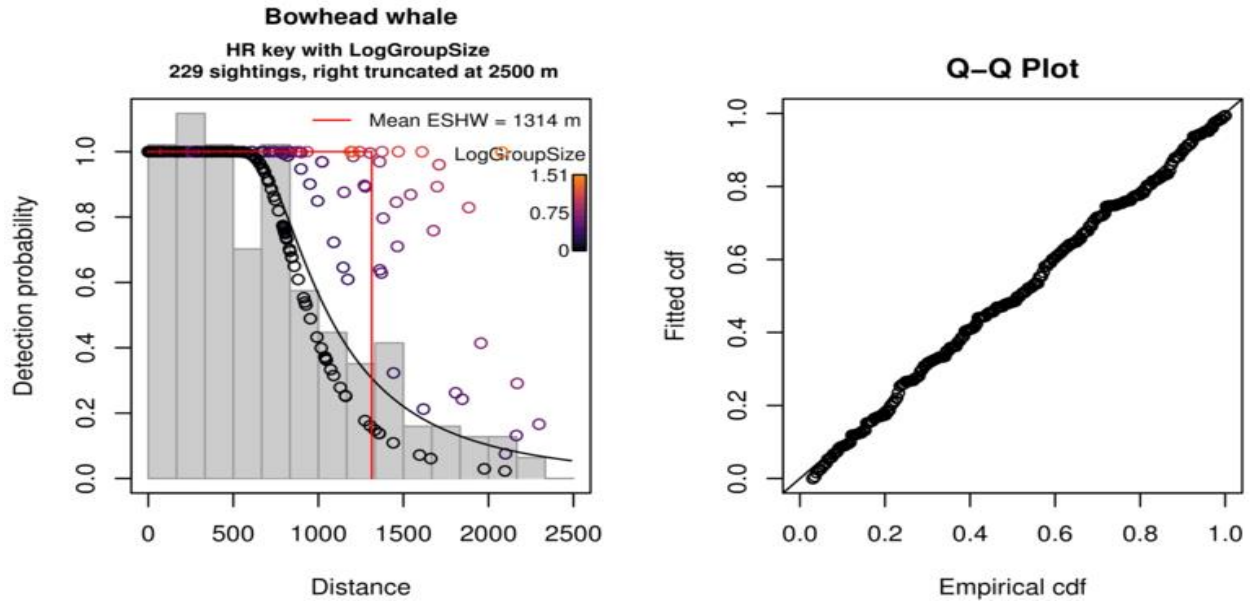


Figure 53. Final detection function chosen for the MML Otter platform for bowhead whales. The single covariate included indicates that as bowhead group size increases, so does detection probability.

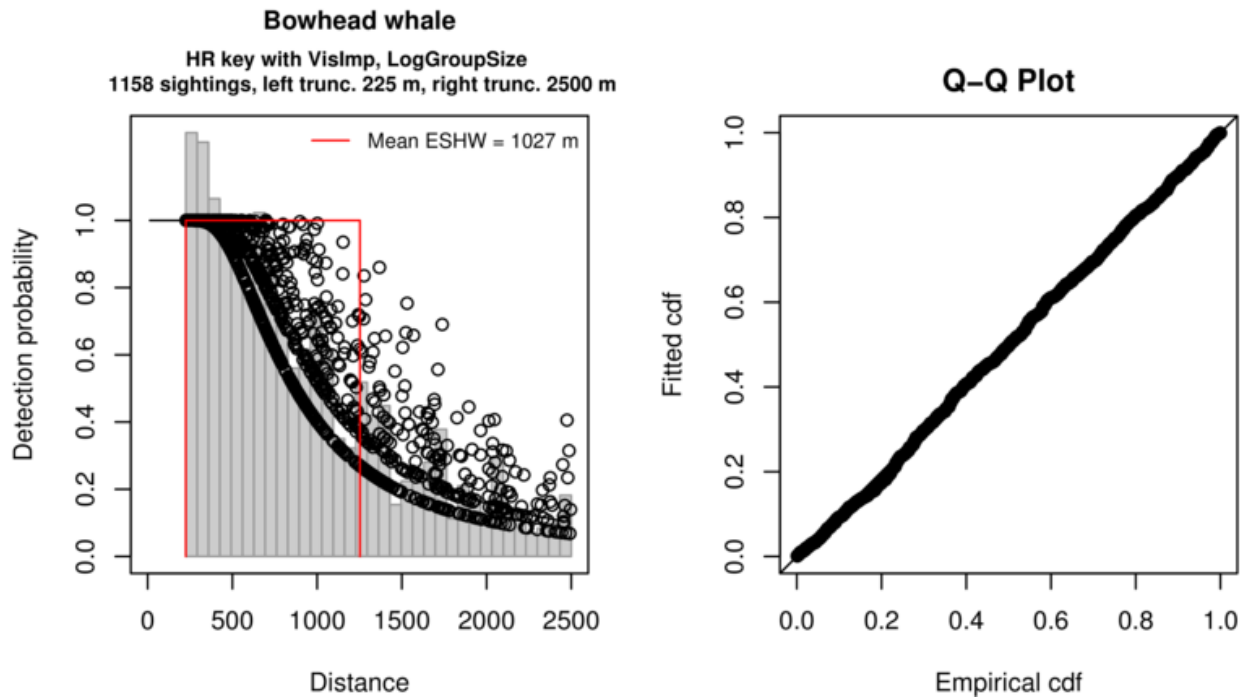


Figure 54. Final detection function chosen for the MML Commander platform for bowhead whales includes covariates for both glare (*VisImp*) and log group size. As with the MML Otter, as group size increases, so does detectability.

Beluga Whales

With smaller whales (belugas) we have right truncated significantly more than with bowheads (**Figures 55, 56, 57**). With the MMS Otter, there may be some evidence of heaping with spikes at approximately 200 and 400 m, but the distance breaks are not immediately congruent with obvious distances like 500 m, 1,000 m, etc. Thus, we did not aggregate to coarser distance bins.

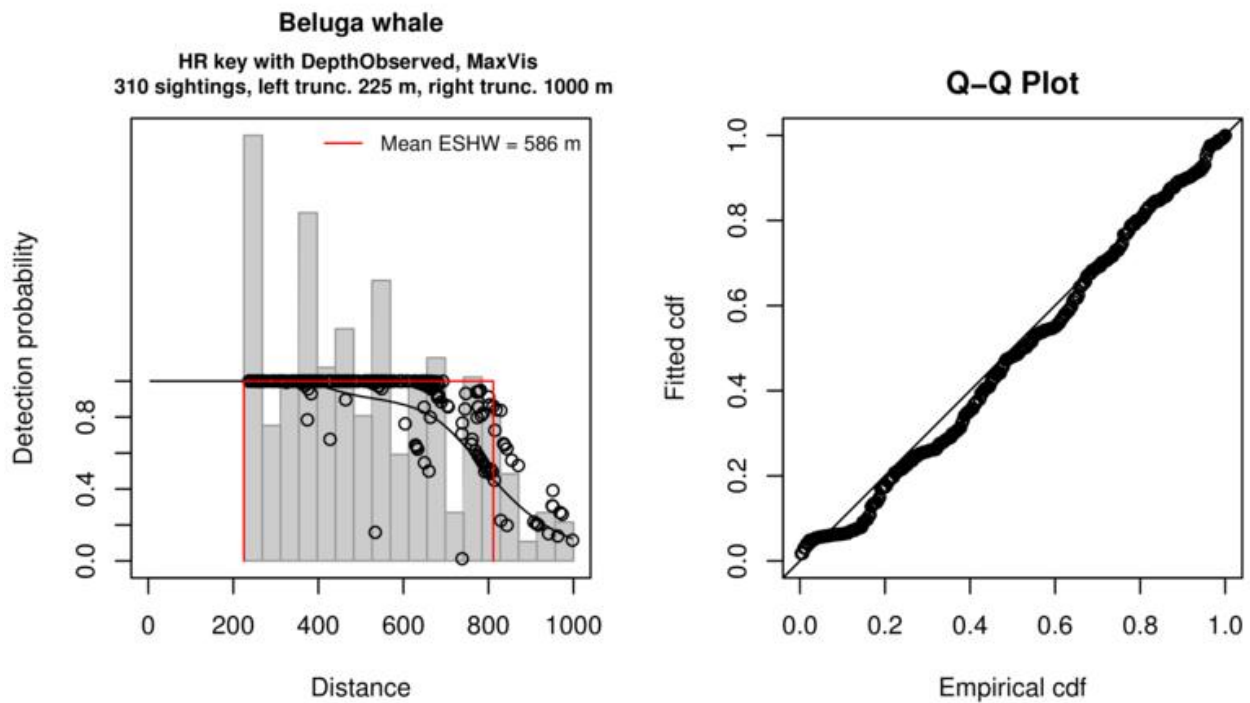


Figure 55. Final detection function chosen for the MMS Otter platform for beluga whales. Some heaping may be evident, but we kept the distance bins as depicted. Left truncation distance was higher than in the MML Otter.

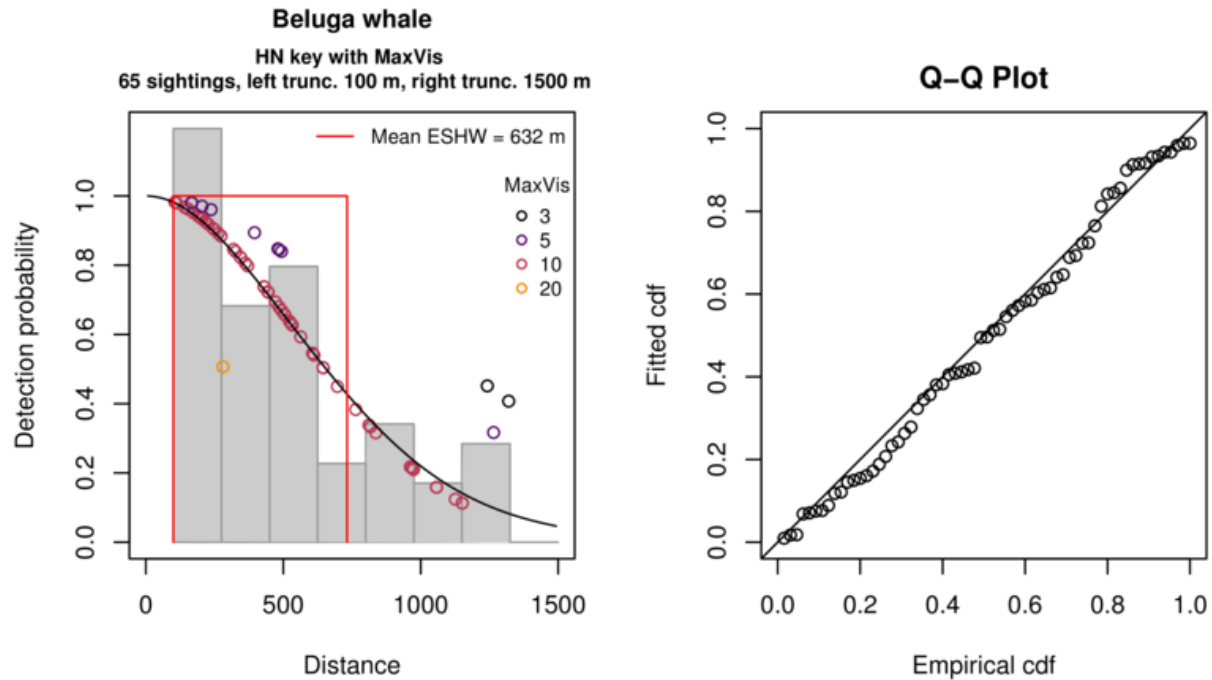


Figure 56. Final detection function chosen for the MML Otter platform for beluga whales. A single covariate—maximum visibility—was included. The detection function indicates somewhat paradoxically that as the visibility improves, detection decreases. It is possible that with a broader search field, observers are scanning over a larger area and thus missing some sightings.

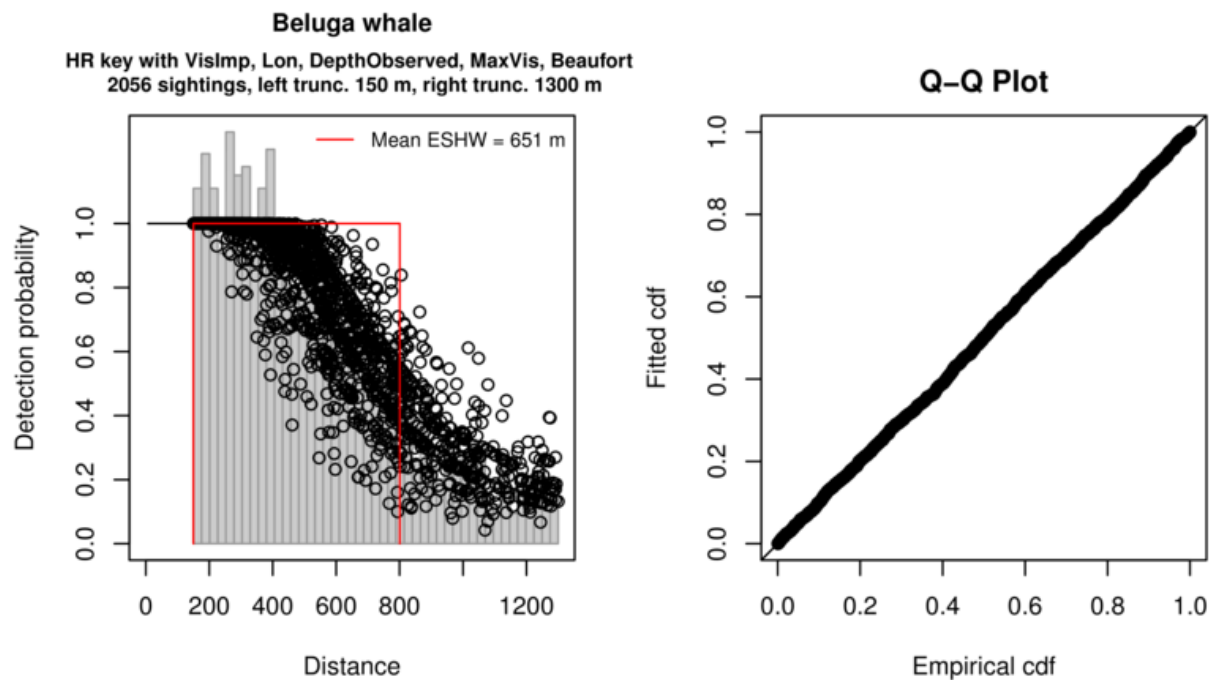


Figure 57. Final detection function chosen for the MML Commander platform for beluga whales. As with bowhead whales, the Commander is the platform with the most sightings and the best fit. Five covariates were included in the best model for detection.

Gray Whales

Because of a lack of sightings for gray whales, we combined the two Otter platforms (**Figure 58**). Here, just one covariate was included, and in contrast to belugas, the results for “Maximum Visibility” are as expected; namely, as visibility increases, so too does detection. Results for the Commander indicate an excellent fit with a larger ESHW than the Otters (**Figure 59**).

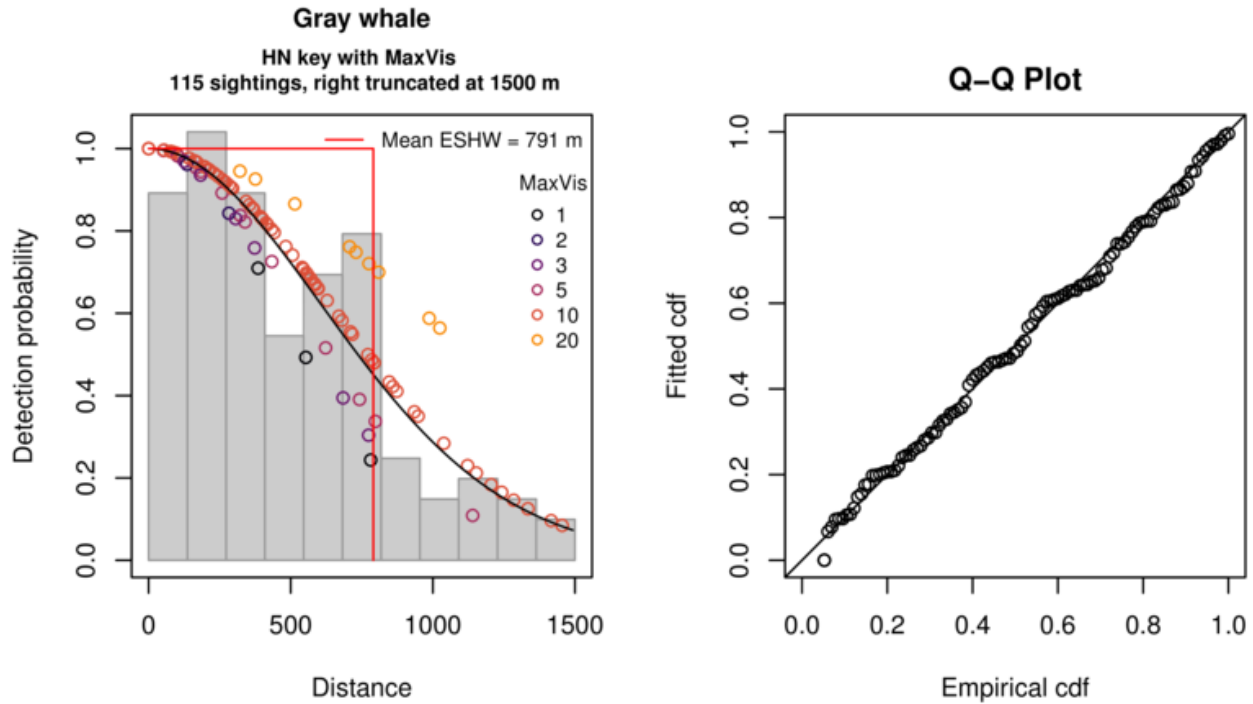


Figure 58. Final detection function chosen for the combined Otter platforms for gray whales. Intuitively, as visibility increases, so does detection.

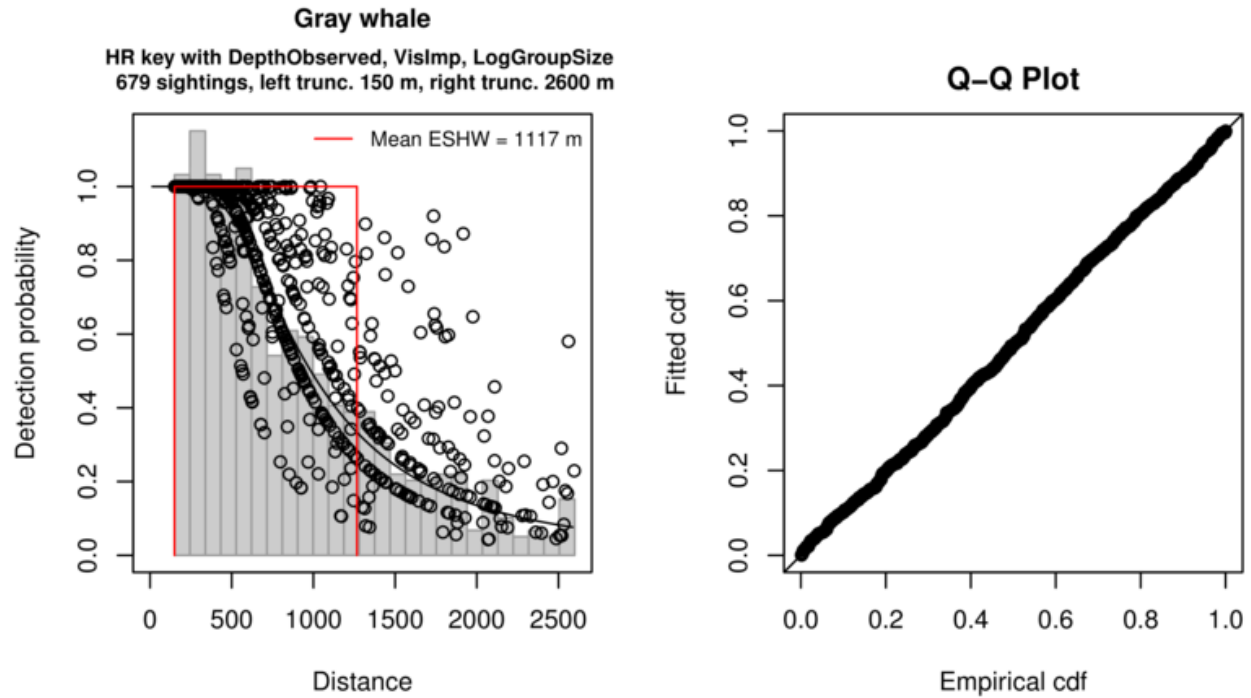


Figure 59. Final detection function chosen for the MML Commander platform for gray whales. While the detection function is more complicated than with the Otters, the fit is excellent.

Walrus

As with previous examples, as the number of sightings increases, so too does the fit (**Figures 60, 61**). In contrast to the previous species the detection function decays very rapidly with very short ESHW for each platform. Unique among the Arctic species, walrus can have extremely large group sizes. This effect can be seen as the near perfect detection rate for some groups even as perpendicular distance increases (**Figures 60, 61**).

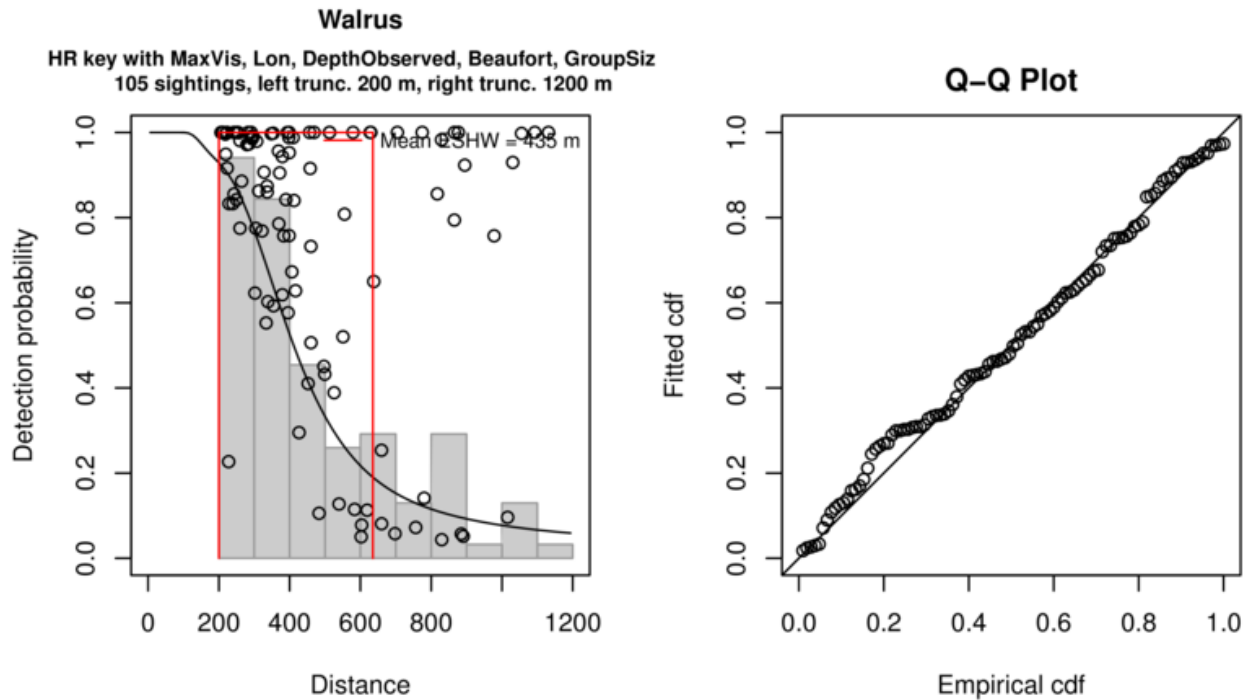


Figure 60. Final detection function chosen for the MML Otter platform for walrus. There were relatively few walrus seen from this platform, and the sightings rate decays very quickly with distance from the trackline.

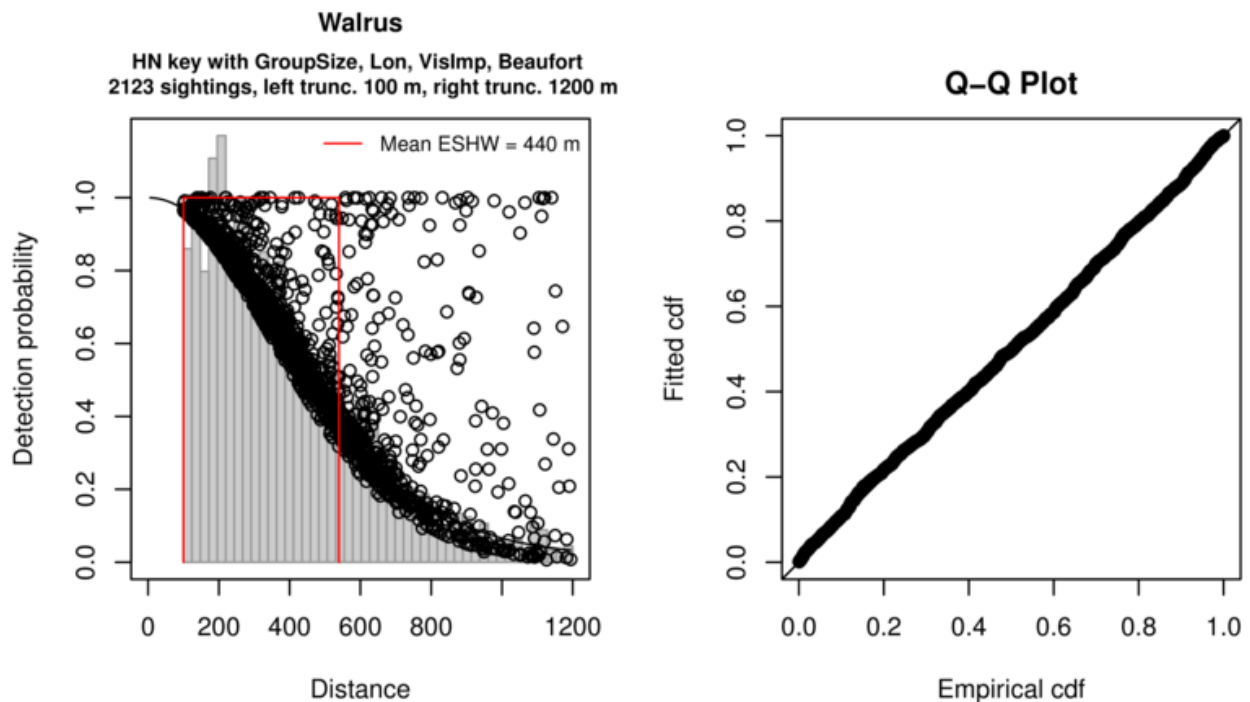


Figure 61. Final detection function chosen for the MML Commander platform for walrus. The detection function decays quickly for this platform as well, though not as quickly as for the Otter.

Bearded Seals

Relatively few bearded seals were seen from either platform. Although, with the higher number of observations seen from the Commander, we do see an improved fit (**Figures 62, 63**). Aboard the MML Otter, a categorical representation of depth indicates that bearded seals are more detectable closer to shore (**Figure 62**). Indeed, for the coastal observations (green) and the inner shelf observations (orange), the detection probability is high.

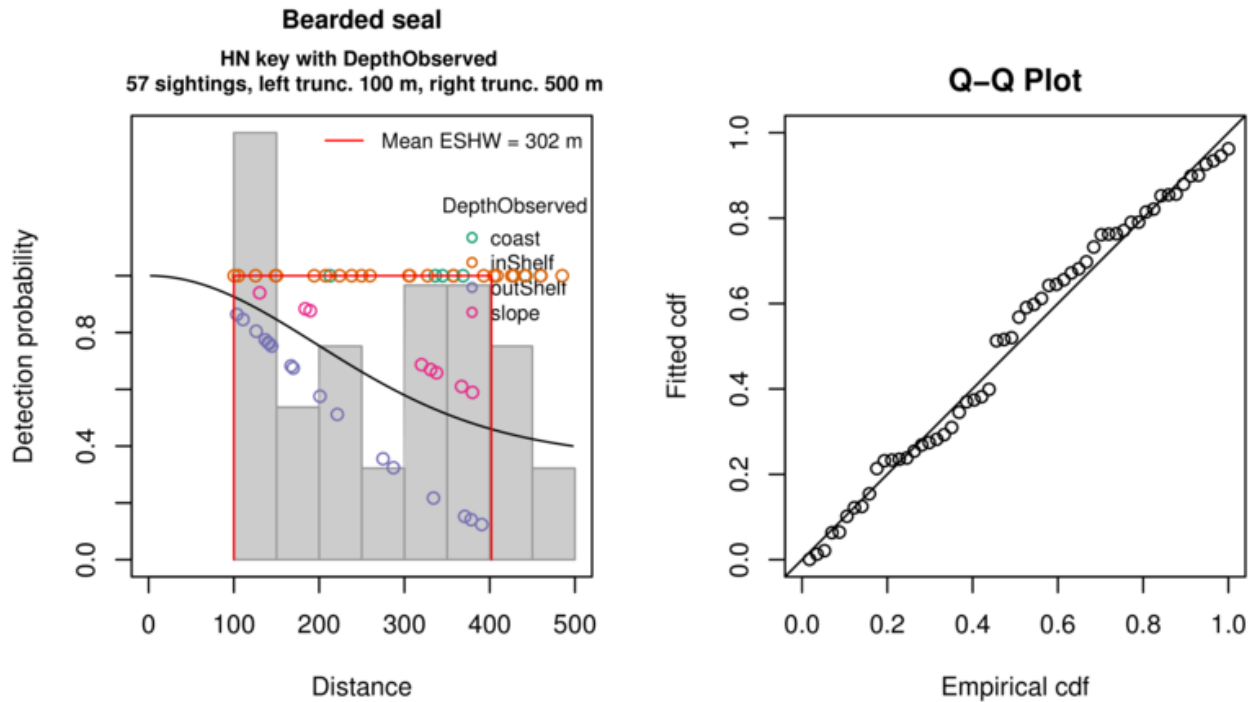


Figure 62. Final detection function chosen for the MML Otter platform for bearded seals.

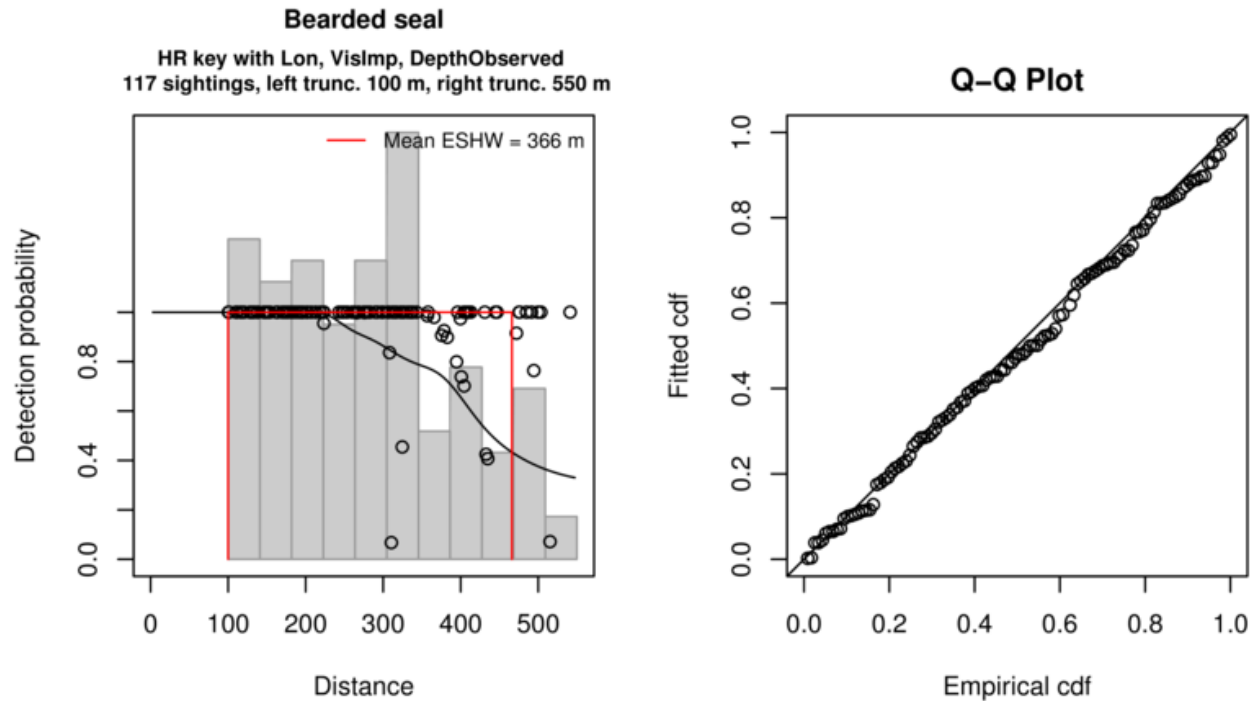


Figure 63. Final detection function chosen for the MML Commander platform for bearded seals. With approximately double the number of observations, the fit is improved; however the ESHW for both platforms is still quite short.

Small Pinnipeds

In each platform, the detection function fit is quite good (**Figures 64, 65**), although the ESHW for the MML Otter is quite short. With many more sightings in the Commander, the fit in the Q-Q plot is excellent, and the ESHW is approximately double that of the Otter (**Figure 65**).

In the Otter the detection is worse when there is no glare (orange circles) (**Figure 64**). While counterintuitive, field observers often note that the presence of glare can add contrast to an otherwise featureless ocean surface (Janet Clarke, Leidos Corporation, *pers. comm.*).

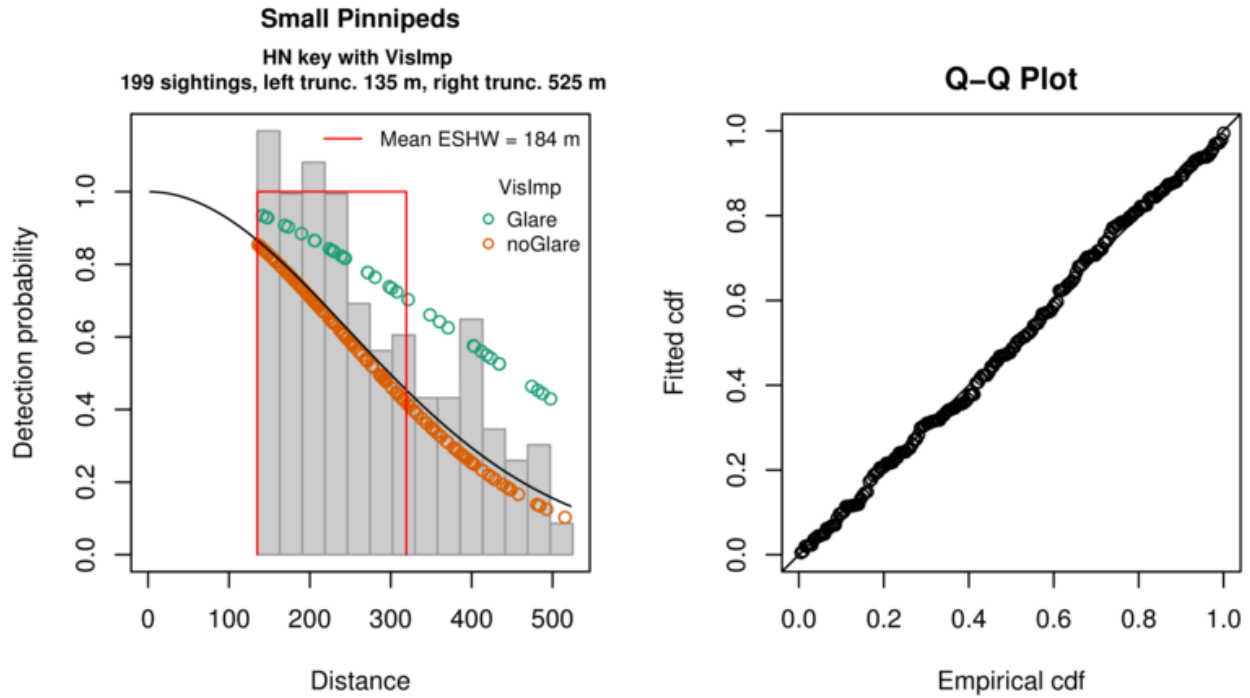


Figure 64. Final detection function chosen for the MML Otter platform for small pinnipeds. Though there are relatively few sightings—especially as compared to the Commander—the fit is still quite good.

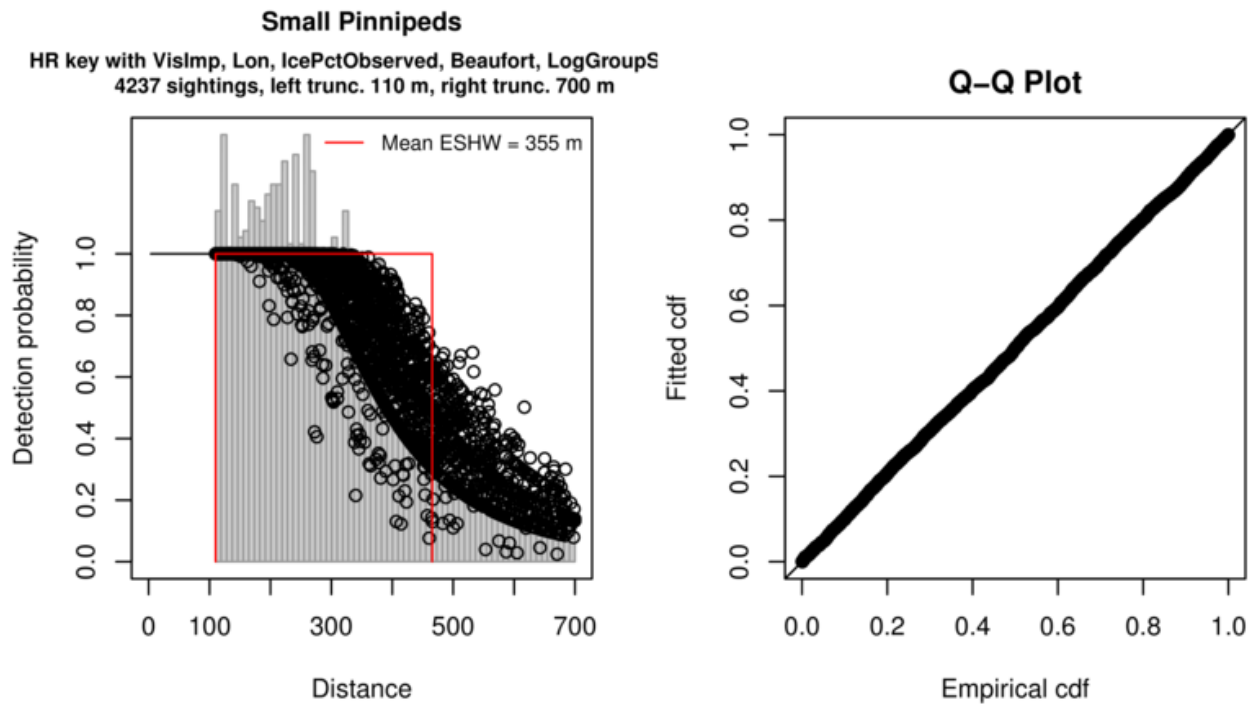


Figure 65. Final detection function chosen for the MML Commander platform for small pinnipeds.

Unidentified Pinnipeds

The fit for the Otter is generally quite poor (**Figure 66**), though with so few sightings, this is not surprising. One concerning feature is that the rate seems to roughly increase with distance from the trackline. Anecdotal evidence indicates that this trend often occurs with unidentified animals; although they are observed, as their distance from the trackline increases, they become harder to identify to individual species (Megan Ferguson, MML, *pers. comm.*). Because of this poor fit, in future modeling efforts we may exclude the data from this platform. In contrast, the fit from the Commander is quite good (**Figure 67**).

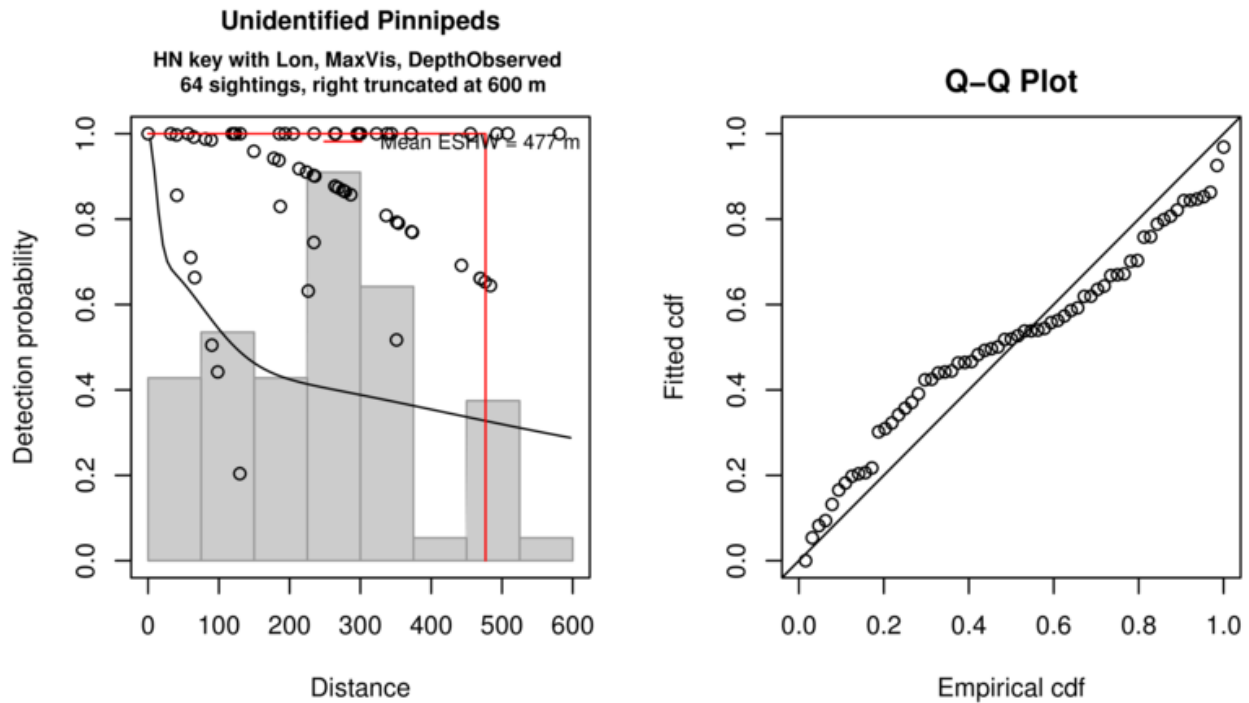


Figure 66. Final detection function chosen for the MML Otter platform for unidentified pinnipeds. Though the ESHW is higher than the Commander, the fit is generally poor.

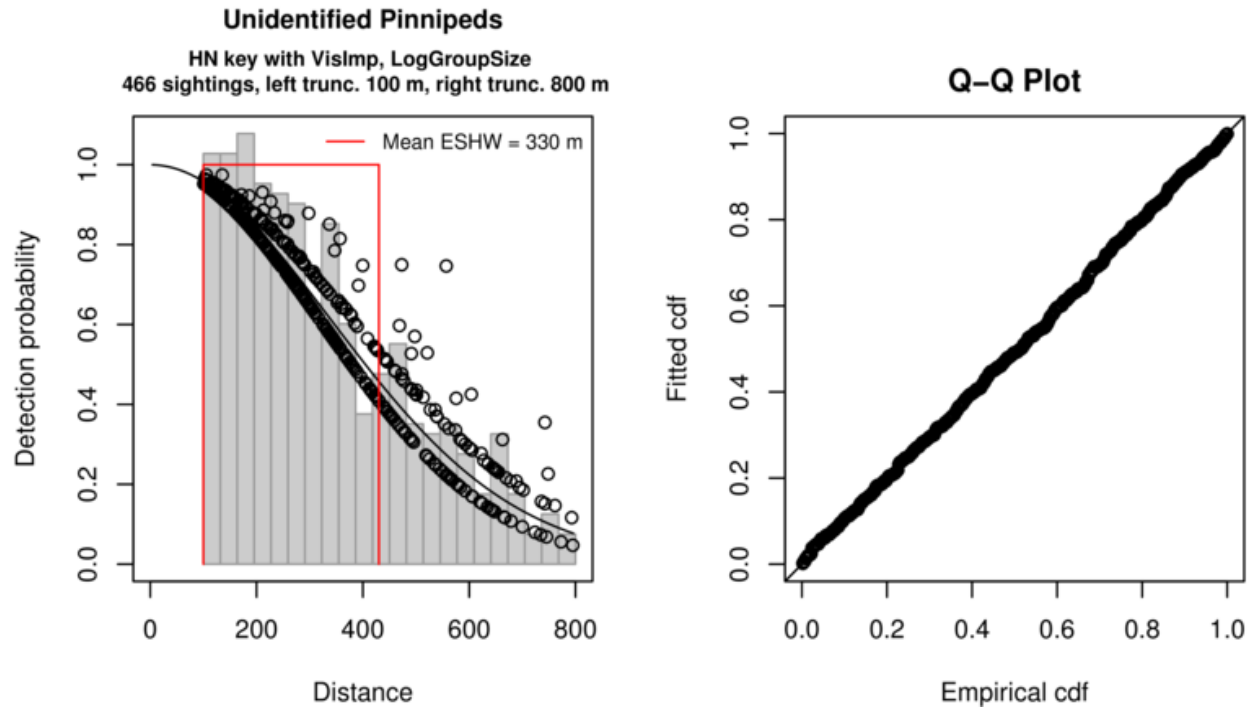


Figure 67. Final detection function chosen for the MML Commander platform for unidentified pinnipeds.

Baleen Whales

In contrast to the unidentified pinniped guild, **Figure 68** highlights how we have approached the cases with few sightings of known-identification species. In particular, we have restricted the set of covariates in the detection function models to only include one covariate at a time. Here the explanatory covariate for the detection function is the species covariate.

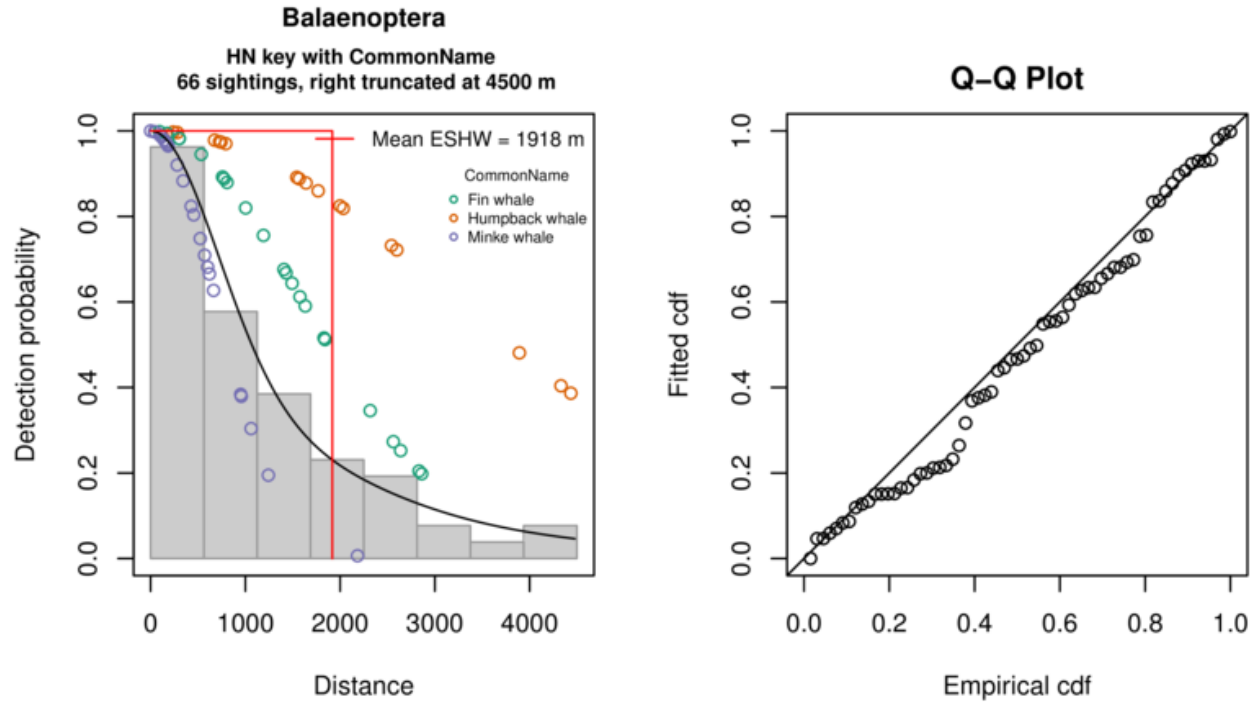


Figure 68. Final detection function chosen for baleen whale (fin, humpback, and minke whale). There is a large ESHW, though this appears driven by humpbacks which are seen at farther distances from the trackline. Minke whales have the lowest detection rate of the three baleen whale species.

This page intentionally left blank.

Appendix B - Generalized Additive Models

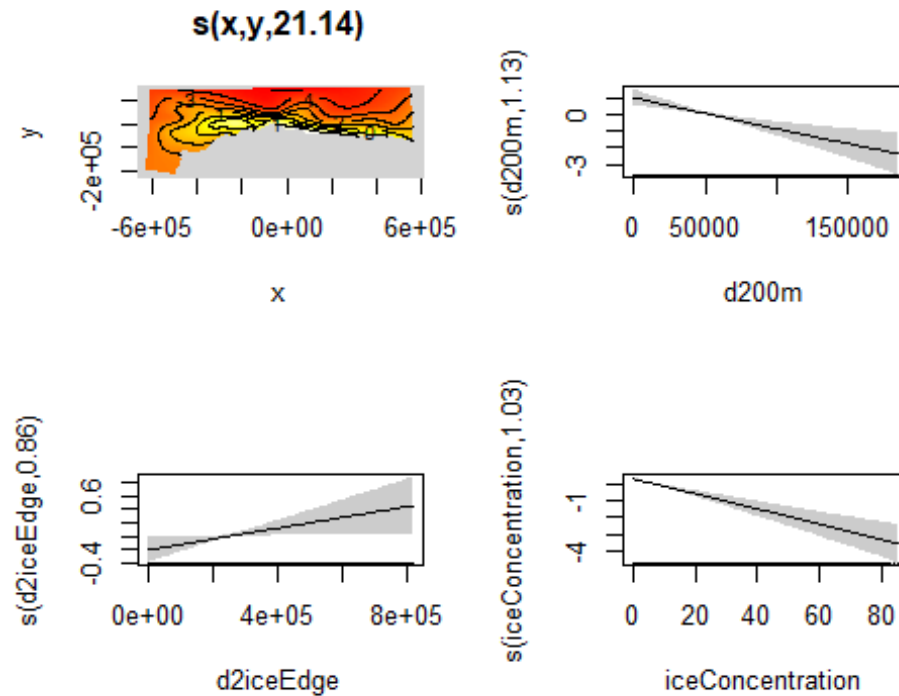
Detailed Summaries of the GAM Models for Each Species

Bowhead Whales

In this instance the final model selected - based on AIC - included a soap film smoother for the land/ocean boundary. In addition to the spatial smooth, the final model included one static covariate and two dynamic covariates. Despite the inclusion of the dynamic predictors (Distance to Ice Edge, and ice concentration) predicted monthly densities are dominated by the spatial smooth.

Below is the text and graphical summary of the final model for bowhead whales:

```
##
## Family: Negative Binomial(0.011)
## Link function: log
##
## Formula:
## Abundance ~ offset(log(Area)) + s(x, y, bs = "so", xt = list(bnd = list(boundary))) +
##      s(d200m, bs = "ts") + s(d2iceEdge, bs = "ts") + s(iceConcentration,
##      bs = "ts")
##
## Parametric coefficients:
##              Estimate Std. Error z value Pr(>|z|)
## (Intercept) -6.09482    0.06235  -97.76   <2e-16 ***
## ---
## Signif. codes:  0 '***' 0.001 '**' 0.01 '*' 0.05 '.' 0.1 ' ' 1
##
## Approximate significance of smooth terms:
##              edf Ref.df Chi.sq p-value
## s(x,y)         21.1435     62 301.321 < 2e-16 ***
## s(d200m)         1.1319      9  17.119 7.35e-08 ***
## s(d2iceEdge)     0.8555      9   4.858 0.0155 *
## s(iceConcentration) 1.0304      9  43.467 8.65e-12 ***
## ---
## Signif. codes:  0 '***' 0.001 '**' 0.01 '*' 0.05 '.' 0.1 ' ' 1
##
## R-sq.(adj) = 0.0184   Deviance explained = 19.5%
## -REML = 6084.4   Scale est. = 1           n = 29908
```



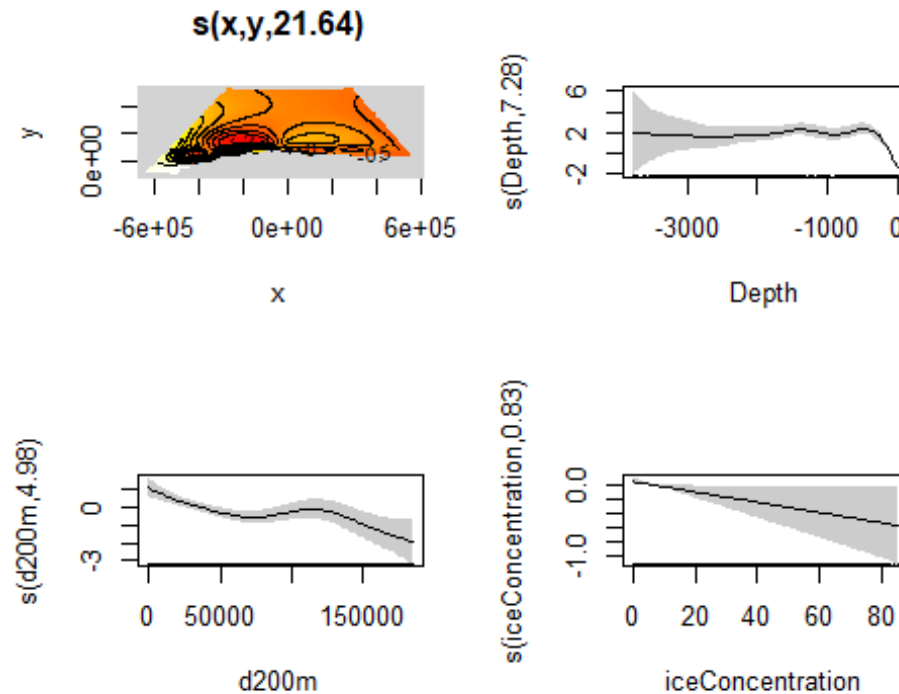
Beluga Whales

For beluga whales, the final model includes a spatial smooth, two static predictors--both of which are highly significant--and one weakly significant dynamic predictor.

```
##
## Family: Negative Binomial(0.017)
## Link function: log
##
## Formula:
## Abundance ~ offset(log(Area)) + s(x, y, bs = "so", xt = list(bnd = list(boundary))) +
##       s(Depth, bs = "ts") + s(d200m, bs = "ts") + s(iceConcentration,
##       bs = "ts")
##
## Parametric coefficients:
##               Estimate Std. Error z value Pr(>|z|)
## (Intercept) -4.95196    0.04925  -100.6   <2e-16 ***
## ---
## Signif. codes:  0 '***' 0.001 '**' 0.01 '*' 0.05 '.' 0.1 ' ' 1
##
## Approximate significance of smooth terms:
##               edf Ref.df Chi.sq p-value
## s(x,y)         21.6354    75 174.481 < 2e-16 ***
## s(Depth)        7.2763     9 131.664 < 2e-16 ***
## s(d200m)        4.9765     9  35.701 3.19e-10 ***
## s(iceConcentration) 0.8268     9   4.441   0.02 *
```



```
## ---
## Signif. codes:  0 '***' 0.001 '**' 0.01 '*' 0.05 '.' 0.1 ' ' 1
##
## R-sq.(adj) =  0.0165   Deviance explained = 23.4%
## -REML = 9023.7   Scale est. = 1           n = 30852
```

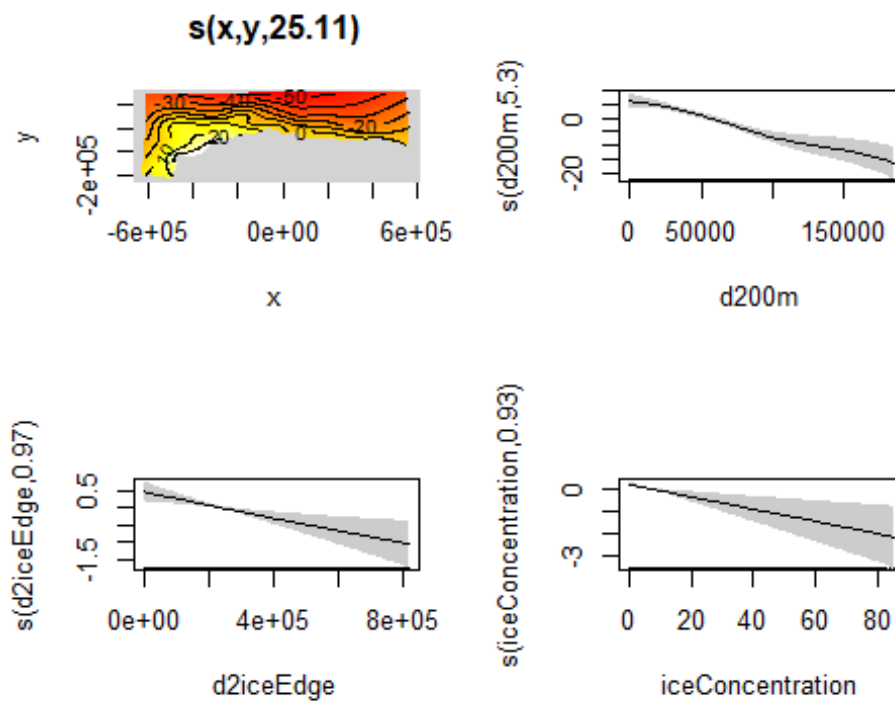


Gray Whales

The spatial smooth is the dominant predictor for gray whales, with a highly significant predictor in the Distance to 200m Isobath. Both dynamic ice-related covariates, while significant, do not appear to explain much of the pattern in gray whale abundance:

```
##
## Family: Negative Binomial(0.026)
## Link function: log
##
## Formula:
## Abundance ~ offset(log(Area)) + s(x, y, bs = "so", xt = list(bnd = list(boundary))) +
##       s(d200m, bs = "ts") + s(d2iceEdge, bs = "ts") + s(iceConcentration,
##       bs = "ts")
##
## Parametric coefficients:
##               Estimate Std. Error z value Pr(>|z|)
## (Intercept)  -13.336      1.086   -12.28   <2e-16 ***
## ---
## Signif. codes:  0 '***' 0.001 '**' 0.01 '*' 0.05 '.' 0.1 ' ' 1
```

```
##
## Approximate significance of smooth terms:
##               edf Ref.df Chi.sq  p-value
## s(x,y)         25.1086    62 483.94 < 2e-16 ***
## s(d200m)        5.3037     9  66.56 < 2e-16 ***
## s(d2iceEdge)     0.9696     9  11.11 0.000436 ***
## s(iceConcentration) 0.9251     9  10.07 0.000698 ***
## ---
## Signif. codes:  0 '***' 0.001 '**' 0.01 '*' 0.05 '.' 0.1 ' ' 1
##
## R-sq.(adj) = 0.0823  Deviance explained = 71.8%
## -REML = 2334.4  Scale est. = 1          n = 29908
```



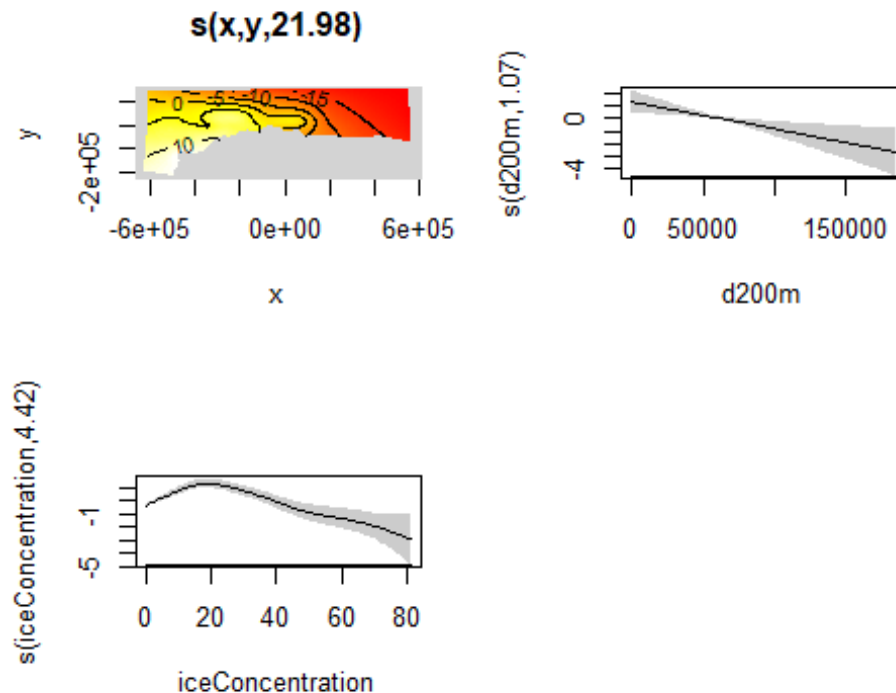
Walrus

While the spatial smooth is highly significant—as it is with previous species—here the distance to ice covariate is highly significant, and explains a great share of the deviance than with other species models.

The strong relationship is apparent in the plot of the smooth, where abundance peaks at around 20% ice concentration, before falling off as ice concentration increases.

```
##
## Family: Negative Binomial(0.016)
## Link function: log
##
## Formula:
```

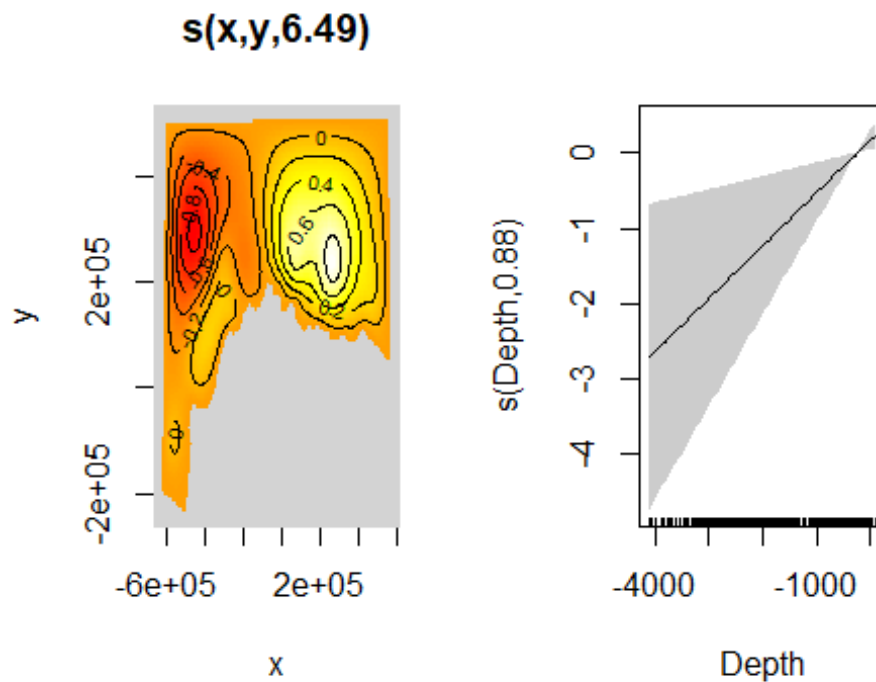
```
## Abundance ~ offset(log(Area)) + s(x, y, bs = "so", xt = list(bnd = list(boundary))) +
##       s(d200m, bs = "ts") + s(iceConcentration, bs = "ts")
##
## Parametric coefficients:
##               Estimate Std. Error z value Pr(>|z|)
## (Intercept)   -8.427      1.011   -8.332   <2e-16 ***
## ---
## Signif. codes:  0 '***' 0.001 '**' 0.01 '*' 0.05 '.' 0.1 ' ' 1
##
## Approximate significance of smooth terms:
##               edf Ref.df Chi.sq p-value
## s(x,y)         21.984     63 585.955 < 2e-16 ***
## s(d200m)        1.068      9   8.679 0.000163 ***
## s(iceConcentration) 4.420      9  91.988 < 2e-16 ***
## ---
## Signif. codes:  0 '***' 0.001 '**' 0.01 '*' 0.05 '.' 0.1 ' ' 1
##
## R-sq.(adj) =  0.0251   Deviance explained = 48.1%
## -REML = 7294.6   Scale est. = 1           n = 25842
```



Bearded Seals

The fit for bearded seals is generally fairly poor with only ~5% of the deviance explained. While the two terms are significant, it is apparent this model can be improved.

```
##
## Family: Negative Binomial(0.003)
## Link function: log
##
## Formula:
## Abundance ~ offset(log(Area)) + s(x, y, bs = "so", xt = list(bnd = list(boundary))) +
##       s(Depth, bs = "ts")
##
## Parametric coefficients:
##               Estimate Std. Error z value Pr(>|z|)
## (Intercept)  -6.6565      0.1149  -57.95   <2e-16 ***
## ---
## Signif. codes:  0 '***' 0.001 '**' 0.01 '*' 0.05 '.' 0.1 ' ' 1
##
## Approximate significance of smooth terms:
##               edf Ref.df Chi.sq p-value
## s(x,y)       6.4907     65 12.615 0.02209 *
## s(Depth)     0.8829      9  7.185 0.00117 **
## ---
## Signif. codes:  0 '***' 0.001 '**' 0.01 '*' 0.05 '.' 0.1 ' ' 1
##
## R-sq.(adj) =  0.000677   Deviance explained = 4.77%
## -REML = 1333.9   Scale est. = 1           n = 36912
```

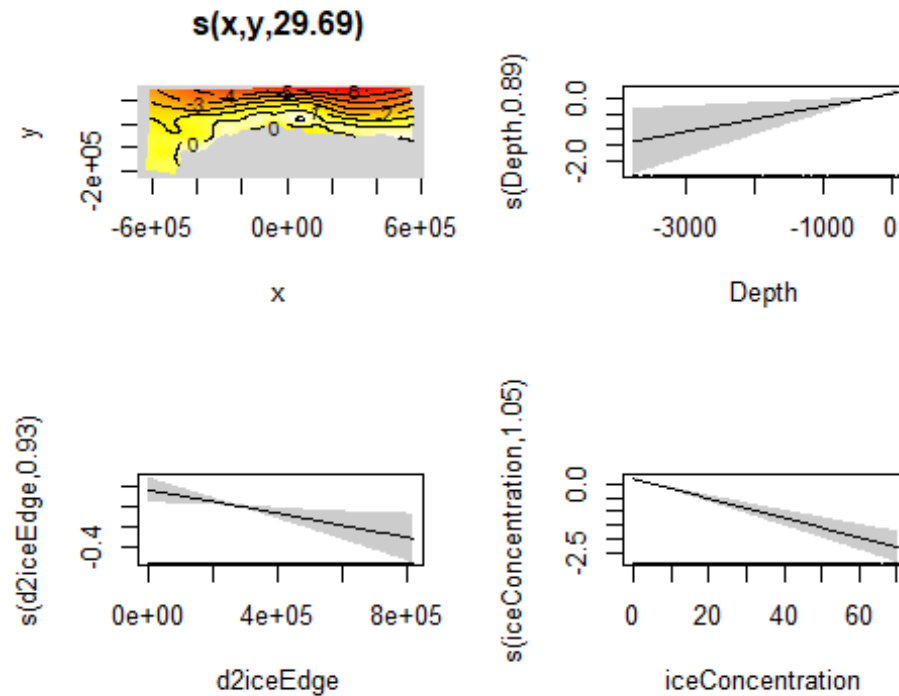


Small Pinnipeds

Though the model fit appears slightly better for small pinnipeds than for bearded seals, it still explains a small portion of the deviance:

The relationship between small pinnipeds and the dynamic covariates is linear; abundance is higher closer to the ice edge, and then decreasing as distance increases:

```
##
## Family: Negative Binomial(0.031)
## Link function: log
##
## Formula:
## Abundance ~ offset(log(Area)) + s(x, y, bs = "so", xt = list(bnd = list(boundary))) +
##       s(Depth, bs = "ts") + s(d2iceEdge, bs = "ts") + s(iceConcentration,
##       bs = "ts")
##
## Parametric coefficients:
##               Estimate Std. Error z value Pr(>|z|)
## (Intercept) -3.26923    0.03387  -96.53   <2e-16 ***
## ---
## Signif. codes:  0 '***' 0.001 '**' 0.01 '*' 0.05 '.' 0.1 ' ' 1
##
## Approximate significance of smooth terms:
##               edf Ref.df Chi.sq p-value
## s(x,y)         29.6917    65 247.479 < 2e-16 ***
## s(Depth)        0.8905     9   7.304 0.00033 ***
## s(d2iceEdge)    0.9339     9   7.501 0.00378 **
## s(iceConcentration) 1.0499     9  76.854 < 2e-16 ***
## ---
## Signif. codes:  0 '***' 0.001 '**' 0.01 '*' 0.05 '.' 0.1 ' ' 1
##
## R-sq.(adj) = 0.00776  Deviance explained = 6.33%
## -REML = 16028  Scale est. = 1          n = 31163
```

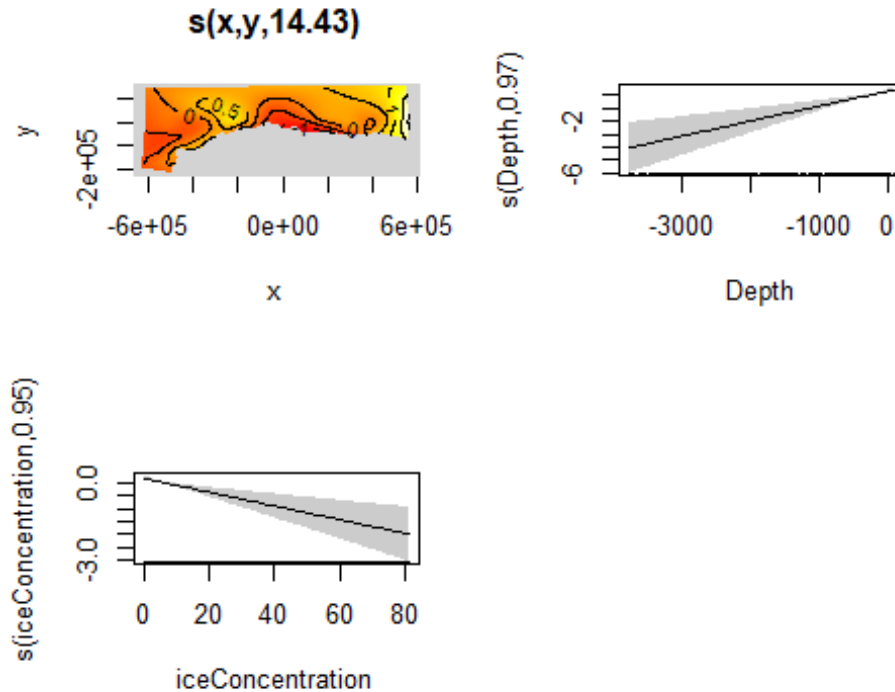


Unidentified Pinnipeds

Below is the text and graphical summary of the final model for unidentified pinnipeds; the response is again dominated by the spatial smooth.

```
##
## Family: Negative Binomial(0.005)
## Link function: log
##
## Formula:
## Abundance ~ offset(log(Area)) + s(x, y, bs = "so", xt = list(bnd = list(boundary))) +
##       s(Depth, bs = "ts") + s(iceConcentration, bs = "ts")
##
## Parametric coefficients:
##               Estimate Std. Error z value Pr(>|z|)
## (Intercept) -5.80176    0.08003   -72.5    <2e-16 ***
## ---
## Signif. codes:  0 '***' 0.001 '**' 0.01 '*' 0.05 '.' 0.1 ' ' 1
##
## Approximate significance of smooth terms:
##               edf Ref.df Chi.sq p-value
## s(x,y)         14.4336    65  64.13 1.56e-10 ***
## s(Depth)        0.9654     9  18.07 4.68e-07 ***
## s(iceConcentration) 0.9522     9  15.01 6.15e-05 ***
## ---
## Signif. codes:  0 '***' 0.001 '**' 0.01 '*' 0.05 '.' 0.1 ' ' 1
```

```
##
## R-sq.(adj) = 0.00411   Deviance explained = 10.1%
## -REML = 3346.7   Scale est. = 1           n = 35448
```



Baleen Whales

Below is the text and graphical summary of the final model for baleen whales. While we explain a large percentage of the deviance, there is only one covariate selected—the spatial smooth.

```
##
## Family: Negative Binomial(0.003)
## Link function: log
##
## Formula:
## Abundance ~ offset(log(Area)) + s(x, y, bs = "so", xt = list(bnd = list(boundary)))
##
## Parametric coefficients:
##               Estimate Std. Error z value Pr(>|z|)
## (Intercept)  -13.531      1.526   -8.869   <2e-16 ***
## ---
## Signif. codes:  0 '***' 0.001 '**' 0.01 '*' 0.05 '.' 0.1 ' ' 1
##
## Approximate significance of smooth terms:
##               edf Ref.df Chi.sq  p-value
## s(x,y) 16.91      65  82.85 1.46e-13 ***
```



```
## ---
## Signif. codes:  0 '***' 0.001 '**' 0.01 '*' 0.05 '.' 0.1 ' ' 1
##
## R-sq.(adj) =  0.0134   Deviance explained = 66.9%
## -REML = 499.3   Scale est. = 1           n = 28819
```

